EFFECTS OF SUBINHIBITORY DOSES OF THE FUNGICIDE IPRODIONE ON THE PLANT PATHOGENS *Fusarium oxysporum* AND *F. proliferatum*

By

VIVIANA ESTEFANIA FREIRE ZAPATA

Bachelor of Science in Biotechnology Engineering

University of the Armed Forces – ESPE

Sangolquí, Ecuador

2016

Submitted to the Faculty of the
Graduate College of the
Oklahoma State University
in partial fulfillment of
the requirements for
the Degree of
MASTER OF SCIENCE
December, 2020

EFFECTS OF SUBINHIBITORY DOSES OF THE FUNGICIDE IPRODIONE ON THE PLANT PATHOGENS *Fusarium oxysporum* AND *F. proliferatum*

Thesis Approved:

Dr. Carla Garzon

Thesis Adviser

Dr. Stephen Marek

Dr. Francisco Flores

Dr. Hassan Melouk

AKNOWLEDGEMENTS

I want to express my sincere gratitude to my advisor Dr. Carla Garzón for her guidance, advice and support during my thesis project. Dr. Garzón's teachings made a great impact on my professional life. I was fortunate to have her as my advisor.

I want to thank my advisory committee members, Dr. Stephen Marek, Dr. Francisco Flores and Dr. Hassan Melouk, for their valuable contributions and insight that helped me to complete my project.

I would also like to express my appreciation for the advice offered by Dr. Darren Hagen during the completion of the last objective of my research.

I want to express my deepest gratitude to the Department of Entomology and Plant Pathology at Oklahoma State University for the scholarship offered to complete my master's program.

Also, I want to express my gratitude to my family. My parents Juan Freire and Cecilia Zapata, my sister Salomé and my brother Juan Andrés for their constant support and encouragement. Their love gives me the strength to keep pursuing my dreams. Finally, I want to thank my beloved fiancé Christian Ayala. His support, patience and love inspire me to complete my goals.

Name: VIVIANA ESTEFANIA FREIRE ZAPATA

Date of Degree: DECEMBER, 2020

Title of Study: EFFECTS OF SUBINHIBITORY DOSES OF THE FUNGICIDE IPRODIONE ON THE PLANT PATHOGENS *Fusarium oxysporum* AND *F. proliferatum*

Major Field: ENTOMOLOGY AND PLANT PATHOLOGY

Abstract: Hormetic stimulatory responses have been widely reported in several economically important plant pathogens. Low doses of commonly applied fungicides can enhance fungal traits in vivo and in vitro conditions. However, little is known about the molecular mechanisms behind hormetic responses. During this study the effects of subinhibitory doses of iprodione on the growth of *Fusarium oxysporum* and *F. proliferatum* in vitro and in vivo were examined. Changes in the relative expression of 5 candidate genes of *F. proliferatum* growing at the suppressive dose, maximum stimulation dose of iprodione and a fungicide-free control were determined using RT-qPCR. Moreover, changes in the gene expression of this fungus growing at the maximum stimulatory dose of iprodione and a fungicide-free control were analyzed using RNAseq data. The results showed that subinhibitory doses of iprodione stimulated the mycelial growth of both pathogens in vitro and in vivo. In vitro, *F. oxysporum* wild type displayed an average growth stimulation of 6.87% and *F. proliferatum* wild type displayed 8.21% stimulation at 24 hpi. On onion epidermis, *F. oxysporum* demonstrated an average stimulation of 24.66% at 48 hpi and 19.6 % at 72hpi. In the case of *F. proliferatum*, mycelial growth was 23.62% larger than the control at 24hpi, no hormetic responses were observed at 48 and 72hpi. Significant changes in the relative expression of FUM1, HOG1 and HSP70 were observed at the suppressive dose. No significant changes in the expression of the 5 candidate genes were observed at the hormetic dose. Finally, 177 genes were differentially expressed, 117 upregulated and 60 downregulated. Functional annotation of the DEGs revealed that 57 had signal peptides, 24 genes were identified as carbohydrate-active enzymes, 15 were putative fungal effectors and 4 DEGs encoded for secondary metabolites. Upregulated processes included carbohydrate metabolism, detoxification mediated by ABC transporters and cytochrome P450 enzymes.

TABLE OF CONTENTS

Chapter Page

Chapter Page

LIST OF TABLES

Table Page

Table Page

Table Page

Table Page

LIST OF FIGURES

Figure Page

Figure Page

Figure Page

Figure Page

Figure Page

Figure Page

Figure Page

Figure Page

Figure Page

Figure Page

Figure Page

Figure Page

CHAPTER I

INTRODUCTION

The term hormesis describes a toxicological phenomenon where low doses of a stressor (e.g., fungicide) can cause stimulatory responses (e.g., enhanced growth, virulence) while high doses cause inhibition. This is a general phenomenon described across kingdoms (Calabrese and Blain 2011; Calabrese and Mattson 2017). Fungicide hormesis studies examine the effects of subinhibitory doses of fungicides in plant pathogens and their subsequent effects on agricultural systems (Pradhan et al. 2017a). Studies in oomycetes and fungi have reported enhancement of growth, sporulation rate, virulence, and mycotoxin production as consequences of exposure to low doses of fungicides (Audenaert et al. 2010; Cendoya et al. 2020; D'mello et al. 1998; Di et al. 2016a; Di et al. 2016b; Di et al. 2015; Flores 2010; Garzón et al. 2011; Kulik et al. 2012; Lu et al. 2018; Magan et al. 2002; Marín et al. 2013; Matthies et al. 1999; Pradhan et al. 2017a; Pradhan et al. 2019; Wang et al. 2017). These studies, and several more, provide compelling evidence that hormetic responses in plant pathogenic microorganisms are a risk to agriculture and possibly also to human and animal health (e.g., overproduction of mycotoxins).

Exact mechanisms behind the hormetic phenomenon remain unclear. Recent studies in plants suggested that mild increases of reactive chemical species, antioxidants, hormones, and upregulation of stress proteins like heat shock are responses to low concentrations of stressors, such as herbicides (Agathokleous et al. 2020). Understanding hormetic mechanisms in plant pathogens using different approaches that include responses in vivo, in vitro, and further molecular analyses can help to determine how hormesis is regulated in plant pathogens and how this knowledge can be applied to develop better management strategies. The main objective of this study was to examine the effects of subinhibitory doses of the fungicide iprodione on the plant pathogens *Fusarium oxysporum* and *F. proliferatum.*

OBJECTIVES

1. Analyze the effect of subinhibitory doses of iprodione under in vitro conditions.

2. Analyze the effect of subinhibitory doses of iprodione in plant tissues.

3. Examine using RT-qPCR the gene expression of virulence-related genes of a *Fusarium proliferatum* isolate growing under three experimental treatments: a suppressive fungicide dose of iprodione, the maximum stimulation dose, and a fungicide-free control.

4.Use mRNA-seq data to perform a differential gene expression analysis of *Fusarium proliferatum* growing at its maximum stimulation dose of iprodione, compared to a fungicide-free control.

CHAPTER II

LITERATURE REVIEW

HORMESIS

Hormesis is a biphasic response of organisms to stressors in which high doses of the stressor cause inhibitory or toxic effects, while low doses produce stimulatory responses (Calabrese and Baldwin 2002). Hormetic observations have been described since antiquity; for example, beneficial effects of small doses of toxic inorganic chemicals were reported by Paracelsus five centuries ago (Calabrese and Baldwin 1998). Hugo Schulz, who worked on yeast growth and fermentation, also described the same phenomena (Schulz 1887, 1888; Stebbing 1997). Later on, his work and the observations of Rudolph Arndt, a homeopathist, were defined as the Arndt-Schulz law (Calabrese and Baldwin 1998, 1999). However, this law was criticized by the research community at the time partially because of its association with homeopathy (Calabrese and Baldwin 2000). Stimulation at low doses and inhibition at high doses of stressors was observed by Hueppe (1896) on bacteria, which later was named "Hueppe's rule". The term "hormesis" was first coined by Southam and Ehrlich in 1943, after describing the effect of red cedar extract on the wood degrader basidiomycete *Fomes officinalis* (Calabrese 2005; Southam 1943).

Over the years, several hormetic responses have been described on plants, microorganisms, and animals, including insects and humans (Calabrese 2017), through the analysis of different biological endpoints and stressors, which have established hormesis as a general and independent phenomenon (Calabrese and Mattson 2017).

The extensive work of Edward Calabrese and collaborators, which includes a proper definition of this phenomenon, its historical background, description of qualitative and quantitative characteristics, and the understanding of molecular mechanism behind it, among other contributions, have been fundamental for the acceptance, development, and expansion of this scientific field (Agathokleous and Calabrese 2019; Calabrese and Baldwin 2002).

Characteristics of hormesis and how to evaluate this phenomenon

As mentioned earlier, hormesis is defined as a biphasic response, thus both zones, inhibition at high doses and stimulation at lower doses, must be present during a hormetic response (Figure 1). Hormetic dose-response relationships display different curve shapes depending on the factors analyzed. Growth, fecundity, and longevity hormetic responses display characteristic β-shape curves. On the other hand, dose responses where low doses produce less damage than higher ones (e.g., mutations, birth defects) are characterized by J or U-shape curves (Calabrese and Baldwin 2002; Calabrese et al. 1999).

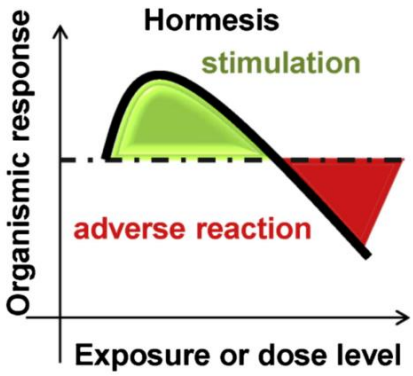

Figure 1. Hormetic dose-response relationship (Agathokleous and Calabrese 2019).

Based on an extensive review of dose-response studies, Calabrese also defined quantitative characteristics of hormetic responses. Most of the reviewed studies described modest stimulation. Where the maximum stimulatory response was 30% to 60% greater than the control, the hormetic zone was located within a 10-fold range and the maximum stimulation response was 3 to 6-fold lower than the no observed adverse effects level (NOAEL) (Calabrese and Baldwin 1997a, b; Calabrese and Blain 2005).

Testing hormetic hypothesis is not a straightforward task; background noise, control group variation, and biological variability affect the resolution of modest stimulation (Calabrese 2004). Thus, having a strong experimental design is fundamental (Calabrese and Blain 2005). There is no single methodology to test hormesis (Calabrese 2017); however, the following criteria must be considered when analyzing a hormetic response: number and space between doses tested must be adequate, the NOAEL must be defined and doses under the NOAEL must be included. Also, hormesis is a dose-time relationship thus selecting a correct time-lapse to collect data is imperative (Calabrese and Baldwin 1997a; Calabrese et al. 1999).

Multiple statistical methods to analyze the significance of hormetic responses have been described (Brain and Cousens 1989; Cedergreen et al. 2005; Deng et al. 2001; Deng et al. 2000; Hunt and Bowman 2004; Schabenberger et al. 1999). Two empirical methods are the most used and widely accepted: the Brain-Cousens model (Brain and Cousens 1989) and the Cedergreen-Ritz-Streibig model (Cedergreen et al. 2005).

Both models are based on log-logistic equations modified to describe hormesis. The Brain-Cousens equation includes the parameter (γ) that represents the stimulation at low doses. The confidence interval in which this parameter is found must not include zero to prove hormetic responses (Brain and Cousens 1989). The Cedergreen-Ritz-Streibig model includes a similar parameter (f), that represents the upper bound of the hormetic effect and which also needs to be greater than zero to statistically support hormesis (Cedergreen et al. 2005).

Proving that a hormetic effect happened or not is not enough, Schabenberger (1999) developed a reparameterization of the Brain-Cousens equation to estimate other informative parameters such as maximum stimulation dose (MSD), the dose at which the hormetic effect ends (NOAEL)' and the dose at which the effect is inhibited 50% compared to the control (EC_{50}) (Schabenberger et al. 1999). The Cedergreen-Ritz-Streibig equation was also reparametrized to calculate those values (Belz and Piepho 2012).

Mechanisms of hormesis

The stimulatory effects observed in hormesis have been described to be the result of several mechanisms (Calabrese 2004, 2008). Overcompensation, induced by a

disruption of homeostasis, is a widely accepted mechanism in hormesis that is time-specific and lasts for the duration of the disruption (Calabrese and Baldwin 2002). Calabrese (1999) stated that this overcompensation results from of overexpressed genes or pathways involved in cell detoxification or protection (Calabrese et al. 1999). Another mechanism for hormesis is direct stimulation. Hormetic responses mediated by both mechanisms seem to display the same qualitative and quantitative characteristics, which lead to suggest that both mechanisms are regulated by the same molecular means (Calabrese and Baldwin 2002; Calabrese and Mattson 2011). Interactions between agonists and low or high affinity receptors have been proposed to describe the biphasic hormetic response; receptors with high-affinity might activate stimulatory pathways while low affinity receptors display inhibitory response (Calabrese 2013; Szabadi 1977).

Calabrese (2013) evaluated around 400 hormetic dose-response experiments with different stressors, endpoints, and cell types (mostly human and from other animals) and proposed possible molecular mechanisms behind hormesis. He proposed two types of mechanisms: one mediated by the interaction between receptors/agonist/antagonist and integration of cell signaling transduction pathways (Calabrese 2013); and a second type where hormetic responses might be mediated by turn-on/turn-off switch mechanisms were the regulation of the response depends on the concentration of the stressor (Zhang et al. 2012).

In the last decade, great advances have been made to understand the mechanisms behind hormetic biphasic responses. It is clear that these responses are very complex and are mediated by an integrative interaction between multiple receptors and cell pathways (Calabrese and Mattson 2017). Analysis in plants have revealed a possible general

mechanism of hormesis (Agathokleous et al. 2020). Plants primed or preconditioned with oxygen, nitrogen, and sulfur reactive species (ROS, RNS, and RSS, respectively) display enhanced tolerance to stress compared to the control. This suggests that those three reactive species mediate responses to stress in plants (Antoniou et al. 2016). Moreover, these same reactive species might naturally control responses to low levels of stressors in plants, thus they can be linked with hormetic responses, given that preconditioning is a form of hormesis (Agathokleous et al. 2020). Additionally, plant responses to mild stress induced by non-essential metal ions are mediated by the action of reactive oxygen species (ROS), which activate antioxidant mechanisms, defense hormones, and mitogen-activated protein kinase (MAPK) pathways (Poschenrieder et al. 2013).

Literature about possible hormetic mechanisms in plant pathogens is lacking. Changes in the expression of virulence genes of *Botrytis cinerea* (Cong et al. 2019a) and *Sclerotinia sclerotiorum* (Hu et al. 2019) growing under the effect of low doses of fungicides has been analyzed. However, no significant changes in the level of expression were observed on the genes studied between fungicide treatments compared to the control. Also, subinhibitory doses of carbendazim did not stimulate the tolerance of *Sclerotinia sclerotiorum* to hydrogen peroxide neither the production of oxalic acid (Di et al. 2015).

Fungicide hormesis

Subinhibitory doses of fungicides have been reported to cause stimulation of vegetative growth, spore formation and germination, and production of virulence factors in fungi and oomycetes (Garzon and Flores 2013).

Sublethal doses of mefenoxam stimulated the radial growth of two *Pythium aphanidermatum* isolates (1 resistant and 1 sensitive) and 4 *Globisporangium cryptoirregulare* isolates (3 resistant and 1 sensitive). One *P. aphanidermatum* mefenoxam-resistant isolate displayed enhanced damping-off severity on geranium seedlings (Garzón et al. 2011). Moreover, low doses of cyazofamid and propamocarb stimulated the mycelial growth of this isolate, 6% larger on average than the control at the maximum stimulation dose (MSD) (Flores and Garzon 2013).

Stimulation of the mycelial growth area and dry mass was described on two mefenoxam resistant isolates of *Globisporangium irregulare* and *G. ultimum* treated with subinhibitory doses of that fungicide. The average mycelial growth area and mycelium dry weight of the *G. irregulare* isolate were 12% and 14% larger than the fungicide-free control; while the *G. ultimum* isolate showed an 8.61% mycelium area increase and 12.6% more dry mass (Pradhan et al. 2017b) in average.

Several studies have described hormetic stimulation of the growth and virulence of the ascomycete *Sclerotinia sclerotiorum* grown at sublethal doses of different fungicides. Dimethaclon resistant isolates showed 12.24 % to 17.24% stimulation of the mycelial growth under in vitro conditions and up to 59.80% enhanced virulence in vivo (Zhou et al. 2014). Seven carbendazim-resistant isolates showed enhanced pathogenicity when inoculated on rapeseed leaves sprayed with subtoxic doses of the fungicide (Di et al. 2015). Moreover, stimulatory effects of carbendazim, trifloxystrobin, and flusilazole on the mycelial growth of this pathogen over detached rapeseed leaves were analyzed at different points in time. Disease symptoms (e.g., necrosis) were observed earlier on fungicide sprayed leaves than in the control: visible symptoms were observed at 18 hours

post inoculation (hpi) on carbendazim, trifloxystrobin and flusilazole treated leaves, visible symptoms on control leaves were observed at 24hpi or later. Based on these results, the authors suggested a direct stimulation mechanism for the observed hormetic responses (Di et al. 2016a; Di et al. 2016b; Lu et al. 2018).

Low doses of dimethaclon, carbendazim and flusilazole did not increase tolerance of the pathogen to oxidative stress and secretion of oxalic acid (Di et al. 2015; Lu et al. 2018; Zhou et al. 2014). Also, the activity of three cell wall degrading enzymes (cellulase, pectinase and polygalacturase) was not affected by low doses of carbendazim (Di et al. 2016b). Zhang et al (2019) reported increased mycelial growth of *S. sclerotiorum* in vitro and increased virulence in planta when growing under the effect of dimethachlone, prochloraz, and mixtures of both fungicides. Dimethachlone caused the highest stimulation (up to 80.6% in one resistant isolate) while prochloraz caused only 9% of stimulation. Mixtures of both fungicides at the stimulating concentrations showed dose-additive effects on the virulence of the pathogen (Zhang et al. 2019) . The same effect was observed with mixtures of carbendazim and iprodione on the virulence of *Botrytis cinerea* (Cong et al. 2019a). In spite of all the studies conducted to date, the molecular mechanisms involved in the hormetic stimulation of growth and virulence of *S. sclerotiorium* and *B. cinerea* have not been elucidated so far.

Seventeen *Clarireedia homoeocarpa* (F.T. Benn.) L.A. Beirn, B.B. Clarke, C. Salgado & J.A. Crouch (formerly *Sclerotinia homoeocarpa* F.T. Benn.) isolates, preconditioned to tolerate the fungicide thiophanate methyl, showed increased growth stimulation at subinhibitory doses. Mycelial area was significantly stimulated, growing between 2.8% to 19.7% more than the control. The study contributed important

knowledge to the hormetic literature in plant pathogens because of the number of isolates analyzed, showing that hormetic responses can vary greatly at the intraspecies level in *C. homoecarpa*. The author concluded that observed hormetic effects might be because an overcompensation mechanism (Pradhan et al. 2019).

Several studies have linked increases of mycotoxin production in *Fusarium* spp. with exposure to sublethal doses of fungicides. Matthies et al. (1999) reported enhanced production of the trichothecene deoxynivalenol (DON) by *F. graminearum* grown in vitro at low doses of tebuconazole and thiabendazole. Similar results were reported on *F. graminearum* and *F. culmorum* treated with 0.1 µg/ml of tebuconazole (D'mello et al. 1998). This overproduction of secondary metabolites might be a stress response to exposure to sublethal doses of fungicides (Matthies et al. 1999).

Audenaert et al. (2010) described enhanced DON production by a *F. graminerum* isolate after 48 hours of being in contact with sublethal doses of prothioconazole and fluxastrobin in vitro and in vivo. Moreover, these fungicides increased the production of hydrogen peroxide in the first 4 hours of the experiment. This led the authors to suggest an interaction between ROS production and the fungicides effects, resulting in the stimulation of DON biosynthesis (Audenaert et al. 2010). Another study in the same pathogen reported an increase of trichothecenes transcripts and in DON and nivalenol (NIV) production when the pathogen was treated with sublethal doses of propiconazole and tebuconazole (Kulik et al. 2012). Tini et al. (2020) observed stimulation of the mycelial growth (evaluated as mycelial dry weight) *in vitro* of *F. avenaceum* and *F. poae* under the effects of low doses of tebuconazole, metconazole, prothioconazole, and prochloraz (Tini et al. 2020).

Twenty-nine out of 130 *Fusarium virguliforme* isolates showed mycelial growth stimulation at low concentrations of fluorypam (1 µg/ml and 0.5 µg/ml). The data of the isolates that fitted better the Brain-Cousens model (Wang et al. 2017).

Marin et al. (2013) reported the increase of the relative expression of the fumonisin biosynthetic polyketide synthase (FUM1) gene on *F. verticillioides* and *F. proliferatum* grown *in vitro* on tebuconazole amended media. Moreover, these findings were evident when the pathogens were under mild water stress and low temperature, suggesting that the increase of mycotoxins biosynthesis was also affected by abiotic factors (Marín et al. 2013). Similar results were described in the work of Cendoya et al. (2020) since two *F. proliferatum* strains showed enhanced production of fumonisins B1, B2, and B3 when treated with fungicides used to control *Fusarium* spp. that belong to the Fusarium head blight complex, tebuconazole, and combinations of epoxiconazole + metconazole and puraclostrobin + epoxiconazole (Cendoya et al. 2020).

ONION PRODUCTION

Onions (*Allium cepa* L.) are monocotyledons herbs belonging to the family Liliaceae, order Liliales (Jakše and Bohanec 2003; USDA 2020b). This important vegetable had a production of nearly 100M metric tons worldwide in 2018. The United States is the third major onion producer country behind China and India (FAOSTAT 2018). The total onion production in the USA was 69.9 million cwt in 2019. California, Washington, and Oregon are the largest producing states (USDA 2020a).

Onions are cold-season plants grown as annual crops for commercial purposes (Smith et al. 2011). Onion production can start from seeds or transplants, with the latter

being the most common. Production of onions in the Pacific Northwest, for example, starts in April. After 7 to 30 days seeds germinate, then the first true leaves appear between days 30 to 50. Onions start producing bulbs in the middle of June and bulb development continues through July and August until the plant is mature and ready to be harvested and stored (Sullivan et al. 2001).

Onion production can be affected by several pests, including weeds, insects, fungi, oomycetes, bacteria, viruses, and nematodes. The best integrated pest management strategies include sanitation, crop rotation, use of resistant varieties, use of certified pest-free seeds and bulbs, and chemical treatments (Schwartz and Mohan 2008; Smith et al. 2011). Most onion diseases are caused by fungi and oomycetes, which can infect onion at any developmental stage during production or in storage. Soil-borne diseases are mostly caused by *Fusarium* spp., *Rhizoctonia* spp., *Pythium* spp., *Sclerotinia sclerotiorum*, *Sclerotium* spp., and *Macrophomina phaseolina* (Behrani et al. 2015). In addition, *Aspergillus* spp., *Penicillium* spp., *Alternaria* spp., *Fusarium* spp., *Rhizopus* spp., *Colletotrichum* spp., and *Botrytis* spp. are fungal species causing bulb rot during storage (Kumar et al. 2015).

Fusarium oxysporum

Fusarium oxysporum is a soil-borne asexual fungus (Lombard et al. 2019) that belongs to the phylum Ascomycota, subphylum: Pezizomycotina, class: Sordariomycetes, subclass: Hypocreomycetidae, order: Hypocreales, family: Nectriaceae (NCBI 1988).

Fusarium species form characteristic structures that can be used for identification: microconidia and macroconidia. Microconidia are born in two types of conidiogenous

cells: monophialides and polyphialides. Macroconidia are born in sporodochia and vary in size, shape, number of septa and form of the apical and basal cells. *F. oxysporum* produces microconidia in short monophialides in false heads. Its macroconidia have 3-septa with a curved apical cell and foot-shaped basal cell. This species can also produce chlamydospores as survival structures (Leslie and Summerell 2008; Summerell et al. 2003).

Fusarium oxysporum is a member of the *Fusarium oxysporum* species complex (FOSC). This complex comprises pathogenic and nonpathogenic strains with a wide host range, including important ornamental and agricultural crops (Michielse and Rep 2009; O'Donnell et al. 2009). Human pathogens have also been described within this complex (O'Donnell et al. 2004). Because of the wide range of hosts and the significant economic damage it can cause, *Fusarium oxysporum* is considered one of the most important plant pathogens, ranking fifth on the top 10 fungal pathogens (Dean et al. 2012).

Some pathogenic strains are adapted to infect a specific host and are denoted as forma specialis. Lombard et al. (2019) reported a total of 144 *F. oxysporum* forma specialis described; some examples are *F. oxysporum* forma specialis (f. sp.) *cepae* that causes basal rot of onion; *F. oxysporum* f. sp. *cubense* which infects banana and asparagus; *F. oxysporum* f. sp. *lycopersici* and f. sp. *radicis- lycopersici* which infect tomato; *F. oxysporum* f. sp. *chrysanthemi* which affects chrysanthemum, gerbera, paris, and African daisy; *F. oxysporum* f. sp. *vasinfectum* which affects cotton, and many more (Edel-Hermann and Lecomte 2019; Lombard et al. 2019).

Fusarium spp. survive in the soil as chlamydospores for multiple years (30 years). Additionally, mycelium, macroconidia and microconidia can be present in plants debris or infecting asymptomatic hosts (Leoni et al. 2013). Once weather conditions are appropriate spores can germinate. Infection usually occurs near plant roots (soil borne disease) but it can also start in aerial tissue due to spores that were transported by rain, wind or insects (Xu et al. 2003). Some factors, such as plant exudates in the soil, favor spore germination and germ tube growth. Exudates from the specific host (for example, tomato for *F. oxysporum* f. sp. *lycopersici*) are more stimulatory than other plants' root exudates (Steinkellner et al. 2005). The pathogen penetrates the tissue directly or by creating hyphal swellings (appressoria). Natural openings (e.g., stomata, hydathodes) and lesions on roots and bulbs favor pathogen invasion (Gordon 2017; Nguyen et al. 2016). Once inside the tissue, it can grow as a biotroph intercellularly without damaging the plant during the endophytic phase, or it can secrete cell degrading enzymes and mycotoxins to destroy the plant tissue, during the necrotrophic phase (Gordon 2017).

Phylogenetic studies have revealed that some forma specialis withing the FOSC are polyphyletic while others are paraphyletic. O'Donnell et al. (2004) described 4 clades inside the species complex using two molecular markers: the translation elongation factor 1-alpha (EF1-α) and the mitochondrial small subunit rDNA (mtSSU) (O'Donnell et al. 2004; O'Donnell et al. 1998). Following studies included the nuclear ribosomal DNA intergenic spacer (IGS) (O'Donnell et al. 2009), topological incongruences were found between EF1-α and IGS phylogenetic trees. *Fusarium oxysporum* f. sp. *cepae* (FOC) is present in two of the four clades, indicating that this forma specialis is not monophyletic. Moreover, a phylogenetic study performed on FOC isolates demonstrated the formation

of a tree with 8 clades when using the IGS gene and 2 clades when using the EF1-α gene (Sasaki et al. 2015). Similar results were found on FOC isolates from UK, a phylogenetic tree of EF1-α gene grouped FOC isolates on one clade with 2 subclades (Taylor et al. 2016).

Fusarium basal rot is a devastating disease that affects *Allium* species. Cramer et al (2000) reported up to 40.3% of pathogen incidence on onion cultivars in New Mexico (Cramer 2000). The economic impact of FOC on onion production have been reported to reach 35% of losses (Lacy and Roberts 1982). The disease can impact onion production on field and storage. Losses of £10 to 11 million have been reported in the UK (Taylor et al. 2013).

Fusarium oxysporum f. sp. *cepae* infection starts at the onion roots and bulb basal plate. FOC conidia near onion roots germinate forming a germ tube that can form extensive mycelia on the root surface. Pathogen invasion of plant tissue can occur by direct penetration without the formation of appressorium. Additionally, wounds on roots or bulbs caused by nematodes, other pathogens, or agricultural practices are used by FOC to invade the plant. Inside the root, the pathogen grows intercellularly before branching and growing, colonizing the whole root cortex. Eventually, the mycelia fills the root cortex cells and decompose them. Then, the pathogen reaches the vascular tissue, and continues growing onto the xylem where clogging occurs. Xylem clogging is more often observed on the basal plate tissue. Once the fungal pathogen reaches the basal plate it can infect fresh scales of the bulb and grow extensively (Abawi and Lorbeer 1971; Brayford 1996; Cramer 2000).

Pathogen infection of seedlings can cause sudden death, delayed emergence, damping-off and stunted growth. One of the first symptoms of FOC infection on mature plants is chlorosis and necrosis of the leaves beginning at the tips. Under the ground, bulbs show discoloration at the basal plate, roots rot and detach from the bulb. Infection eventually reaches the stem plate and the external scales, where white mycelium can often be observed (Cramer 2000; Schwartz and Mohan 2008).

Pathogenic effectors released during infection have been described in *F. oxysporum*. Fourteen secreted in xylem (SIX) proteins were identified during the infection of tomato plants by *F. oxysporum* f. sp. *lycopersici*, further analysis described that some of these genes were necessary for pathogenicity (Gawehns et al. 2015; Houterman et al. 2007). Homologs of SIX genes have been reported to be related with pathogenicity of FOC on onions (SIX3, SIX5, SIX7, SIX9, SIX10, SIX12 and SIX14) (Sasaki et al. 2015; Taylor et al. 2016). Taylor et al (2016) suggested that the SIX genes and putative effectors might be located on "lineage-specific mobile pathogenicity chromosomes" as observed on *F. oxysporum* f. sp. *lycopersici* (FOL), the species where those dispensable chromosomes were discovered (Ma et al. 2010; Taylor et al. 2016).

Fusarium species biosynthesize different secondary metabolites, mycotoxins are some of the most important because of the economic losses and health issues associated with them (Munkvold 2017). Mycotoxins of concern are trichothecenes (deoxynivalenol (DON), T-2 toxin); zearalenone (ZEN) and fumonisins (e.g., fumonisin B1). Trichothecenes and zearalenones are mainly produced by *F. graminearum* and closely related species, zearalenone can also be produced by members of the *F. sambucinum* species complex, while fumonisins are produced mainly by *F. verticilliodes*, *F.*

proliferatum, and some species inside the *Fusarium fujikuroi* species complex (FFSC) (Bakker et al. 2018). High doses of these toxins can cause serious diseases in humans and animals. For example, fumonisin B1 has been reported as a potential carcinogenic agent for humans (Anttila et al. 2002). Neuro-, hepato- and nephrotoxicity effects have been described in animals feeding on fumonisin contaminated feed (Stockmann-Juvala and Savolainen 2008). For example, horses developed leukoencephalomalacia commonly known as "moldy corn poisoning" after ingesting *Fusarium* contaminated feed grain (Devreese et al. 2013).

Fusarium oxysporum species produce few mycotoxins, including enniatins, fusaric acid and moniliformin (Munkvold 2017). Production of fumonisins has been reported only in one strain from Korea (Proctor et al. 2004).

Fusarium proliferatum

Fusarium proliferatum belongs to the *Fusarium fujikuroi* species complex (FFSC). Initially, Matsushima described it as *Cephalosporium* species until Nirenberg recognized it as a *Fusarium* species (Leslie and Summerell 2008). Its host range is as extensive as that of *F. oxysporum* and includes conifers, monocots and dicots (Proctor et al. 2009). *Fusarium proliferatum* can infect economically important crops, such as maize (Zainudin et al. 2017), wheat (Conner et al. 1996), rice (Amatulli et al. 2012), asparagus (Bargen et al. 2009), garlic (Stankovic et al. 2007), onions (Isack et al. 2014), soybean (Chang et al. 2015), tomato (Gao et al. 2016), pea (Waśkiewicz et al. 2013), cotton (Zhu et al. 2019), banana (Jimenez et al. 1993), and grapevine (Yurchenko et al. 2019), among others. This pathogen also affects ornamentals, including orchids (Srivastava et al. 2018),

sugar pine trees and other conifers (Stewart et al. 2016) and palms (Armengol et al. 2005).

Fusarium proliferatum produces microconidia in mono and polyphialides usually forming chains. They have club shape and are abundant in aerial mycelium. Macroconidia are produced on tan to orange sporodochia. Each macroconidium has 3 to 5 septa, the apical cell has a curved shape and the basal cell is not well developed. *F. proliferatum* does not form chlamydospores (Leslie and Summerell 2008).

Fusarium proliferatum together with *F. verticillioides* are the principal producers of fumonisins (Smith 2018). To date at least 28 fumonisins have been described and divided into groups (A, B, C and P) based on their structure (Gutleb et al. 2002; Musser and Plattner 1997). Fumonisin B, especially fumonisin B1, is the most prevalent and of main interest because of the cancer risk associated with its consumption. Several studies have described the biosynthetic pathway of fumonisins, which includes at least 17 clustered genes (designed FUM genes) as well as a transcription factor and an ABC transporter (Alexander et al. 2009; Proctor et al. 2003). Additionally, *F. proliferatum* biosynthesizes other mycotoxins: beauvericin, enniatins, fusaric acid, fusarin, moniliformin and fusaproliferin, which was first discovered in this specie (Munkvold 2017; Ritieni et al. 1995).

Studies have reported a high genetic variation within *Fusarium proliferatum*. Phylogenetic analysis based on sequences of the EF1-α gene of *F. proliferatum* from different hosts and locations showed that isolates formed groups and subgroups that were not related to the host or place of collection. Isolates from maize were observed in all the

clusters of the phylogenetic tree, suggesting a high genetic variation of this population which might be associated with the extensive distribution of the host itself (Jurado et al. 2010). Similar findings were described by Stępień et al. (2011), who found that 36 *F. proliferatum* isolates from a wide variety of host and origins did not cluster together neither by host nor by geographic location when an EF1-α tree was analyzed. However, a phylogenetic tree based on partial sequences of the FUM1 gene showed that isolates clustered by host. Also, fumonisin production of the isolates was described, showing a variable biosynthetic potential of the mycotoxin within the species (Stępień et al. 2011). Palacios et al. (2015) reported similar results, high genetic variability was observed by analyzing *F. proliferatum* isolated from wheat between 2008 and 2011, using EF1-α and calmodulin genes. Additionally, isolates demonstrated high variability in fumonisin biosynthesis, with fumonisin B1 being the most abundant. However, isolates that produced fumonisins type B2 and B3 were reported too (Palacios et al. 2015). *Fusarium proliferatum* isolates causing basal rot of garlic in Spain also showed genetic variation demonstrated as the formation of 5 clusters in an EF1-α based tree. Mating type analysis revealed possible sexual reproduction within this population (Gálvez et al. 2017).

The draft genome of a *F. proliferatum* isolated from an onion with basal rot disease have been recently reported. It has a size of 45.8 Mb, 597 contigs and 15,418 genes. Comparing the genome with RNA-seq data allowed to identify 15,448 proteins. Of these 1,254 were secreted proteins, 258 were putative effectors, and 341 were secreted carbohydrate-active enzymes (CAZYmes). Also, 58 secondary metabolite clusters, homologs to the effectors SIX2 of *F. oxysporum*, and 6 miniature impala (mimp) sequences were present in the genome (Armitage et al. 2019).

Fusarium proliferatum causes bulb rot of onion. It has been isolated in several regions worldwide from field and stored bulbs (Bayraktar and Dolar 2011; Dissanayake et al. 2009b; Galván et al. 2008; Gálvez et al. 2017; Kalman et al. 2020; Mohan et al. 1997; Stankovic et al. 2007; Toit et al. 2003). Symptoms of the disease include yellowish, water-soaked, translucent areas in the scales that with time become brown, necrotic and soft. Later stages of the infection can produce a brown liquid exudate as well as the presence of white mycelia between affected scales. This disease can be distinguished from onion basal rot in that the basal plate is usually not affected (Schwartz and Mohan 2008). Other symptoms consist of a salmon-pink discoloration of the outer three to four external scales of white onions (Toit et al. 2003). Even though *F. proliferatum* does not form chlamydospores it can persist saprophytically in the field for long periods of time (Schwartz and Mohan 2008).

CONTROL OF FUSARIUM DISEASES

Fusarium diseases cause several yield and quality losses in economically important crops. One management strategy against *Fusarium* diseases is the application of chemicals and fungicides: *F. oxysporum* and *F. proliferatum* causing hypocotyl and root rot on conifers were controlled by soil fumigation with trichloronitromethane (chloropicrin) and methyl bromide (currently restricted) (Gordon et al. 2015). *Fusarium oxysporum* f. sp *lycopersi* affecting tomato has been controlled by fungicides such as bromuconazole, prochloraz, azoxystrobin, benomyl, carbendazim and fludioxonil; however, soil fumigants are used to manage soilborne pathogens of this crop more often than fungicides (McGovern 2015). Crown and root rot of asparagus (caused by *F. oxysporum* and *F. proliferatum*) can be treated with thiabendazole, however the fungicide

application is not cost effective (Elmer 2015). Fungicides mancozeb, fludioxonil, pyraclostrobin, and iprodione have been used to control *Fusarium* diseases on orchids (Srivastava et al. 2018). FOC disease can be controlled with carbendazim, mancozeb, hexaconazole, iprodione, tebuconazole, prochloraz and thiram (Abd-Elrazik et al. 1990; Behrani et al. 2015; Futane et al. 2018; Özer and Köycü 1998; Saravanakumari et al. 2019). Dipping garlic on fludioxonil and thiophanate can reduce Fusarium bulb rot caused by *F. proliferatum* (Schwartz and Mohan 2008*)*.

Dicarboximides are fungicides that belong to group 2, as defined by the Fungicide Resistance Action Committee (FRAC). This group includes the fungicides chlozolinate, dimethachlone, iprodione, procymidone and vinclozolin (FRAC 2020). Although the action site of dicarboximides has not been entirely elucidated yet, studies in *B. cinerea* have reported that the putative target site of iprodione is a class III histidine kinase gene (OS1). *Botrytis cinerea* iprodione-resistant isolates showed an amino acid substitution at the codon 365 of this gene, where isoleucine was substituted with serine (I365S) or asparagine (I365N). However, other types of mutations have also been described (Cui et al. 2002; Ma et al. 2007; Oshima et al. 2002).

Iprodione activates oxidative and osmotic stress responses (Hayes et al. 2014). Sensitivity to iprodione was increased by activation of the HOG1 pathway by phosphorylation, while *Botrytis cinerea* HOG1 mutants showed resistance to iprodione (Segmüller et al. 2007). Phenylpyrrole fungicides (e.g., fludioxonil) also stimulate HOG1 phosphorylation (Tanaka and Izumitsu 2010). Moreover, it has been reported that strains of other fungi (*Aspergillus nidulans* and *Neurospora crassa*), with mutations on class III histidine kinases, such as OS1, display increased resistance to dicarboxamides and

phenylpyrroles (Hagiwara et al. 2007; Ochiai et al. 2001; Viaud et al. 2006). These observations suggested a possible target upstream on the HOG1 pathway (Turrà et al. 2014)

CHAPTER III

EFFECT OF SUBINHIBITORY DOSES OF IPRODIONE ON *FUSARIUM* SPP. GROWING UNDER IN VITRO CONDITIONS

INTRODUCTION

Hormesis is a phenomenon characterized by stimulation at subinhibitory (low) doses of a stressor and inhibition at higher doses (Calabrese and Baldwin 2002). This dose-response concept has been demonstrated in a wide range of biological systems including bacteria, fungi, oomycetes, plant and animals using different stressors and endpoints (Calabrese and Mattson 2017).

Fungicide hormesis is a growing field of research. There are increasing reports of stimulatory effects of commonly applied fungicides in important plant pathogens. Fungi and oomycetes have been shown to increase their growth, sporulation and virulence when they are in contact with low doses of commonly applied fungicides (Garzon and Flores 2013). For example, subinhibitory doses of thiophanate-methyl stimulated preconditioned *Sclerotinia homeocarpa* isolates to grow up to 19.7% more than the control (Pradhan et al. 2019). Carbendazim and iprodione applied alone or in a mixture were shown to increase the virulence of *Botrytis cinerea* isolates on cucumber leaves (Cong et al. 2019a;

Cong et al. 2019b). Different fungicides were demonstrated to produce hormetic effects on dimethachlon-sensitive and -resistant isolates of *Sclerotinia sclerotiorum* (Zhou et al. 2014). All isolates that were exposed to low doses of the fungicide were more virulent and grew significantly faster than those growing on non-amended medium (Zhou et al. 2014). The same effect was observed with prochloraz and mixtures of both chemicals (Zhang et al. 2019). Additional stimulatory responses have been described with the fungicides carbendazim (Di et al. 2015), trifloxystrobin (Di et al. 2016a), and flusilazole (Lu et al. 2018) in *S. sclerotiorum*.

Similar results have been reported in studies involving oomycetes. Mycelial stimulation and increased damping-off on geranium seedlings were reported on *Pythium aphanidermatum* growing under low doses of mefenoxam (Garzón et al. 2011). Further studies by Flores and Garzon (2013) described the increment of radial growth of *Pythium aphanidermatum* when growing on media amended with cyazofamid or propamocarb. The mycelial growth areas of *Globisporangium ultimum* and *G. irregulare* under the effect pf low doses of mefenoxam were significantly larger than the controls (Pradhan et al. 2017b).

Fusarium spp. are cosmopolitan soilborne plant pathogens with an extremely wide range of hosts that include agriculturally important crops. They cause multiple diseases such as rots of roots, stalks, ears and fruits, vascular wilts, blights, leaf spots, seedling damping-off and diebacks (Summerell et al. 2003). An important feature of these pathogens is the production of several mycotoxins that can contaminate human food and animals feed thus representing an important threat to health and crop production (Santos Pereira et al. 2019).

Fungicide hormesis has been previously reported in few *Fusarium* species. *Fusarium graminearum*, which causes Fusarium head blight (FHB) in grain cereals, showed increased production of the mycotoxin deoxynivalenol (DON) under in vitro and in vivo conditions when treated with sublethal doses of prothioconazole and a mixture of fluoxastrobin + prothioconazole (Audenaert et al. 2010). *Fusarium avenaceum* and *F. poae*, other species from the FHB complex, showed increased mycelial growth at low doses (0.001 mg/L and 0.0001 mg/L) of tebuconazole, metconazole, prothioconazole and prochloraz (Tini et al. 2020). A study that determined the sensitivity of a collection of *Fusarium virguliforme* isolates from soybean fields to the fungicide fluorypam, demonstrated that 22% of isolates analyzed showed increased mycelial growth at the subinhibitory dose (1µg/ml) in comparison to the control (Wang et al. 2017).

Several studies have found an increase in mycotoxin production in *Fusarium* spp. treated with sublethal doses of fungicides; however, the association of stimulatory responses with hormesis were not explored (D'mello et al. 1998; Kulik et al. 2012; Magan et al. 2002; Matthies et al. 1999). *Fusarium verticillioides* and *Fusarium proliferatum* growing at sublethal doses of tebuconazole, under water stress and lower temperatures increased the expression of FUM1 gene (Marín et al. 2013). Moreover, sublethal doses of tebuconazole and mixtures of epoxiconazole + metconazole and pyraclostrobin + epoxiconazole fungicides accompanied with abiotic factors such as temperature and water stress contributed to the overproduction of fumonisins in *F. proliferatum* (Cendoya et al. 2020).

The aim of this study was to examine the effects of subinhibitory doses of iprodione on the mycelial growth of *Fusarium oxysporum* and *F. proliferatum* isolated from onion under in vitro conditions.

MATERIALS AND METHODS

Fusarium spp. inoculum

Fusarium oxysporum and *F. proliferatum* were isolated from white onion bulbs (*Allium cepa*) obtained from a grocery store in Stillwater, OK, and transformed to express the green fluorescent protein (GFP) and tdTomato protein (tdTom) (Table 1) (Gard and Arias, not published). Species identities of the wild type strains were previously determined by morphology (Arias and Gard, not published) and confirmed by PCR amplification and sequencing of translation elongation factor gene using primers EF1 and EF2 (O'Donnell et al. 2010).

Table 1. *Fusarium* spp. isolates included in the study.

Species	**Wild type sample name**	**Isolate name**	**Transformation**	**Isolated from**
F. oxysporum	A1WT	FO-A1R1-4	tdTom	White onion bulbs (*Allium cepa*)
		FO-A1G4-2	GFP	
F. proliferatum	A7WT	FP-A7R8	tdTom	
		FP-A7G32	GFP	

Determination of the Benchmark dose and iprodione doses preparation

The experimental doses were calculated using the recommended rate for ground application in dry bulb onions (Rovral 1.5 pints a.i. per acre transformed to parts per million (ppm)). This dose was the minimum application rate used in following studies.

In order to find the benchmark dose (BMD), the following serial dilutions of the minimum application rate (MAR) (1,797.396 ppm) dose were prepared: $MARx10^{2}$ (179,740 ppm), $MARx10^{1}$ (17,974 ppm), MAR (1,797.4 ppm), $MARx10^{-1}$ (179.74 ppm), $MARx10^{-2}$ (17.97 ppm), $MARx10^{-3}$ (1.797 ppm), $MARx10^{-4}$ (0.179 ppm), $MARx10^{-5}$ (0.0179 ppm), and $MARx10^{-6}$ (0.00179 ppm). The growth of *F. proliferatum* transformant isolates was tested using the previously mentioned concentrations plus a fungicide-free treatment on Spezieller Nährstoffarmer Agar (SNA) (Leslie and Summerell 2008). The experiment included three replicates per each of the treatments.

The benchmark dose was calculated with the Environmental Protection Agency (EPA) Benchmark Dose software version 3.1.1. using the standard continuous Hill model (Flores 2010). Doses that produced total inhibition of fungal mycelium were excluded. The calculated benchmark dose was 10.74 ppm.

In order to model a hormetic curve, 11 new iprodione doses were calculated using the benchmark dose as reference (Flores 2010). The BMD was diluted as follows: $BMDx10^{1.5}$, $BMDx10^{1}$, BMD $x10^{0.5}$, BMD, $BMDx10^{-0.5}$, $BMDx10^{-1}$, $BMDx10^{-1.5}$, $BMDx10^{-2}$, $BMDx10^{-2.5}$, $BMDx10^{-3}$, $BMDx10^{-3.5}$. These dilutions corresponded to the following concentrations of iprodione: 316.23 ppm, 100 ppm, 31.623 ppm, 10 ppm,

3.1623 ppm, 1 ppm, 0.31623 ppm, 0.1 ppm, 0.031623 ppm, 0.01 ppm and 0.003163 ppm. Water was used as the fungicide-free control.

In vitro dose response of *Fusarium oxysporum and F. proliferatum* to subinhibitory doses of iprodione

The experiment followed the protocol designed by (Flores 2010) and modified by (Pradhan et al. 2017a). Fungicide dilutions were prepared in autoclaved reverse osmosis (RO) water, in a final volume of 100 ml. The fungicide Iprodione 2SE (active ingredient (a.i.): iprodione 240 g/L, BASF Corporation) was diluted at the highest dose (316.2278 ppm a.i.) and mixed for 15 minutes at medium velocity. Then 31.62 ml of this solution was transferred to a 250 ml flask containing 68.4 ml of water and mixed for 5 minutes to reach the iprodione concentration of the second treatment (100 ppm). This process was repeated ten times until the lowest concentration (0.003162 ppm) was prepared.

The growing medium (SNA) prepared with 10% less amount of water, was amended with iprodione, one flask per dose, plus a fungicide-free control to which only water was added. Petri dishes containing 15 ml of amended SNA were inoculated with 5 mm agar plugs, one per plate, of actively growing fungal culture (concentrically collected from mycelia margins) from 5 days old *Fusarium oxysporum* and *F. proliferatum* isolates growing on SNA (one wild type and two transformants each of *F. oxysporum* = FO-A1, and *F. proliferatum* = FP-A7). Assays using each wild type isolate included 3 replicates per dose. Each experiment was repeated 5 times over time. The number of replicates per dose was increased to 5 for transformant isolates, and each experiment was repeated 3 times over time.

Inoculated petri dishes were sealed with parafilm and incubated in a growth chamber (Percival Scientific, Perry, IA) at 22 ± 2 ºC in the dark for 3 days. Replicates of each treatment were randomly sorted in columns. Non-inoculated petri dishes containing SNA medium were placed at the top and bottom of each column and around the columns to minimize variation of temperature in the experimental media due to exposure moving air. Columns were then randomly placed in the middle of the growth chamber.

Finally, petri dishes were scanned at 24, 48 and 72 hours post inoculation (hpi) using a CanoScan 8400F (Canon, Melville, NY). Mycelial growth areas were measured using the ImageJ 1.52a software (Abràmoff et al. 2004).

Effect of subinhibitory doses of iprodione on *Fusarium* spp. growing over cellophane sheets

Fusarium oxysporum (FO-A1WT) and *F. proliferatum* (FP-A7WT) wild type isolates were used in this experiment in order to determine the isolate that underwent the highest hormetic stimulation, which was selected to conduct the assays related to the third and fourth objectives (Chapter V and VI) of this work.

Iprodione treatments were prepared following the same protocol mentioned above, with the following addition: working with one fungicide dilution at that time, autoclaved cellophane disks (7 cm) were immersed for 5 minutes in the appropriate fungicide solution contained in autoclaved glass petri dishes. Excess of fungicide solution on the cellophane disks was briefly removed using autoclaved paper towels. Cellophane sheets were then placed over petri dishes containing 15 ml SNA media amended with the respective fungicide dose. Petri dishes prepared this way were inoculated over the

cellophane disk with a 5 mm agar plug containing 5-day old cultures of *Fusarium* spp. Five replicates of each treatment were included, and the experiment was repeated 3 times over time.

Borders of the mycelia growing over the cellophane sheet were marked with points forming 2 perpendicular diameters and the petri dishes were scanned using a CanoScan 8400F (Canon, Melville, NY) at 24, 48 and 72 hpi. Growth area was measured using the software ImageJ 1.52a (Abràmoff et al. 2004).

Data analysis

The presence of hormetic stimulation was tested using the Brain and Cousens (Brain and Cousens 1989) model with mycelial growth data, as defined by Equation 1.

Equation 1

$$E\left[\frac{y}{x}\right] = \delta + \frac{\alpha - \delta + \gamma x}{1 + \omega\ exp\left[\beta ln\left(\frac{x}{EC_{50}}\right)\right]}$$

where,

$$\omega = 1 + \frac{2\gamma EC_{50}}{\alpha - \delta}$$

$E\left[\frac{y}{x}\right]$: average response at dosage x

α: upper bound

δ: lower bound

β: slope at the EC_{50} dose

γ: rate of increase at low doses

In this model, gamma (γ) must not include zero or negative values for hormetic stimulation to be significant. When $\gamma \leq 0$ hormetic hypotheses were rejected.

To conduct statistical analyses, the mycelial growth area was transformed to percentages of the growth of the fungicide-free control of each replicate after the subtraction of the agar plug area (Flores and Garzon 2013). In order to test the fitting of the data to the model equation, a nonlinear regression analysis was performed using custom scripts using the R version 3.6.2 (R Core Team 2019) packages: nlstools (Baty et al. 2015), nls2 (Grothendieck 2013) and minpack.lm (Elzhov et al. 2016). Some initial parameters where fixed as follows: $\alpha = 100$, which corresponded to the stimulation of the fungicide-free control, and $\delta = 0$, which represented the response at the inhibitory dose. For other parameters such as EC_{50}, β and γ, initial values were estimated by visual inspection of the data (Flores and Garzon 2013).

When hormetic stimulation was statistically supported, the no observed adverse effect level (NOAEL) and the maximum stimulation dose (MSD) were calculated using the modified Brain-Cousens equation (Schabenberger et al. 1999). The values estimated as described above were used to plot the dose-response curve of each isolate and each time point using the tidyverse package of R (Wickham et al. 2019)

Additionally, an analysis of dose response curves was performed using the R package “drc” (Ritz et al. 2015). Dataset fitting was tested using two hormetic models, the Brain-Cousens model (Brain and Cousens 1989) with five parameters (BC.5) and the Cedergreen-Ritz-Streibing model (Cedergreen et al. 2005) also with five parameters

(CRS.5a). Hormetic stimulation was statistically supported if the parameter 'f', which correspond to the magnitude of the hormetic response, was positive and its 95% confidence limits did not include zero. Also, a 'lack of fit test' was performed using the function modelFit of the drc package. This function tests fitting of the data to the dose response model by comparing the model with a general ANOVA using a *F*-test. If the *P*-value was significant it was concluded that the dose-response model did not fit the data (Ritz et al. 2016).

RESULTS

Dose response of *Fusarium oxysporum* to iprodione

Wild type isolates

Fusarium oxysporum wild type isolate FO-A1WT showed significant mycelial growth stimulation, with γ confidence limits ranging from 5.52 to 31.76, which supported a hormetic response to subinhibitory doses of iprodione. Mycelial growth area at the MSD (0.74 ppm) was estimated to be 6.87% greater on average than the control at 24 hpi. The parameters β, EC_{50} and NOAEL were 2 ppm, 4.87 ppm and 1.57 ppm, respectively (Table 2). These parameters were used to model a biphasic dose-response curve presented in Figure 1. At 48 hpi and 72 hpi, γ limits remained positive supporting a hormetic stimulation. Average mycelial growth area stimulation at the MSD decreased with time, with 3.23% increase at 48hpi and 1.54% at 72hpi (Table 2, Figure 2 and Figure 3).

Table 2. Dose response parameters that describe the effect of subinhibitory doses of iprodione on the mycelial growth area of *Fusarium oxysporum* wild type (FO-A1WT) at 24, 48 and 72 hpi. Analysis performed after 5 repetitions with 3 replicates per treatment.

Parameters	24 HPI			48 HPI			72 HPI		
	Value (ppm)	Lower limit (2.5%)	Upper limit (97.5%)	Value (ppm)	Lower limit (2.5%)	Upper limit (97.5%)	Value (ppm)	Lower limit (2.5%)	Upper limit (97.5%)
β	2.00	1.75	2.25	2.10	1.90	2.30	2.26	2.00	2.52
EC_{50}	4.87	4.32	5.42	4.04	3.77	4.31	3.76	3.54	3.99
γ	18.64	5.52	31.76	11.32	4.06	18.58	6.12	0.30	11.95
NOAEL	1.57	1.17	1.97	1.10	0.79	1.41	0.87	0.46	1.29
MSD	0.74	0.54	0.93	0.54	0.39	0.70	0.45	0.24	0.66
Stimulation at the MSD (%)	6.87%			3.23%			1.54%		

β= slope at the EC_{50} dose; EC_{50}= effective concentration at which the growth is inhibited 50% compared to the control; γ= rate of increase at small doses; NOAEL= No observed adverse effect level; MSD= Maximum stimulation dose

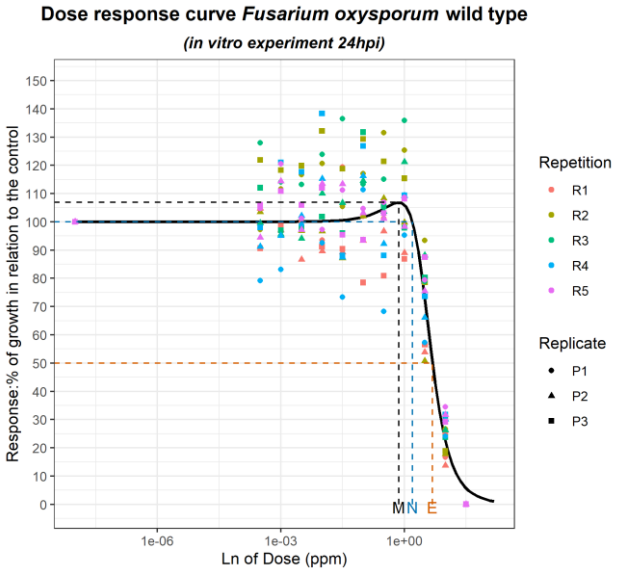

Figure 2. Dose-response curve showing the effect of 11 subinhibitory doses of iprodione and a fungicide-free control on the mycelial growth area of *Fusarium oxysporum* wild type isolate FO-A1WT at 24 hpi. Parameters of the modeled curve were: maximum stimulation dose (M), no observed adverse effect level NOAEL (N) and the effective concentration at which the growth is inhibited 50% compared to the control EC_{50} (E).

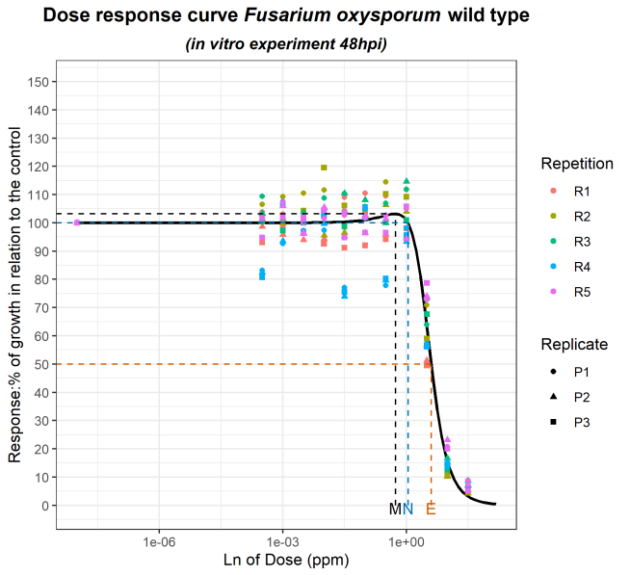

Figure 3. Dose-response curve showing the effect of 11 subinhibitory doses of iprodione and a fungicide-free control in the mycelial area growth of *Fusarium oxysporum* wild type isolate FO-A1WT at 48hpi. Parameters that model the curve are showed: maximum stimulation dose (M), no observed adverse effect level NOAEL (N) and the effective concentration at which the growth is inhibited 50% compared to the control EC_{50} (E).

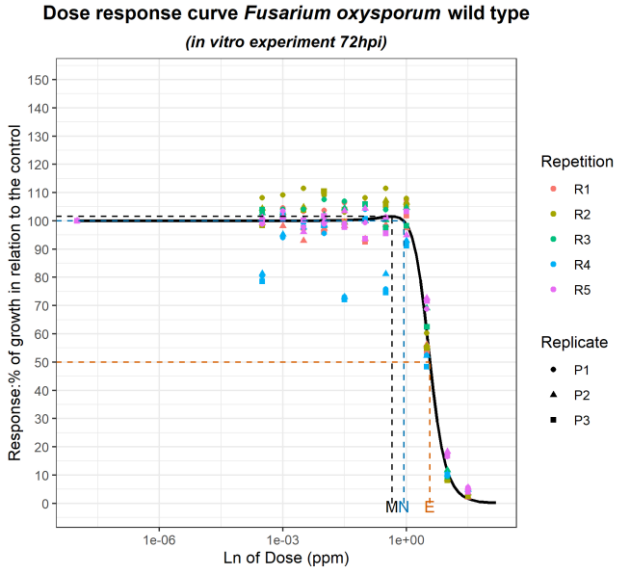

Figure 4. Dose-response curve showing the effect of 11 subinhibitory doses of iprodione and a fungicide-free control in the mycelial area growth of *Fusarium oxysporum* wild type isolate FO-A1WT at 72 hpi. Parameters that model the curve are showed: maximum stimulation dose (M), no observed adverse effect level NOAEL (N) and the effective concentration at which the growth is inhibited 50% compared to the control EC_{50} (E).

Transformant isolates

Fusarium oxysporum isolates transformed to express the GFP and tdTom proteins, FO-A1G4-2 and FO-A1R1-4 respectively, showed significant stimulation at subinhibitory doses of iprodione. At 24 hpi, isolate FO-A1G4-2 showed a mycelial growth area 5.9% greater than the fungicide-free control at the MSD (0.94 ppm). Meanwhile, the tdTom transformant showed a maximum growth stimulation of 6.92% greater than the control at the MSD (0.87 ppm). β, EC_{50} and NOAEL were calculated for both isolates (Table 3 and Table 4) and dose response curves were modeled using these parameters (Figure 5 and Figure 8).

At 48 hpi, both isolates had significant growth stimulation with positive γ 95% confidence limits (ranging from 3.87 to 14.8 in FO-A1G4-2, and from 5.63 to 15.45 in FO-A1R1-4). Mycelial growth stimulation was less intense than at 24 hpi, with 3.3% and 3.08% at the MSDs (FO-A1G4-2 = 0.72 ppm, and FO-A1R1-4 = 0.61 ppm) (Table 3 and Table 4;Figure 6 and Figure 9). At 72 hpi the GFP transformant showed small but significant stimulation (0.74%) at the MSD (0.38 ppm) (Table 3 and Figure 7). Meanwhile, *Fusarium oxysporum* tdTom transformant isolate (FO-A1R1-4) did not show a hormetic response at 72 hpi (Table 4). FO-A1R1-4 β and EC_{50} were calculated (1.92 ppm and 5.3 ppm, respectively) using a log logistic model and the dose response curve was modeled with these parameters (Figure 10) (Flores and Garzon 2013; Schabenberger et al. 1999).

Table 3. Dose response parameters that describe the effect of subinhibitory doses of iprodione on the mycelial growth area of *Fusarium oxysporum* GFP transformant (FO-A1G4-2) at 24, 48 and 72 hours post inoculation. Analysis performed after 3 repetitions with 5 replicates per treatment.

Parameters	24 HPI			48 HPI			72 HPI		
	Value (ppm)	**Lower limit (2.5%)**	**Upper limit (97.5%)**	**Value (ppm)**	**Lower limit (2.5%)**	**Upper limit (97.5%)**	**Value (ppm)**	**Lower limit (2.5%)**	**Upper limit (97.5%)**
B	1.98	1.77	2.20	1.97	1.84	2.10	2.01	1.91	2.10
EC_{50}	6.54	5.81	7.27	5.90	5.51	6.29	5.28	5.05	5.51
Γ	12.63	2.87	22.39	9.34	3.87	14.80	3.85	0.81	6.88
NOAEL	2.00	1.49	2.51	1.49	1.12	1.86	0.77	0.37	1.18
MSD	0.94	0.70	1.18	0.72	0.55	0.89	0.38	0.18	0.58
Stimulation at the MSD (%)	5.90%			3.30%			0.74%		

β= slope at the EC_{50} dose; EC_{50}= effective concentration at which the growth is inhibited 50% compared to the control; γ= rate of increase at small doses; NOAEL= No observed adverse effect level; MSD= Maximum stimulation dose.

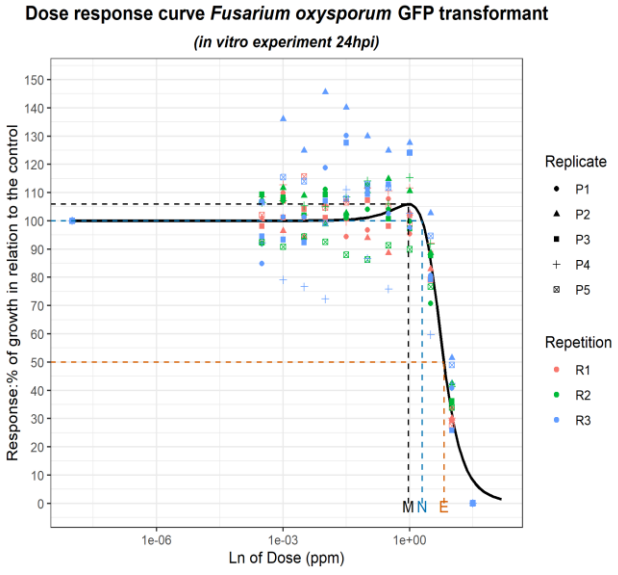

Figure 5. Dose-response curve showing the effect of 11 subinhibitory doses of iprodione and a fungicide-free control in the mycelial area growth of *Fusarium oxysporum* GFP transformant isolate FO-A1G4-2 at 24hpi. Parameters that model the curve are showed: maximum stimulation dose (M), no observed adverse effect level NOAEL (N) and the

effective concentration at which the growth is inhibited 50% compared to the control EC_{50} (E).

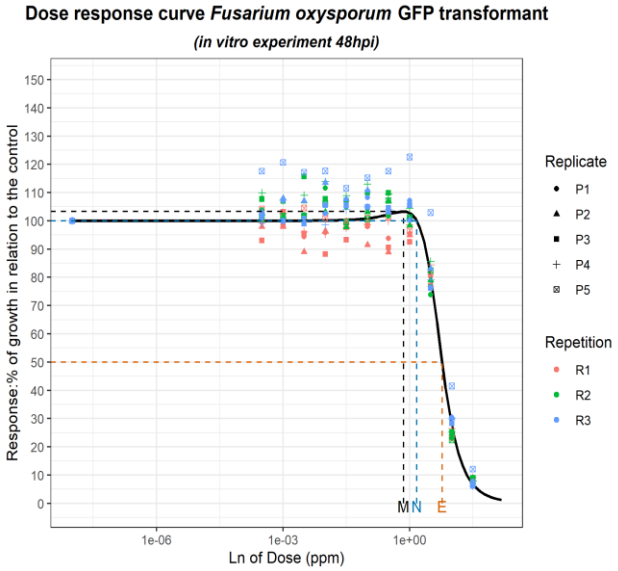

Figure 6. Dose-response curve showing the effect of 11 subinhibitory doses of iprodione and a fungicide-free control in the mycelial area growth of *Fusarium oxysporum* GFP transformant isolate FO-A1G4-2 at 48 hpi. Parameters that model the curve are showed: maximum stimulation dose (M), no observed adverse effect level NOAEL (N) and the effective concentration at which the growth is inhibited 50% compared to the control EC_{50} (E).

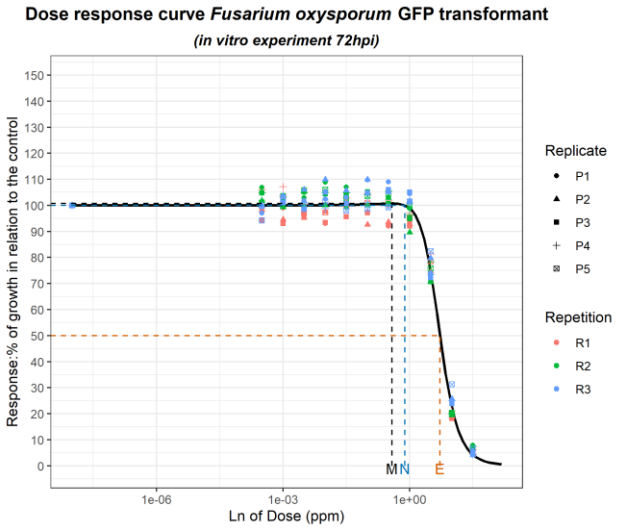

Figure 7. Dose-response curve showing the effect of 11 subinhibitory doses of iprodione and a fungicide-free control in the mycelial area growth of *Fusarium oxysporum* GFP transformant isolate FO-A1G4-2 at 72 hpi. Parameters that model the curve are showed:

maximum stimulation dose (M), no observed adverse effect level NOAEL (N) and the effective concentration at which the growth is inhibited 50% compared to the control EC_{50} (E).

Table 4. Dose response parameters that describe the effect of subinhibitory doses of iprodione on the mycelial growth area of *Fusarium oxysporum* tdTom transformant (FO-A1R1-4) at 24, 48 and 72 hours post inoculation. Analysis performed after 3 repetitions with 5 replicates per treatment.

Parameters	24 HPI			48 HPI			72 HPI		
	Value (ppm)	Lower limit (2.5%)	Upper limit (97.5%)	Value (ppm)	Lower limit (2.5%)	Upper limit (97.5%)	Value (ppm)	Lower limit (2.5%)	Upper limit (97.5%)
β	1.90	1.62	2.17	1.90	1.81	2.00	1.92	1.78	2.06
EC_{50}	6.32	5.29	7.35	5.54	5.25	5.84	5.30	5.05	5.55
γ	16.84	0.38	33.30	10.54	5.63	15.45	NA		
NOAEL	1.91	1.26	2.55	1.30	1.02	1.58	NA		
MSD	0.87	0.57	1.17	0.61	0.49	0.74	NA		
Stimulation at the MSD (%)	6.92			3.08			NA		

β= slope at the EC_{50} dose; EC_{50}= effective concentration at which the growth is inhibited 50% compared to the control; γ= rate of increase at small doses; NOAEL=No observed adverse effect level; MSD= Maximum stimulation dose. NA= not applicable, gamma confidence limits include negative values.

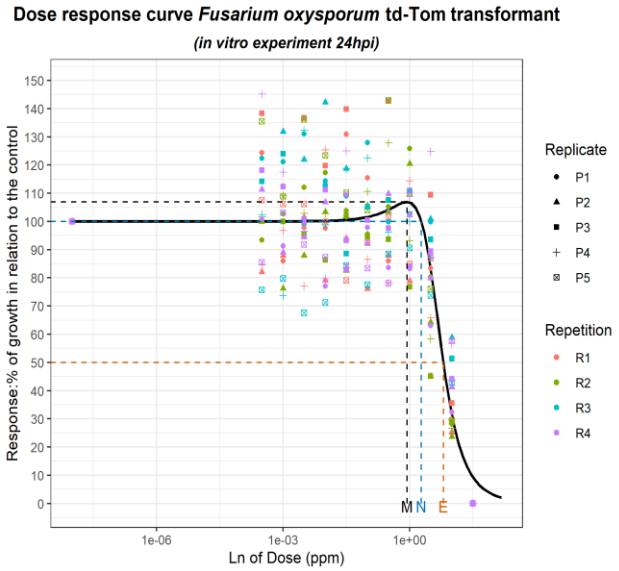

Figure 8. Dose-response curve showing the effect of 11 subinhibitory doses of iprodione and a fungicide-free control in the mycelial area growth of *Fusarium oxysporum* tdTom transformant isolate FO-A1R1-4 at 24 hpi. Parameters that model the curve are showed: maximum stimulation dose (M), no observed adverse effect level NOAEL (N) and the

effective concentration at which the growth is inhibited 50% compared to the control EC_{50} (E).

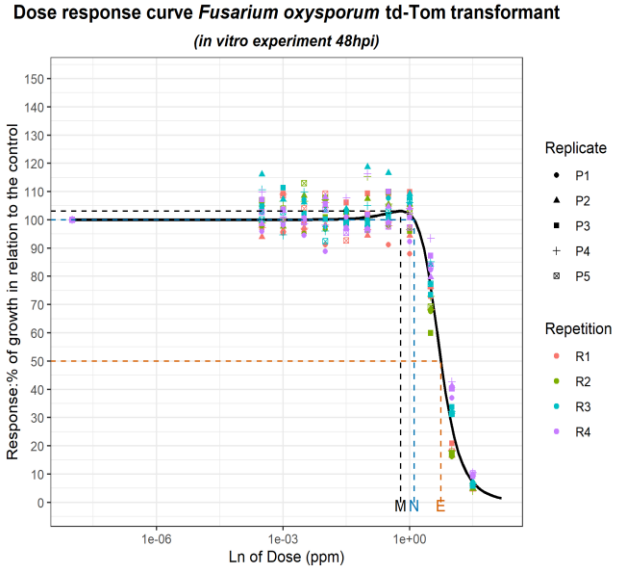

Figure 9. Dose-response curve showing the effect of 11 subinhibitory doses of iprodione and a fungicide-free control in the mycelial area growth of *Fusarium oxysporum* tdTom transformant isolate FO-A1R1-4 at 48. Parameters that model the curve are showed: maximum stimulation dose (M), no observed adverse effect level NOAEL (N) and the effective concentration at which the growth is inhibited 50% compared to the control EC_{50} (E).

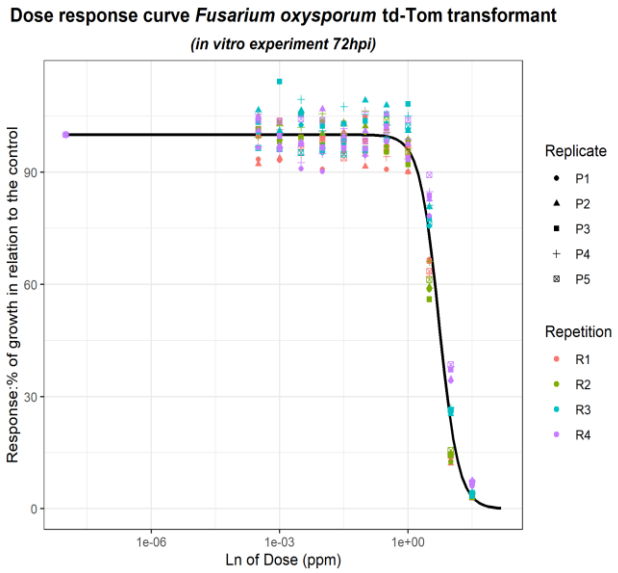

Figure 10. Dose-response curve showing the effect of 11 subinhibitory doses of iprodione and a fungicide-free control in the mycelial area growth of *Fusarium oxysporum* tdTom transformant isolate FO-A1R1-4 at 72 hpi. No hormetic effect was found at this point time.

Experiment performed over cellophane sheets

The *F. oxysporum* wild type isolate growing over cellophane sheets placed on fungicide amended SNA petri dishes showed significant hormetic stimulation at 24 hpi. Gamma confidence limits ranged from 46.74 to 1223.49. The percentage of stimulation at the MSD (0.21 ppm) was 15.23%. Beta, EC_{50} and NOAEL were estimated as 1.13 ppm, 333.63 ppm and 1.59 ppm, respectively (Table 5). The MSD and the calculated hormetic curve parameters differed from the in vitro experiment results without cellophane. The modeled biphasic dose response curve is shown in Figure 11. There was no significant hormetic stimulation at 48 and 72 hpi (Table 5).

Table 5. Dose response parameters that describe the effect of subinhibitory doses of iprodione on the mycelial growth area of *F. oxysporum* wild type isolate FO-A1WT at 24, 48 and 72 hpi. Analysis performed after 3 repetitions with 5 replicates per treatment.

Parameters	**24 HPI**	**48 HPI**	**72 HPI**

	Value (ppm)	Lower limit (2.5%)	Upper limit (97.5%)	Value (ppm)	Lower limit (2.5%)	Upper limit (97.5%)	Value (ppm)	Lower limit (2.5%)	Upper limit (97.5%)
β	1.13	1.09	1.17	1.35	0.92	1.78	1.52	1.01	2.03
EC_{50}	333.63	-128.55	795.82	31.30	24.71	37.89	27.50	22.07	32.93
γ	635.11	46.74	1223.49	NA	NA				
NOAEL	1.59	0.87	2.32	NA	NA				
MSD	0.21	0.07	0.34	NA	NA				
Stimulation at the MSD (%)	15.23			NA			NA		

β= slope at the EC_{50} dose; EC_{50}= effective concentration at which the growth is inhibited 50% compared to the control; γ= rate of increase at small doses; NOAEL=No observed adverse effect level; MSD= Maximum stimulation dose. NA= not applicable, gamma confidence limits include negative values.

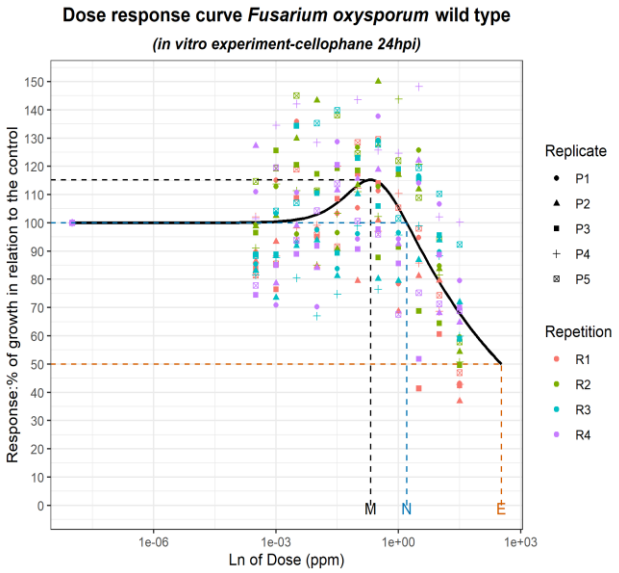

Figure 11. Dose-response curve showing the effect of 11 subinhibitory doses of iprodione and a fungicide-free control in the mycelial area growth of *Fusarium oxysporum* wild type isolate FO-A1WT growing over cellophane sheets. Results at 24 hpi. Parameters that model the curve are showed: maximum stimulation dose (M), no observed adverse effect level NOAEL (N) and the effective concentration at which the growth is inhibited 50% compared to the control EC_{50} (E).

Dose response of *Fusarium proliferatum* to iprodione

Wild type isolate

Fusarium proliferatum wild type isolate FP-A7WT showed significant stimulation growing on SNA media under the effect of subinhibitory doses of iprodione after 24, 48 and 72 hpi. The percentages of stimulation over the control were 8.21% at 24 hpi, 6.97% at 48 hpi and 5.65% a 72 hpi at the MSD (0.82 ppm). Parameters β, EC_{50} and NOAL were estimated (Table 6) and used to model dose response curves at each time point (Figure 12, Figure 13 and Figure 14).

Table 6. Dose response parameters that describe the effect of subinhibitory doses of iprodione on the mycelial growth area of *Fusarium proliferatum* wild type (FP-A7WT) after 24, 48 and 72 hours post inoculation. Analysis performed after 5 repetitions with 3 replicates per treatment.

Parameters	24 HPI			48 HPI			72 HPI		
	Value (ppm)	**Lower limit (2.5%)**	**Upper limit (97.5%)**	**Value (ppm)**	**Lower limit (2.5%)**	**Upper limit (97.5%)**	**Value (ppm)**	**Lower limit (2.5%)**	**Upper limit (97.5%)**
β	1.98	1.76	2.20	2.06	1.86	2.27	2.17	1.97	2.37
EC_{50}	5.36	4.77	5.95	5.07	4.64	5.51	4.93	4.58	5.28
γ	20.22	7.73	32.71	16.68	7.63	25.74	12.85	6.17	19.53
NOAEL	1.79	1.40	2.17	1.71	1.38	2.03	1.66	1.35	1.97
MSD	0.82	0.63	1.01	0.81	0.65	0.97	0.82	0.66	0.97
Stimulation at the MSD (%)	8.21%			6.97%			5.65%		

β= slope at the EC_{50} dose; EC_{50}= effective concentration at which the growth is inhibited 50% compared to the control; γ= rate of increase at small doses; NOAEL= No observed adverse effect level; MSD= Maximum stimulation dose.

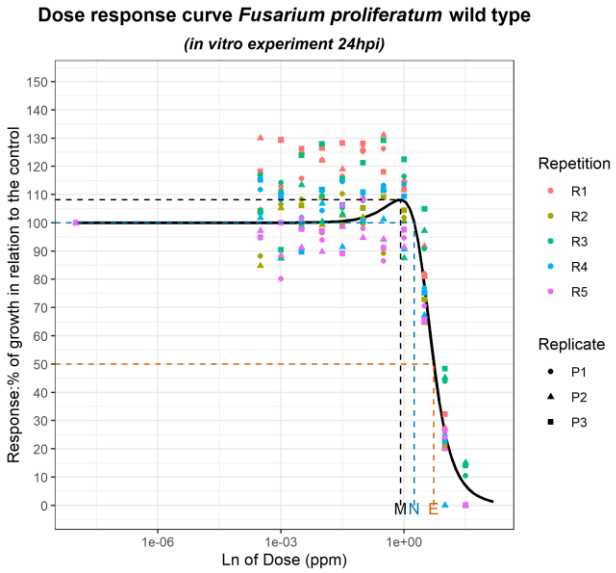

Figure 12. Dose-response curve showing the effect of 11 subinhibitory doses of iprodione and a fungicide-free control in the mycelial area growth of *Fusarium proliferatum* wild type isolate FP-A7WT. Results at 24 hpi. Parameters that model the curve are showed: maximum stimulation dose (M), no observed adverse effect level NOAEL (N) and the effective concentration at which the growth is inhibited 50% compared to the control EC_{50} (E).

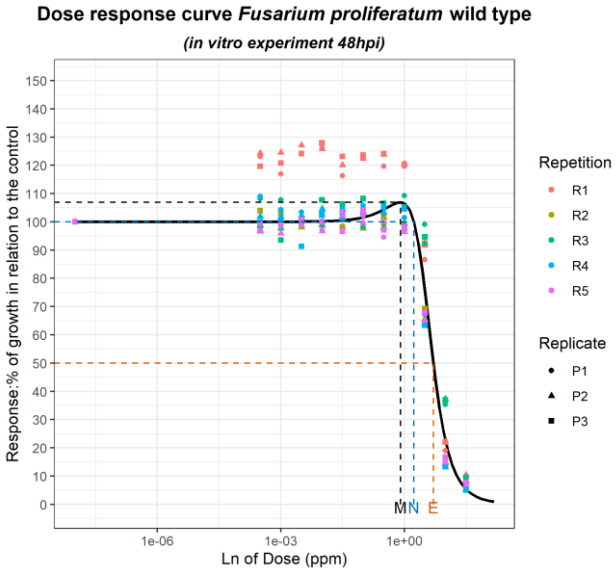

Figure 13. Dose-response curve showing the effect of 11 subinhibitory doses of iprodione and a fungicide-free control in the mycelial area growth of *Fusarium proliferatum* wild type isolate FP-A7WT. Results at 48 hpi. Parameters that model the curve are showed: maximum stimulation dose (M), no observed adverse effect level

NOAEL (N) and the effective concentration at which the growth is inhibited 50% compared to the control EC_{50} (E).

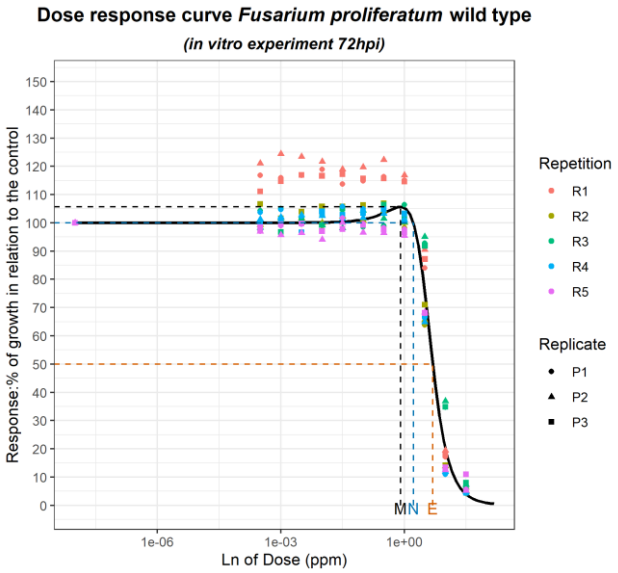

Figure 14. Dose-response curve showing the effect of 11 subinhibitory doses of iprodione and a fungicide control in the mycelial area growth of *Fusarium proliferatum* wild type isolate FP-A7WT. Results at 72 hpi. Parameters that model the curve are showed: maximum stimulation dose (M), no observed adverse effect level NOAEL (N) and the effective concentration at which the growth is inhibited 50% compared to the control EC_{50} (E).

Transformant isolates

Fusarium proliferatum GFP transformant isolate FP-A7G32 showed significant hormetic stimulation only at 48 hpi. The stimulation was 2.14% greater than the control at the MSD (0.47 ppm) with positive γ confidence limits (ranging from 2.19 to 17.50). Beta, EC_{50} and NOAEL parameters were calculated (1.87 ppm, 4.89 ppm and 0.98 ppm, respectively; Table 7). The modeled dose response curve showed a peak at the MSD (Figure 15). A log logistic model was used to calculate β and EC_{50} at 24 and 72 hpi (Table 7) and these parameters were used to model the dose-response curves (Figure 16 and Figure 17).

Table 7. Dose response parameters that describe the effect of subinhibitory doses of iprodione on the mycelial growth area of *Fusarium proliferatum* GFP transformant (FP-A7G32) after 24, 48 and 72 hpi. Analysis performed after 3 repetitions with 5 replicates per treatment.

Parameters	24 HPI			48 HPI			72 HPI		
	Value (ppm)	**Lower limit (2.5%)**	**Upper limit (97.5%)**	**Value (ppm)**	**Lower limit (2.5%)**	**Upper limit (97.5%)**	**Value (ppm)**	**Lower limit (2.5%)**	**Upper limit (97.5%)**
β	1.79	1.31	2.27	1.87	1.73	2.02	1.97	1.74	2.19
EC_{50}	6.58	5.80	7.36	4.89	4.50	5.27	4.96	4.61	5.31
γ	NA	9.85	2.19	17.50	NA				
NOAEL	NA	0.98	0.55	1.41	NA				
MSD	NA	0.47	0.27	0.66	NA				
Stimulation at the MSD (%)	NA			2.14%			NA		

β= slope at the EC_{50} dose; EC_{50}= effective concentration at which the growth is inhibited 50% compared to the control; γ= rate of increase at small doses; NOAEL= No observed adverse effect level; MSD= Maximum stimulation dose. NA= not applicable, gamma confidence limits include negative values.

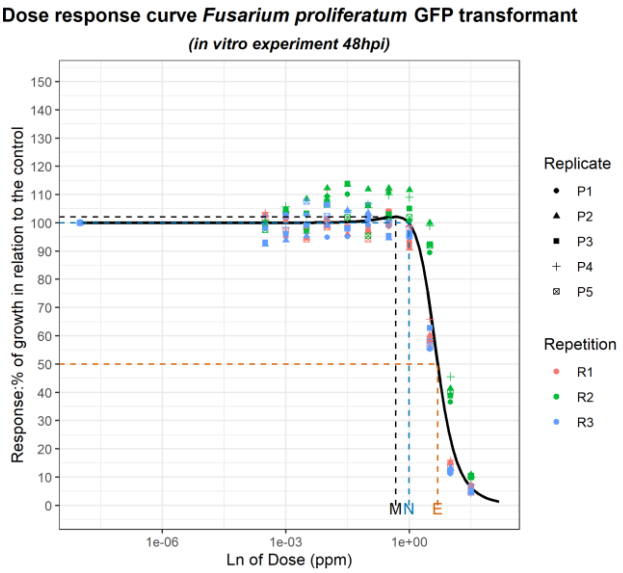

Figure 15. Dose-response curve showing the effect of 11 subinhibitory doses of iprodione and a fungicide control in the mycelial area growth of *Fusarium proliferatum* GFP transformant isolate FP-A7G32. Results at 48 hpi. Parameters that model the curve are showed: maximum stimulation dose (M), no observed adverse effect level NOAEL (N) and the effective concentration at which the growth is inhibited 50% compared to the control EC_{50} (E).

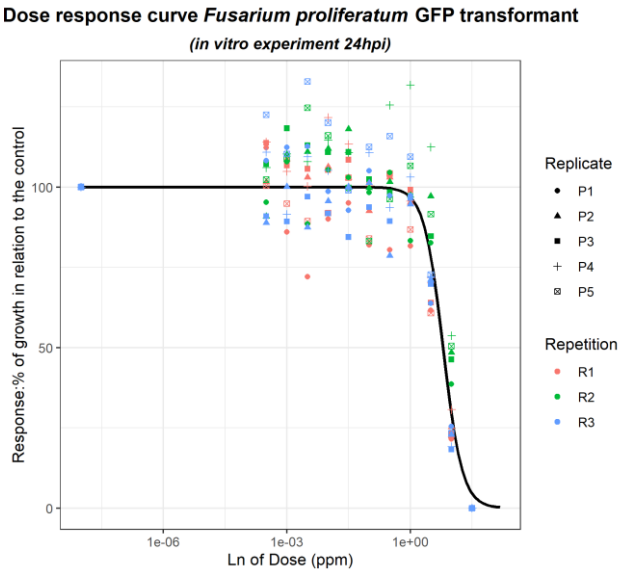

Figure 16. Dose-response curve showing the effect of 11 subinhibitory doses of iprodione and a fungicide-free control in the mycelial area growth of *Fusarium proliferatum* GFP transformant isolate FP-A7G32. Results at 24 hpi. No hormetic effect was found at this time point.

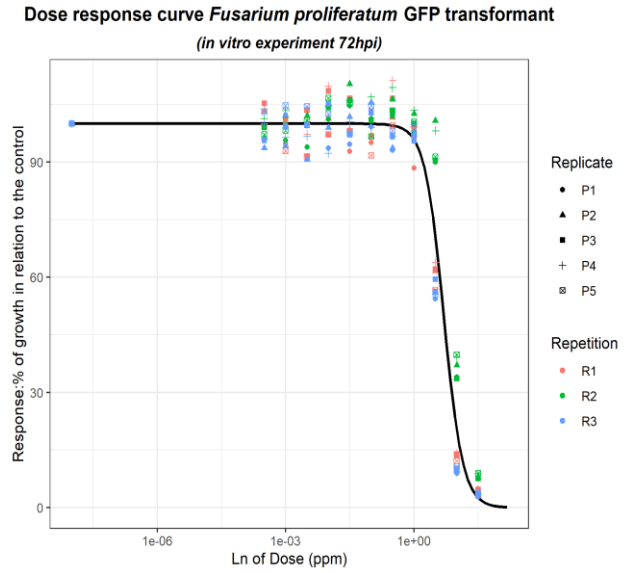

Figure 17. Dose-response curve showing the effect of 11 subinhibitory doses of iprodione and a fungicide-free control in the mycelial area growth of *Fusarium proliferatum* GFP transformant isolate FP-A7G32. Results at 72 hpi. No hormetic effect was found at this time point.

On the other hand, *F. proliferatum* tdTom transformant (FP-A7R8) showed significant stimulation at 48 and 72 hpi, with growth stimulation of 1.85% and 3.13% greater than the control at the MSD (0.46 ppm and 0.59 ppm, respectively). No significant hormetic response was observed at 24 hpi. At 48 hpi, the estimated values of β was 1.74 ppm, EC_{50} was 5.93 ppm, and NOAEL was 0.99 ppm. At 72 hpi, the parameters were 1.83 ppm, 5.71 ppm and 1.27 ppm respectively (Table 8). Dose response curves were modeled and presented in Figure 19 and Figure 20. The calculated β and EC_{50} at 24 hpi were graphed in the modeled dose response curve in Figure 18.

Table 8. Dose response parameters that describe the effect of subinhibitory doses of iprodione on the mycelial growth area of *Fusarium proliferatum* tdTom transformant isolate FP-A7R8 at 24, 48 and 72 hpi. Analysis performed after 3 repetitions with 5 replicates per treatment.

Parameters	24 HPI			48 HPI			72 HPI		
	Value (ppm)	**Lower limit (2.5%)**	**Upper limit (97.5%)**	**Value (ppm)**	**Lower limit (2.5%)**	**Upper limit (97.5%)**	**Value (ppm)**	**Lower limit (2.5%)**	**Upper limit (97.5%)**
β	1.76	1.56	1.95	1.74	1.65	1.84	1.83	1.73	1.94
EC_{50}	6.69	6.19	7.18	5.93	5.51	6.34	5.71	5.33	6.10
γ	NA	NA	NA	9.46	3.14	15.78	11.67	5.24	18.11
NOAEL	NA	NA	NA	0.99	0.58	1.40	1.27	0.93	1.60
MSD	NA	NA	NA	0.46	0.27	0.64	0.59	0.44	0.74
Stimulation at the MSD (%)	NA			1.85%			3.13%		

β = slope at the EC_{50} dose; EC_{50} =effective concentration at which the growth is inhibited 50% compared to the control; γ=rate of increase at small doses; NOAEL=No observed adverse effect level; MSD= Maximum stimulation dose. NA= not applicable, gamma confidence limits include negative values.

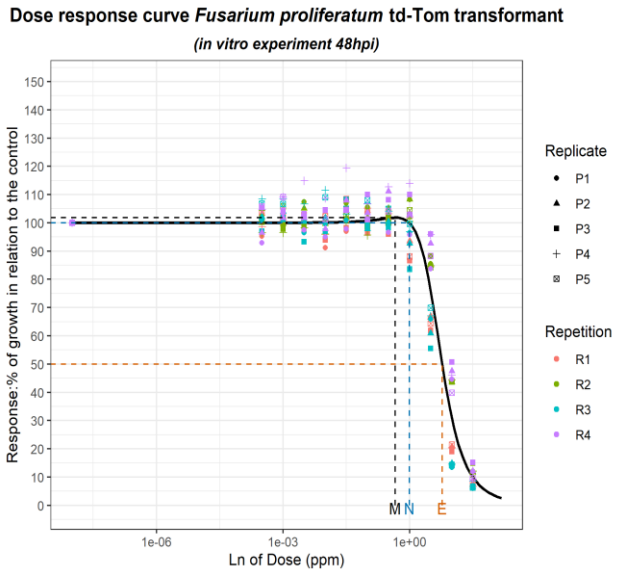

Figure 18. Dose-response curve showing the effect of 11 subinhibitory doses of iprodione and a fungicide-free control in the mycelial area growth of *Fusarium proliferatum* tdTom transformant isolate FP-A7R8. Results at 48 hpi, significant stimulation observed. Parameters that model the curve are showed: maximum stimulation dose (M), no observed adverse effect level NOAEL (N) and the effective concentration at which the growth is inhibited 50% compared to the control EC_{50} (E).

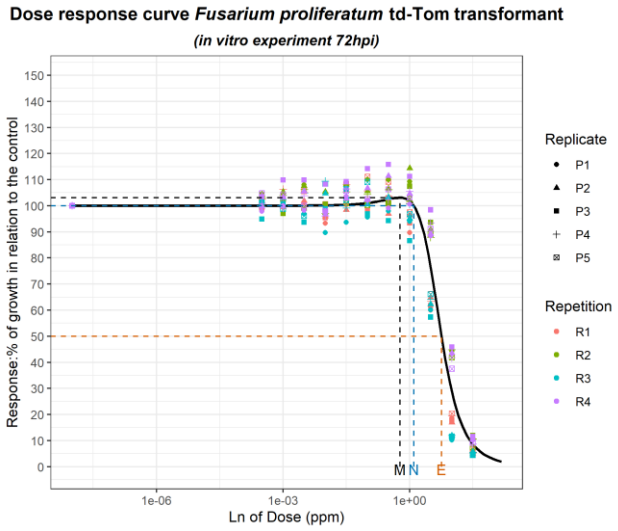

Figure 19. Dose-response curve showing the effect of 11 subinhibitory doses of iprodione and a fungicide-free control in the mycelial area growth of *Fusarium proliferatum* tdTom transformant isolate FP-A7R8. Results at 72 hpi, significant stimulation observed. Parameters that model the curve are showed: maximum stimulation dose (M), no observed adverse effect level NOAEL (N) and the effective concentration at which the growth is inhibited 50% compared to the control EC_{50} (E).

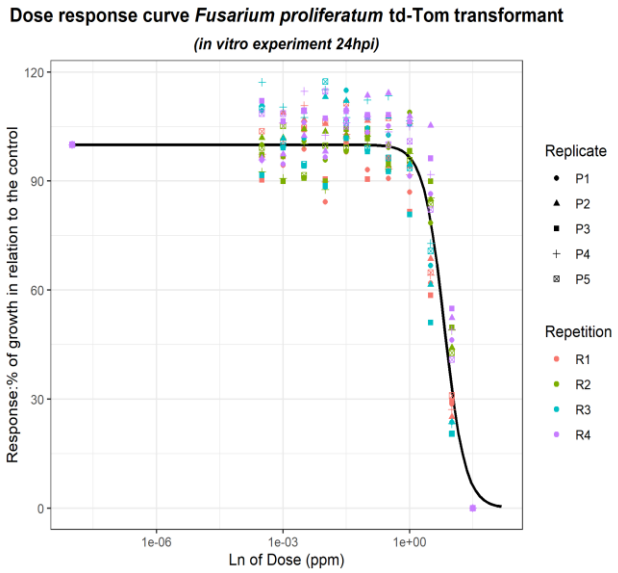

Figure 20. Dose-response curve showing the effect of 11 subinhibitory doses of iprodione and a fungicide-free control in the mycelial area growth of *Fusarium proliferatum* tdTom transformant isolate FP-A7R8. Results at 24 hpi. No hormesis effect was found at this time point.

Experiment performed over cellophane sheets

Fusarium proliferatum wild type demonstrated a significant stimulation at 24, 48, and 72 hpi in mycelial growth area over cellophane sheets. The stimulation at the MSD was 22.83% greater than the control at 24 hours, 28.12% at 48 hpi, and 22.66% at 72 hpi. The MSDs were estimated to be 0.16 ppm, 0.19 ppm, and 0.55 ppm, respectively. Beta, $EC_{50,}$ and NOAEL were calculated at each time (Table 9). Biphasic dose-response curves were modeled and showed clear stimulation peaks at the MSD (Figure 21, Figure 22 and Figure 23).

Table 9. Dose response parameters that describe the effect of subinhibitory doses of iprodione on the mycelial growth area of *F. proliferatum* wild type isolate FP-A7WT

growing over cellophane sheets at 24, 48 and 72 hours post-inoculation. Analysis performed after 3 repetitions with 5 replicates per treatment.

Parameters	24 HPI			48 HPI			72 HPI		
	Value (ppm)	Lower limit (2.5%)	Upper limit (97.5%)	Value (ppm)	Lower limit (2.5%)	Upper limit (97.5%)	Value (ppm)	Lower limit (2.5%)	Upper limit (97.5%)
β	1.15	1.10	1.19	1.18	1.12	1.23	1.28	1.17	1.39
EC_{50}	202.08	-82.78	486.94	97.24	-16.75	211.23	39.22	7.78	70.67
γ	1098.42	112.79	2084.06	971.22	167.17	1775.28	166.87	6.83	326.92
NOAEL	1.71	0.93	2.50	1.95	1.12	2.77	2.95	1.68	4.21
MSD	0.16	0.06	0.27	0.19	0.08	0.31	0.55	0.21	0.90
Stimulation at the MSD (%)	22.83			28.12			22.66		

β= slope at the EC_{50} dose; EC_{50}= effective concentration at which the growth is inhibited 50% compared to the control; γ= rate of increase at small doses; NOAEL= No observed adverse effect level; MSD= Maximum stimulation dose.

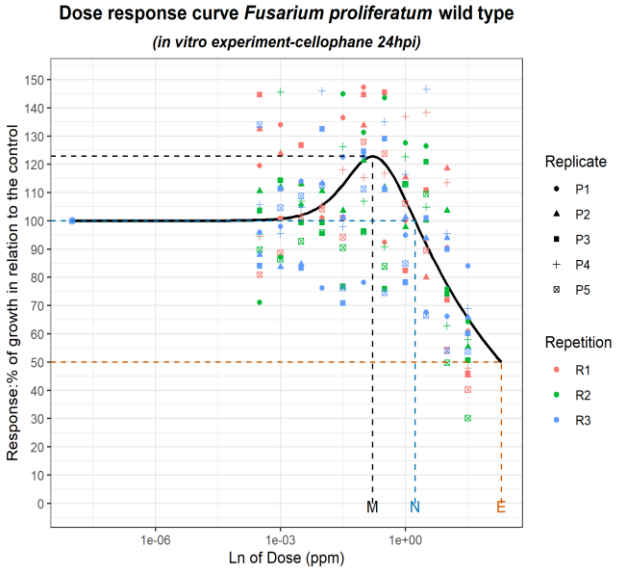

Figure 21. Dose-response curve showing the effect of 11 subinhibitory doses of iprodione and a fungicide-free control in the mycelial area growth of *F. proliferatum* wild type isolate FP-A7WT growing over cellophane sheets. Results at 24 hpi. Parameters that model the curve are showed: maximum stimulation dose (M), no observed adverse effect level NOAEL (N), and the effective concentration at which the growth is inhibited 50% compared to the control EC_{50} (E).

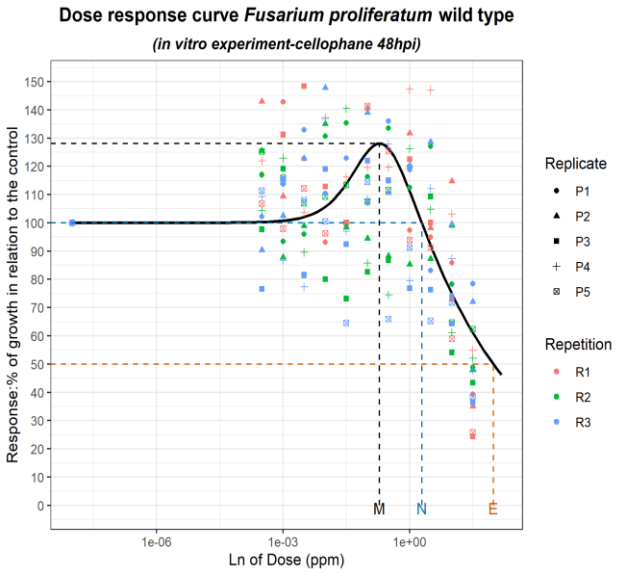

Figure 22. Dose-response curve showing the effect of 11 subinhibitory doses of iprodione and a fungicide-free control in the mycelial area growth of *F. proliferatum* wild type isolate FP-A7WT growing over cellophane sheets. Results at 48 hpi. Parameters that model the curve are showed: maximum stimulation dose (M), no observed adverse effect level NOAEL (N), and the effective concentration at which the growth is inhibited 50% compared to the control EC_{50} (E).

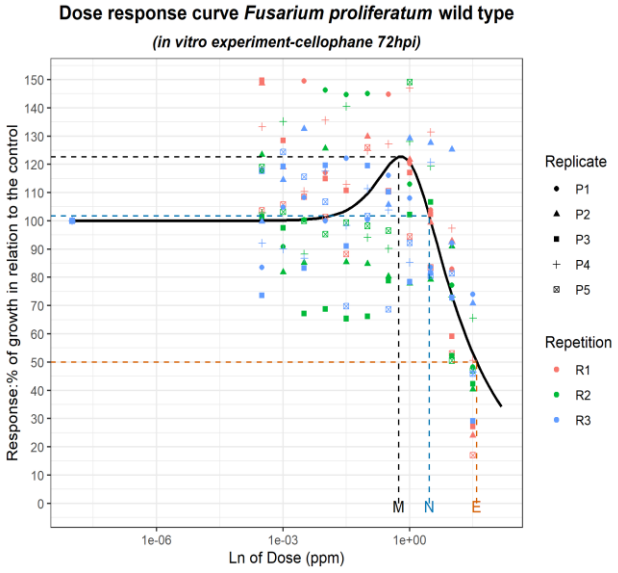

Figure 23. Dose-response curve showing the effect of 11 subinhibitory doses of iprodione and a fungicide-free control in *F. proliferatum* wild type isolate FP-A7WT growing over cellophane sheets. Results at 72 hpi. Parameters that model the curve are showed: maximum stimulation dose (M), no observed adverse effect level NOAEL (N),

and the effective concentration at which the growth is inhibited 50% compared to the control EC_{50} (E).

Analysis using the 'drc' R package

Hormetic effects were identified using two models, Brain-Cousens (BC.5) and Cedergreen-Ritz-Streibing (CRS.5a), in most of the datasets tested. *Fusarium oxysporum* wild type isolate A1WT showed hormetic responses at 24, 48, and 72 hpi with both models in the experiment on SNA media. The 'lack of fit test' showed that both models fitted the data with *P*-values > 0.05 (non-significant *P*-values show a fit of the model). The EC_{50} and the standard error was calculated for each model. At 24hpi, the EC_{50} calculated with the Brain-Cousens model was 6.07 ppm and 5.30 ppm with the Cedergreen-Ritz-Streibing model (Table 10).

Fusarium oxysporum tdTom transformant isolate A1R1-4 showed hormetic responses at 24, 48, and 72 hpi using the BC.5 model, the EC_{50} values calculated were 6.92 ppm, 5.52 ppm, and 5.13 ppm, respectively. The CRS.5a model did not found hormesis at 24 hpi. The EC_{50} values at 48 and 72 hpi were 5.37 ppm and 5.08 ppm (Table 10). The GFP transformant showed significant hormetic responses at 24 and 48 hpi using the Brain-Cousens model, and only at 48 hpi using the Cedergreen-Ritz-Streibing model. No hormesis was found at 72 hpi with any of the models.

Fusarium proliferatum wild type isolate A7WT hormetic response was tested with both models, "f" parameters were positive in both cases, and the p-values of the "lack of fit test" were not significant. The EC_{50} value calculated using the Brain-Cousens model was 5.50 ppm at 24 hpi and 4.6 ppm at 48 and 72 hpi. Using the Cedergreen-Ritz-

Streibing model, the EC_{50} values were similar: 5.59 ppm at 24hpi, and 4.6 ppm at 48 and 72hpi (Table 10).

Fusarium proliferatum tdTom transformant isolate A7R8 showed significant hormetic stimulation at 24 hpi only with the Cedergreen-Ritz-Streibing model. The EC_{50} calculated was 8.53 ppm. Both models confirmed hormetic responses after 48 and 72 hpi and fitted the dataset (*P*-value > 0.05). The EC_{50} values estimated using both models were similar (Table 9). GFP transformant isolate A7G32 did not show hormetic stimulation at 24 hpi with any of the models. After 48 and 72 hpi, both the Brain-Cousens and the Cedergreen-Ritz-Streibing models fitted the dataset. EC_{50} values calculated with both models were similar (Table 10).

Table 10. Dose-response analysis using two hormetic models: Brain-Cousens model (BC.5) and Cedergreen-Ritz-Streibig model (CRS.5) using the functions of the "drc" R package. Analysis performed with *F. oxysporum* and *F. proliferatum* wild type and transformant isolates growing *in vitro* conditions at 24, 48, and 72 hpi. EC_{50} values and the corresponding standard error were calculated only if the models proved the hormetic response. The fit of the models to the respective datasets was analyzed using the function modelFit; non-significant *P*-values (> 0.05) represent a correct fit of the model.

Isolate	HPI	Brain-Cousens model (BC.5)		Cedergreen-Ritz-Streibig model (CRS.5)		Lack of fit test (p value)	
		EC_{50}	Standard error	EC_{50}	Standard error	BC.5	CRS.5
A1WT	24	6.07	1.25	5.30	0.54	0.19	0.22
	48	3.73	0.17	3.77	0.17	0.07	0.12
	72	3.58	0.14	3.62	0.14	0.08	0.15
A1R1-4	24	6.92	1.04	NA	NA	0.30	NA
	48	5.52	0.29	5.37	0.22	0.84	0.69
	72	5.13	0.21	5.08	0.19	0.98	0.98
A1G4_2	24	7.21	0.42	NA	NA	0.09	NA
	48	5.54	0.25	5.53	0.24	0.68	0.67
	72	NA					

A7WT	24	5.50	0.35	5.59	0.51	0.60	0.46
	48	4.64	0.29	4.64	0.28	0.63	0.61
	72	4.61	0.23	4.62	0.23	0.73	0.66
A7R8	24	NA	NA	8.53	0.93	NA	0.28
	48	5.89	0.50	5.62	0.31	0.73	0.61
	72	5.83	0.46	5.53	0.29	0.57	0.31
A7G32	24	NA					
	48	4.70	0.32	4.62	0.27	0.78	0.68
	72	4.64	0.27	4.60	0.24	0.86	0.79

EC_{50}= effective concentration at which the growth is inhibited 50% compared to the control, NA= not applicable, the model analyzed did not found a hormetic effect.

DISCUSSION

Fusarium oxysporum and *F. proliferatum* growing exposed to subinhibitory doses of iprodione displayed a significant hormetic stimulation in the mycelial growth area in vitro. The stimulation of both pathogens was moderate, showing less than 10% stimulation on average at MSD doses on SNA medium. Average growth stimulation on cellophane sheets at the MSD increased to 15% in *F. oxysporum* and over 20% in *F. proliferatum*. According to Calabrese and Baldwin (1997), hormetic stimulatory effects range from 30% to 60% greater than the control (Calabrese and Baldwin 1997a). However, a recent study analyzed around 70,000 stimulatory responses on animals, plants, and microbes, in vivo and in vitro, and demonstrated that the maximum hormetic stimulation response (MHSR) increases with the number of doses below the control analyzed. Their compilation of studies of hormetic effects on microbes showed that the average of the MHSR ranges from 24%, when analyzing one dose below the control, to 65%, when analyzing 6 doses below the control (Calabrese et al. 2019).

In my study, which analyzed more than 6 doses below the control, the stimulatory responses observed on *F. oxysporum* and *F. proliferatum* wild type at 24 hpi reached up to 40% and 30%, respectively. However, because of the high variability between repetitions, the average stimulations at the MSD were 6.87% and 8.21%. This change in the size of the MSD because of the variability of experimental factors is a common experimental error observed in studies of hormetic responses (Calabrese et al. 2019). Furthermore, several studies on plant pathogens have shown moderate hormetic responses (stimulation between 10% to 25%) in vitro and an increase of the stimulation effect in vivo conditions (Flores 2010; Garzón et al. 2011; Pradhan et al. 2017a; Pradhan et al. 2017b; Pradhan et al. 2019; Zhang et al. 2019).

Hormetic responses are characterized by having less than a 10-fold difference between the NOAEL and MSD (Agathokleous et al. 2018; Calabrese and Blain 2011). The hormetic responses observed on *Fusarium oxysporum* wild type and transformant isolates fulfilled this hormetic quantitative characteristic since the MSDs were less than 2-fold different from the NOAEL (i.e., *F. oxysporum* wild type MSD= 0.74 ppm and NOAEL=1.57 ppm). However, *Fusarium oxysporum* wild type growing over cellophane showed a 7-fold difference between the MSD and the NOAEL. Similarly, in all *F. proliferatum* isolates, the NOAEL was 2-fold larger than the MSD. However, in the experiment using cellophane sheets, the NOAEL was 10-fold larger than the MSD at 24 hpi and 48 hpi and 5-fold at 72 hpi.

Fusarium oxysporum transformant isolates behaved similar to the wild type, GFP and tdTom transformant isolates had significant but moderate hormetic stimulatory responses at 24 and 48 hpi. In contrast, *F. proliferatum* transformants demonstrated

different responses to the subinhibitory doses of iprodione than the wild type. While the wild type had significant stimulatory responses at 24, 48, and 72 hpi, the GFP transformant isolate showed hormetic stimulation only at 48 hpi and the tdTom transformant, both at 48 and 72 hpi. However, the maximum stimulation on *F. proliferatum* transformants was not greater than 5% in any of the cases. Phenotypic differences between wild type and transformant isolates can be expected. For example, *F. verticillioides* transformed to express the GFP protein showed decreased growth compared to the wild type when growing at a pH of 4 and 5.5 (Wu et al. 2016). The present study noticed that GFP transformant isolates of both *Fusarium* species produced smaller colonies than the wild type. Therefore, it is possible that factors involved in growth were affected by the transformation. Hence, hormetic responses were not significantly demonstrated in these transformants. However, the difference in the hormetic responses between wild type and transformant isolates of *F. proliferatum* might just be the result of variability between experimental repetitions rather than genetic changes. Further assays are needed to examine these alternative hypotheses.

In the experiment performed over cellophane sheets, *Fusarium oxysporum* showed a maximum stimulation response greater than 10% at the MSD at 24 hpi and did not show significant hormetic responses at 48 and 72 hpi. Meanwhile, *F. proliferatum* had growth stimulations greater than 20% at each of the time points of the assay, showing the greatest average stimulation overall at 48 hpi. Maximum stimulation responses on the assay without cellophane sheets were observed at 24 hpi and decreased after 48 and 72 hpi, consistent with an adaptive response.

Hormetic responses have been previously described on the causal agent of sudden death syndrome in soybean, *Fusarium virguliforme*. A concentration of 1 µg/ml of the fungicide fluopyram increased the mycelial growth of 29 isolates. Moreover, the authors demonstrated that the Brain-Cousens model fitted the data better than the log-logistic model using the R package "drc". The calculated EC_{50} values ranged from 3.79 to 9.34 µg/ml (Wang et al. 2017). In another study, members of the Fusarium head blight complex, *F. avenaceum* and *F. poae*, showed increased mycelial growth, measured as dry weight, when treated with low concentrations of tebuconazole, metconazole, prothioconazole, and prochloraz. (Tini et al. 2020). Furthermore, several studies have reported the increase of mycotoxin production on *Fusarium* species under the effect of low doses of fungicides (Audenaert et al. 2010; Cendoya et al. 2020; D'mello et al. 1998; Kulik et al. 2012; Magan et al. 2002; Marín et al. 2013; Matthies et al. 1999), which will be further discussed in Chapter V.

The study of modest hormetic responses is challenging because the effect can be masked by background noise produced by biological and technical variation and changes in environmental conditions between experiments (Calabrese 2004). In order to obtain reproducible hormetic responses, especially in fungicide hormesis, several experimental factors need to be taken into account, for example, the number of doses below the NOAEL to be analyzed, adequate time to measure the hormetic response, type of growth media used, age of the inoculum, proper mixing of fungicide dilutions (Garzon and Flores 2013; Pradhan et al. 2017a). Also, it is important to control environmental factors like temperature, light, and humidity. Although the present study followed these suggestions, variability was still encountered. One of the main causes of variation might

be changes in temperature and relative humidity inside the growth chamber. Relative humidity inside the growth chamber measured with a digital hygrometer varied from 60% to 30% in a day (data not showed). Fungal growth can be affected by changes in relative humidity, increased rate of growth has been correlated with higher humidity rates (Alam et al. 1996). Nonetheless, relative humidity of the air might not affect the growth of the fungi inside petri dishes as long as the moisture of the media is appropriate (Pasanen et al. 1991). Further studies will be necessary to test if the relative humidity of the growth chamber affects the fungicide hormetic responses or not, considering that environmental factors will affect fungal growth and disease development in the field. Moreover, to avoid experimental error, increasing the number of repeats and replicates is important to obtain statistically significant data.

Fungicide hormesis was corroborated in *F. oxysporum* and *F. proliferatum* by two hormetic models, Brain-Cousens and Cedergreen-Ritz-Streibing in most of the cases. Both models are widely accepted and used in studies testing hormetic responses; however, they have limitations. Since the Brain-Cousens equation fails to confirm hormetic effects when the value of the slope (b) is lower than 1, Cedergreen et al. (2005) modified the equation to solve this drawback. Moreover, Cedergreen model seems to be more flexible and it describes better different hormetic responses. However, it has been reported that this model fails when drops in the curve precede the hormetic response (Belz and Piepho 2012). Reparameterization using both models allowed not only to prove hormetic effects but to estimate hormetic parameters defining the effect such as NOAEL, MSD, and EC_{50} (Belz and Piepho 2012; Schabenberger et al. 1999).

Despite the advantages and disadvantages encountered when analyzing different sets of data using these models, the use of both of them will always offer a more powerful conclusion (Belz and Piepho 2012). In my datasets, the Cedergreen-Ritz-Streibig model failed to prove a hormetic response by *F. oxysporum* tdTom and GFP transformants at 24 hpi. However, the Brain-Cousens model confirmed the hormetic effect using our custom script and the "BC.5" function of the R package "drc".

The R package "drc" allowed to analyze of hormetic responses, to calculate the EC_{50} value and to determine the proper fit of the models to the data (Ritz et al. 2016). However, this package does not estimate the previously mentioned hormetic parameters (NOAL, MSD and EC_{50}). In contrast, the custom script used in our study allows the estimation of hormetic parameters by using the Brain-Cousens model reparameterization (Brain and Cousens 1989; Flores 2010; Flores and Garzon 2013; Schabenberger et al. 1999).

Few differences between the analysis with the R package "drc" and the custom script were observed. The "drc" package allowed to prove a hormetic effect on *F. oxysporum* td-Tom transformant at 72 hpi while my script did not. Similar results were observed with the *F. proliferatum* GFP transformant. Contrarily, my script found a hormetic response at 72 hpi on *F. oxysporum* GFP transformant not found by the "drc" package. These differences might appear because our custom script uses fixed values, provided by the users from data observations, as a starting point while the 'BC.5' function for the Brain-Cousens equation of the R package "drc" does not use fixed values as a starting point.

In conclusion, hormetic responses were observed for both *F. oxysporum* and *F. proliferatum,* wild type and transformant isolates, in vitro. These observations were confirmed using two different statistical approaches and two mathematical models.

CHAPTER IV

EFFECT OF SUBINHIBITORY DOSES OF IPRODIONE ON *FUSARIUM* SPP. GROWING IN VIVO CONDITIONS

INTRODUCTION

Subinhibitory doses of fungicides trigger stronger responses when plant pathogens grow in planta. Garzon et al. (2011) showed that *Pythium aphanidermatum* (Edson) Fitzp. isolates grown at low doses of mefenoxam caused more severe rates of damping-off in geranium seedlings. The percentage of disease severity increase on plants reached up to 61% compared to the non-amended treatment (Garzón et al. 2011).

Similarly, *Sclerotinia sclerotiorum* (Lib.) de Bary previously grown on dimethachlon amended media, showed increased virulence stimulation (42%-59.8% increase) when inoculated on detached oilseed leaves. In the case of mycelia previously grown on fungicide-free media, when inoculated on detached oilseed rape leaves and leaves of potted plants sprayed with subinhibitory doses of dimethachlon, virulence stimulation was observed with 57% and 62.99% more disease than the control (Zhou et al. 2014). Furthermore, other studies have demonstrated that *S. sclerotiorum* growing on rapeseed leaves had increased rates of virulence when in contact with subinhibitory doses of different fungicides such as carbendazim (Di et al. 2015), trifloxystrobin (Di et al. 2016a), flusilazole (Lu et al. 2018), prochloraz, dimethaclone, and mixtures of the last

two (Zhang et al. 2019). Low doses of carbendazim, iprodione, and mixtures of both chemicals caused increased virulence in carbendazim-resistant *Botrytis cinerea* Pers. isolates growing on detached cucumber leaves. The maximum stimulation for each fungicide when applied alone was 16.7% and 18.7%, respectively. Mixtures of each fungicide at their highest doses did not cause stimulatory effects, but at lower doses (10 µg/ml of carbendazim and 0.0005 µg/ ml of iprodione), virulence stimulation was higher than the stimulation when each fungicide was applied alone (Cong et al. 2019b). A study in *Fusarium graminearum* showed that it produced higher concentrations of the mycotoxin deoxynivalenol (DON) when growing in vitro and after being inoculated on wheat kernels treated with sublethal doses of prothioconazole (Audenaert et al. 2010).

Onions (*Allium cepa* L.) are economically important crops worldwide. The United States is the third-largest onion producer, after China and India (FAOSTAT 2018), with 132,400 acres planted and a total production of 69.9 million cwt (approx. 3.9 million US ton) in 2019 (USDA 2020a). Onion production is affected by several *Fusarium* species, including *F. oxysporum, F. verticillioides, F. subglutinans, F. proliferatum, F. solani, F. equisetti* and *F. tricinctum*, which cause damping-off of onions. *Fusarium oxysporum* f. sp. *cepae* (FOC) causes Fusarium basal rot, while *F. proliferatum* causes onion bulb rot (Schwartz and Mohan 2008).

Fusarium basal rot causes significant losses in the field and during storage. The pathogen survives in the soil by forming long-term resting structures (chlamydospores) and on host and non-host plant debris in the form of macroconidia, microconidia, or mycelium (Leoni et al. 2013). Infection is favored by wet conditions and temperatures between 25 ^{o}C and 28 ^{o}C. *Fusarium oxysporum* f. sp. *cepae* infection of onion starts at

the roots and basal plate (Cramer 2000). The first symptoms above the ground include curly leaf tips, yellowing, and necrosis of the leaves (Conn et al. 2012). The onion basal plate shows a characteristic brown discoloration, watery tissue, and necrosis; roots rot and separate from the basal plate, and white mycelia is observed on the stem plate (Parthasarathy et al. 2016).

Fusarium proliferatum is the causal agent of onion bulb rot. Diseased mature bulbs show yellow, watery lesions that end in necrosis of the tissue. White onion cultivars display a characteristic salmon-pink discoloration in the bulb outer dry scales. The infection does not reach the basal plate, which distinguishes it from Fusarium basal rot (Schwartz and Mohan 2008). This pathogen does not produce chlamydospores but can survive saprophytically in the soil for long periods of time (Kalman et al. 2020).

Fusarium spp. can colonize and remain in onion bulbs without causing detectable signs or symptoms of infection. Thus, severe infections can occur during storage, producing important economic losses (Sintayehu et al. 2011). Moreover, *F. oxysporum* and *F. proliferatum* are toxigenic and can produce several mycotoxins such as beauvericin, enniatins, fumonisin, moniliformin, fusaric acid and fusarins, though *F. oxysporum* rarely produces the last. Additionally, *F. proliferatum* can produce fusaproliferin. (Munkvold 2017; Stankovic et al. 2007).

Management strategies to control Fusarium basal rot rely on resistant onion varieties, 4-year crop rotations using non-susceptible crops, soil solarization, biological control, and fungicide application (Conn et al. 2012; Cramer 2000; Leoni et al. 2013). Several fungicides have been reported to control the disease such as iprodione (Abd-

Elrazik et al. 1990), hexaconazole, mancozed, and carbendazim (Futane et al. 2018; Saravanakumari et al. 2019) as well as seed treatments with tebuconazole, prochloraz, and thiram (Özer and Köycü 1998).

This project aims to characterize the effect of subinhibitory doses of iprodione on the longitudinal growth of *F. oxysporum* and *F. proliferatum* growing on onion epidermis.

MATERIAL AND METHODS

Fusarium spp. inoculum and iprodione doses preparation

Fusarium oxysporum and *F. proliferatum* isolates transformed to express the tdTomato protein (td-Tom) (Gard and Arias, unpublished data) were used in this experiment (FO-A1R1-4 and FP-A7R8, respectively).

Twelve experimental treatments were used, which consisted of eleven doses of iprodione, including 2 suppressive and 9 subinhibitory doses, and a fungicide-free control (water). Iprodione solutions were prepared following the protocol described in Chapter III.

Dose response of *Fusarium* spp. to subinhibitory doses of iprodione in vivo

The endpoint for this experiment was the longitudinal mycelial growth of *Fusarium* spp. on onion epidermis. White onion bulbs (*Allium cepa*) were cut in quarters. The external scales were separated and disinfected with 95% ethanol for 1 min, followed by 10% bleach for 15 min, and finally rinsed at least 6 times with autoclaved reverse osmosis (RO) water.

Working with each iprodione dose at the time, three disinfected scales were immersed for 5 minutes in the fungicide solution in sterile 250 ml beakers. Then the adaxial epidermis of each scale was peeled off and placed on square petri dishes containing 15 ml of SNA media amended with the corresponding fungicide dose (Figure 24). Each onion skin was wounded using a sterile needle and inoculated with a 5 mm plug of actively growing mycelium of a 5 days-old culture of each *Fusarium* spp. isolate. Each plug was placed directly over the wound. After inoculation, petri dishes were sealed with parafilm and incubated in a growth chamber (Percival Scientific, Perry, IA) at 22 (± 2) ^{o}C in the dark. The experiment was conducted with three replicates per treatment (3-onion inoculated epidermis per petri dish) and repeated 3 times over time.

The longitudinal mycelial growth over the onion skin was monitored after 24, 48 and 72 hpi using a Nikon Eclipse E800 epifluorescent microscope with a G-2E/C TRITC filter set (Nikon Inc., Tokyo, Japan). Each day the furthermost border of the active hyphae was marked using a red marker. The distance to the marks was measured with a digital caliper (VWR) using the border of the agar plug as the reference point to start the measurements. Additionally, monochromatic grayscale images were taken with a QImaging Retiga 2000R camera (Quantitative Imaging Corp., Surrey, BC, Canada) using G-2E/C TRITC and GFP-3535B epifluorescence filters at 4X objective. The monochromatic grayscale images were merged and digitally colored using the ImageJ version 1.52a software (Abràmoff et al. 2004).

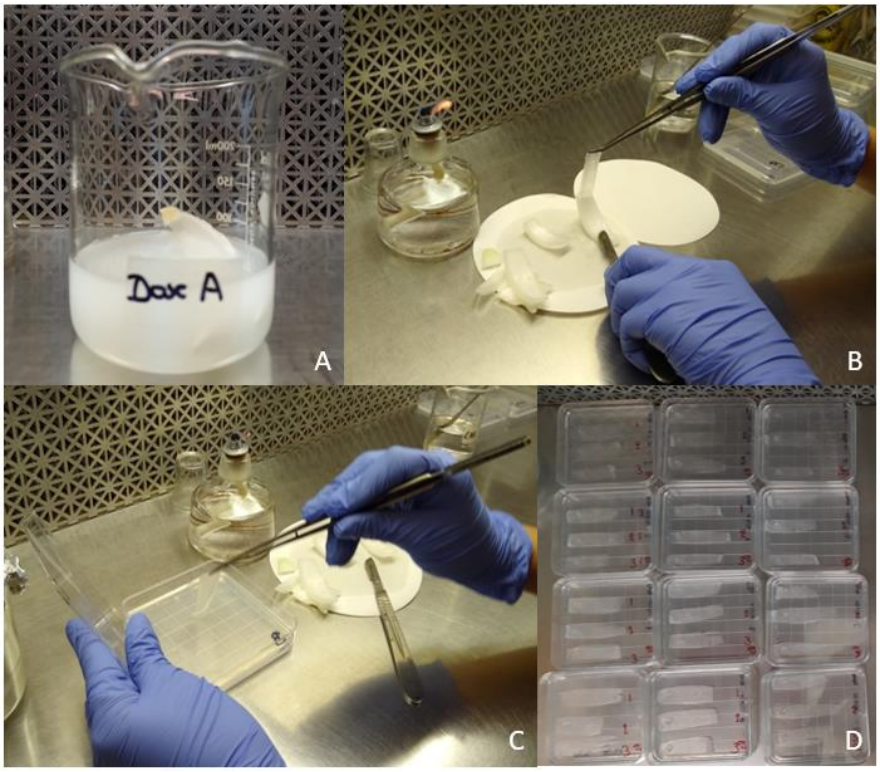

Figure 24. Methodology for studying the response of *Fusarium* spp. to subinhibitory doses of iprodione when growing on onion slides. (A) Onion scales were immersed 5 minutes in their respective fungicide dose. (B) Adaxial epidermis of onion scale was peeled and (C) placed over square petri dishes that contained SNA media amended with the corresponding fungicide dose. (D) Three onion scales were inoculated per dose with a 5 mm agar plug containing 5 days old active mycelium.

Data analysis

Data analysis and hormetic curve modeling were performed following the methods described in Chapter III. The input data was the mycelial longitudinal growth transformed into percentages in relation to the average growth of the three fungicide-free control replicates (Flores and Garzon 2013).

RESULTS

Dose response of *Fusarium oxysporum* to iprodione growing on onion scales

Fusarium oxysporum td-Tom transformant (FO-A1R1-4) growing on onion epidermis treated with 11 subinhibitory doses of iprodione and fungicide-free control showed a significant growth stimulation after 48 and 72 hpi. There was not a hormetic effect after 24 hpi, so the EC_{50} value was estimated using a log-logistic model (EC_{50}= 14.04 ppm) (Figure 25).

At 48 hpi, the isolate showed mycelial longitudinal growth 24.66% greater than the fungicide-free control (Figure 26). The EC_{50}, NOAEL, and MSD were calculated to be 16.68 ppm, 1.9 ppm, and 0.41 ppm respectively. The longitudinal mycelial growth stimulation at the MSD (0.61 ppm) decreased after 72 hpi to 19.6% (Figure 27) and the EC_{50} and NOAEL were estimated to be 12.45 ppm and 2.16 ppm, respectively (Table 11).

Table 11. Dose response parameters that describe the effect of subinhibitory doses of iprodione on the mycelial longitudinal growth of *Fusarium oxysporum* td-Tom transformant (FO-A1R1-4) growing epidermis after 24, 48, and 72 hours post inoculation. Analysis performed after 3 repetitions with 3 replicates per treatment.

Parameters	24 HPI			48 HPI			72 HPI		
	Value (ppm)	**Lower limit (2.5%)**	**Upper limit (97.5%)**	**Value (ppm)**	**Lower limit (2.5%)**	**Upper limit (97.5%)**	**Value (ppm)**	**Lower limit (2.5%)**	**Upper limit (97.5%)**
β	1.33	0.61	2.05	1.32	1.21	1.44	1.42	1.27	1.56
EC_{50}	14.04	8.21	19.87	16.68	6.21	27.15	12.45	7.32	17.57
γ	NA	NA	NA	247.31	15.15	479.46	109.89	9.30	210.49
NOAEL	NA	NA	NA	1.90	1.08	2.72	2.16	1.33	2.99
MSD	NA	NA	NA	0.41	0.16	0.65	0.61	0.29	0.92
Stimulation at the MSD (%)	NA			24.66			19.60		

Beta= slope at the EC_{50} dose; EC_{50}= effective concentration at which the growth is inhibited 50% compared to the control Gamma= rate of increase at small doses; NOAEL= No observed adverse effect level; MSD= Maximum stimulation dose.

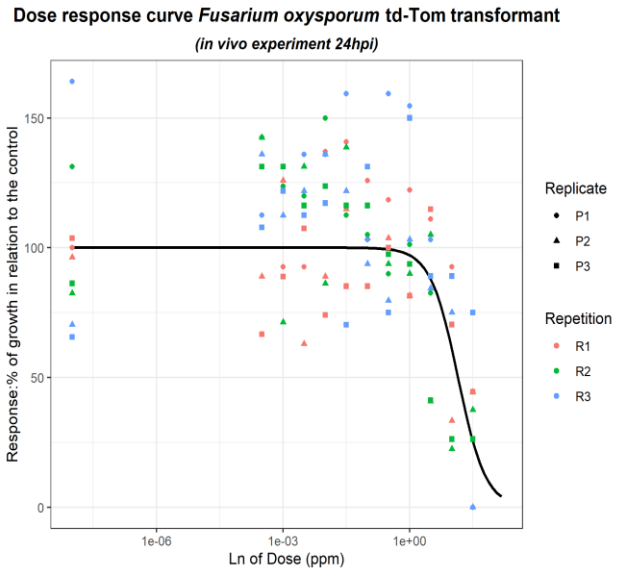

Figure 25. Dose-response curve showing the effect of 11 subinhibitory doses of iprodione and a fungicide-free control in the mycelial longitudinal growth of *Fusarium oxysporum* td-Tom transformant (FO-A1R1-4) on onion epidermis after 24 hpi. No hormetic effect was found at this time point.

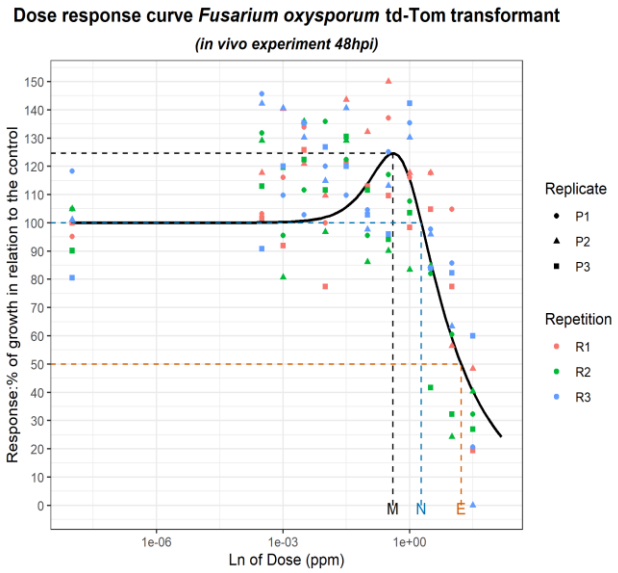

Figure 26. Dose-response curve showing the effect of 11 subinhibitory doses of iprodione and a fungicide-free control in the mycelial longitudinal growth of *Fusarium oxysporum* td-Tom transformant (FO-A1R1-4) on onion epidermis after 48 hpi. Significant stimulation was observed (24.66%). Parameters shown in the modeled curve include maximum stimulation dose (M), no observed adverse effect level NOAEL (N), and the effective concentration at which the growth is inhibited 50% compared to the control, EC_{50} (E).

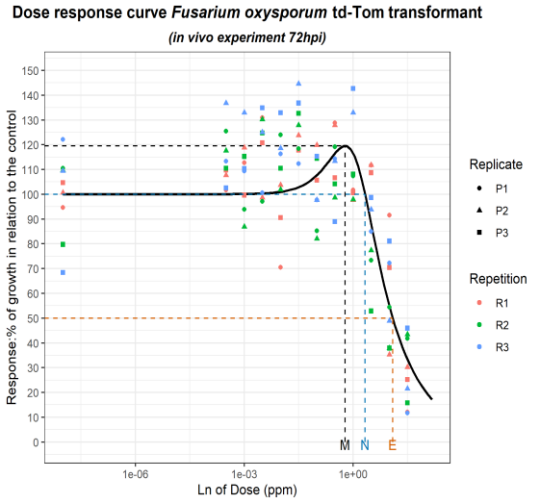

Figure 27. Dose-response curve showing the effect of 11 subinhibitory doses of iprodione and a fungicide-free control in the mycelial longitudinal growth of *Fusarium oxysporum* td-Tom transformant (FO-A1R1-4) on onion epidermis after 72 hpi. Significant stimulation was observed (19.6%). Parameters that model the curve are shown: maximum stimulation dose (M), no observed adverse effect level NOAEL (N), and the effective concentration at which the growth is inhibited 50% compared to the control, EC_{50} (E).

Dose response of *Fusarium proliferatum* to iprodione growing on onion scales

Fusarium proliferatum td-Tom transformant (FP-A7R8) demonstrated a significant hormetic stimulation only at 24 hpi. The maximum stimulation of mycelial longitudinal growth was 23.62% greater than the control at the MSD (0.14 ppm). The EC_{50} was 8.81 ppm, NOAEL 0.71 ppm, and β was 1.28 ppm (Table 12). A dose response curve showing the maximum stimulation peak was modeled with the parameters mentioned before (Figure 28). Mycelial development under the effect of iprodione doses are shown on Figures 6 and Figure 7. No fungal growth was observed at the suppressive dose. At subinhibitory doses (3.162278 ppm, 1 ppm, 0.316228 ppm) and at the MSD (0.1 ppm), an evident difference in growth was observed. Mycelial growth seemed denser on the subinhibitory doses compared to the fungicide-free control, which is more noticeable in the MSD.

At 48 and 72 hpi, a hormetic hypothesis was rejected since γ limits included negative values. EC_{50} values estimated using the log logistic model were 10.47 ppm and 9.15 ppm, respectively (Table 12) and dose response curves were modeled using these parameters (Figure 8 and Figure 9).

Table 12. Dose response parameters that describe the effect of subinhibitory doses of iprodione on the mycelial longitudinal growth of *Fusarium proliferatum* td-Tom transformant (FP-A7R8) growing on onion epidermis after 24, 48, and 72 hours post inoculation. Analysis performed after 3 repetitions with 3 replicates per treatment.

Parameters	24 HPI			48 HPI			72 HPI		
	Value (ppm)	Lower limit (2.5%)	Upper limit (97.5%)	Value (ppm)	Lower limit (2.5%)	Upper limit (97.5%)	Value (ppm)	Lower limit (2.5%)	Upper limit (97.5%)
β	1.28	1.19	1.36	1.00	0.67	1.33	1.00	0.73	1.28
EC_{50}	8.81	3.22	14.39	10.47	7.02	13.93	9.15	6.65	11.65
γ	789.18	33.69	1544.68	NA	NA	NA	NA	NA	NA
NOAEL	0.71	0.38	1.04	NA	NA	NA	NA	NA	NA
MSD	0.14	0.05	0.22	NA	NA	NA	NA	NA	NA
Stimulation at the MSD (%)	23.62			NA			NA		

Beta= slope at the EC_{50} dose; EC_{50}= effective concentration at which the growth is inhibited 50% compared to the control Gamma= rate of increase at small doses; NOAEL= No observed adverse effect level; MSD= Maximum stimulation dose.

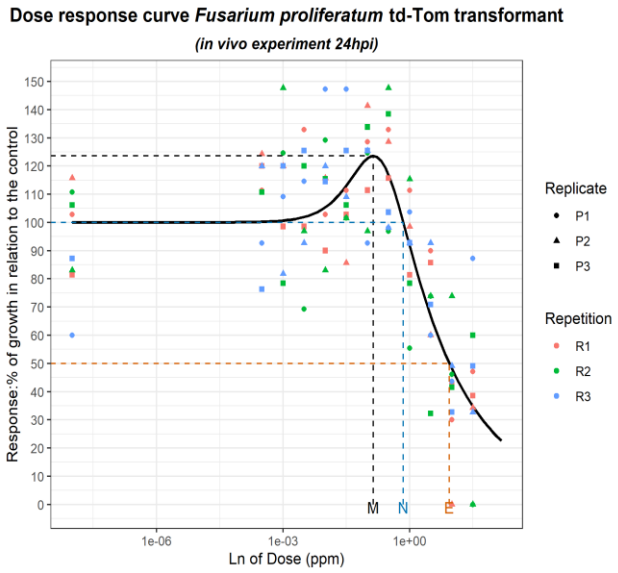

Figure 28. Dose-response curve showing the effect of 11 subinhibitory doses of iprodione and a fungicide-free control in the mycelial longitudinal growth of *Fusarium proliferatum* td-Tom transformant (FP-A7R8) on onion epidermis after 24 hpi. Significant stimulation was observed (23.62%). Parameters that model the curve are shown: maximum stimulation dose (M), no observed adverse effect level NOAEL (N), and the effective concentration at which the growth is inhibited 50% compared to the control, EC_{50} (E).

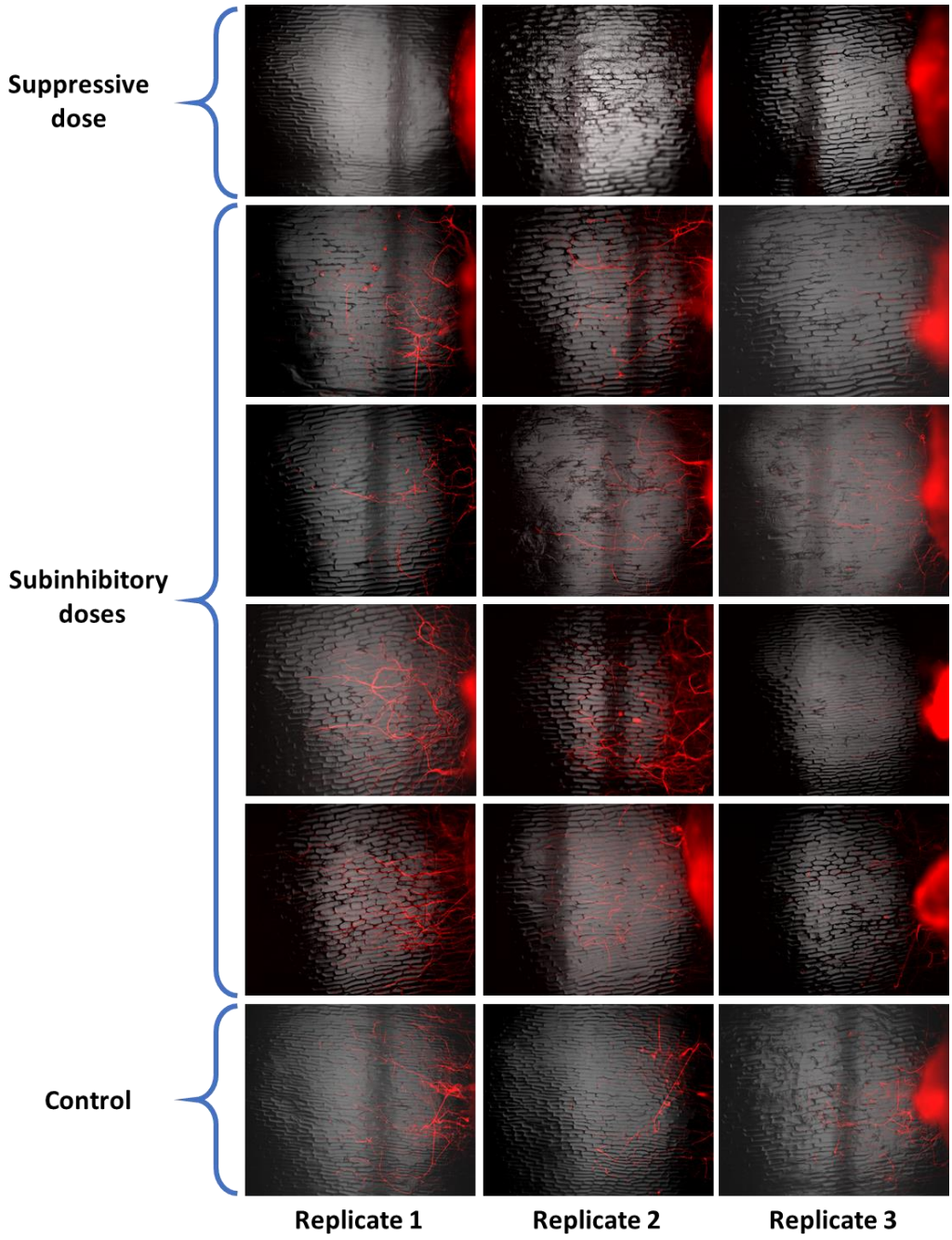

Figure 29. *Fusarium proliferatum* growing on onion epidermis slides treated with iprodione after 24 hpi. Subinhibitory doses showed from top to bottom, 3.162278 ppm, 1 ppm, 0.316228 ppm, and 0.1 ppm. Color composite from GFP-3535B and G-2E/C TRITC epifluorescence filter sets. Direction of the growth from right to left.

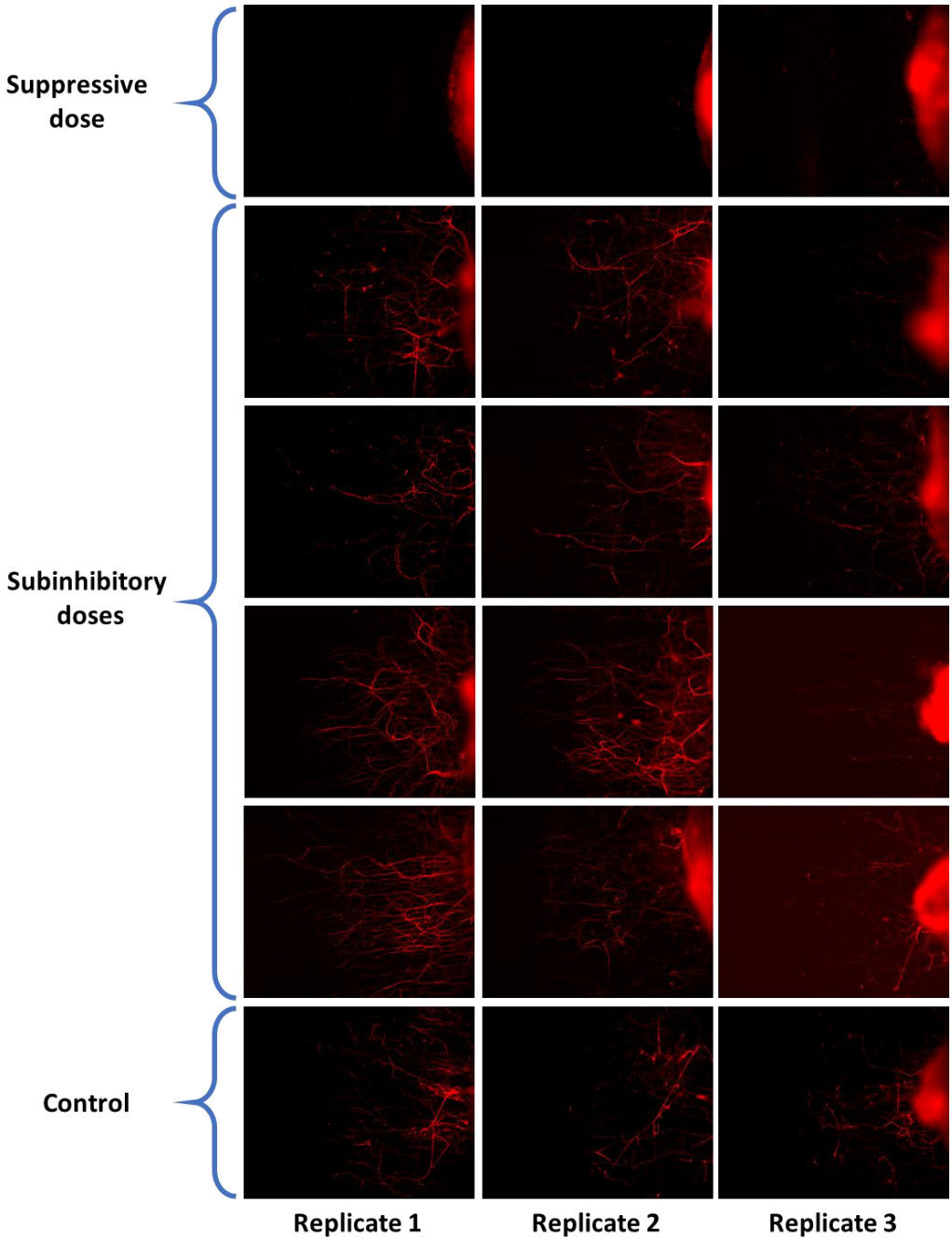

Figure 30. *Fusarium proliferatum* growing on onion epidermis slides treated with iprodione after 24 hpi. Subinhibitory doses showed from top to bottom, 3.162278 ppm, 1 ppm, 0.316228 ppm, and 0.1 ppm. Image was taken with G-2E/C TRITC epifluorescence filter set. Direction of the growth from right to left.

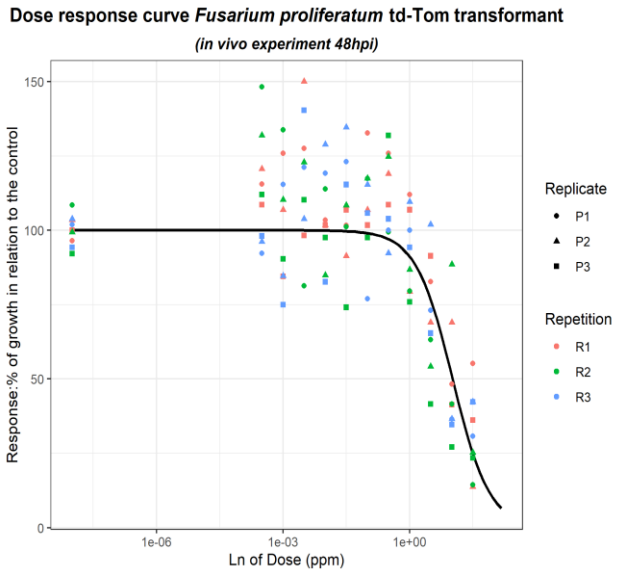

Figure 31. Dose-response curve showing the effect of 11 subinhibitory doses of iprodione and a fungicide-free control in the mycelial longitudinal growth of *Fusarium proliferatum* td-Tom transformant (FP-A7R8) on onion epidermis after 48 hpi. No hormetic effect was found at this time point.

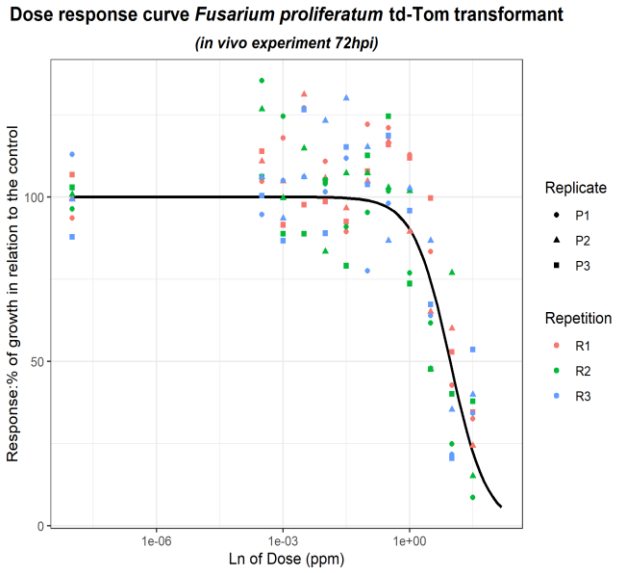

Figure 32. Dose-response curve showing the effect of 11 subinhibitory doses of iprodione and a fungicide-free control in the mycelial longitudinal growth of *Fusarium proliferatum* td-Tom transformant (FP-A7R8) on onion epidermis after 72 hpi. No hormetic effect was found at this time point.

Growth data was also analyzed using the R package "drc" to test the fitness of the hormetic models: Brain-Cousens and Cedergreen-Ritz-Streibig using the functions "BC.5" and "CRS.5" respectively. The *Fusarium oxysporum* isolate showed a positive hormetic stimulation only at 24 hpi. The EC_{50} value calculated with the Brain-Cousens model was 13.84 ppm and the lack of fit test indicated that the model fitted good the data (p-value >0.05) (Table 13). The lack of fit test after 48 and 72 hpi were lower than 0.05, which means that the Brain-Cousens model did not fitted the data. A hormetic hypothesis was not proved using the Cedergreen-Ritz-Streibig model.

The *F. proliferatum* isolate demonstrated a positive hormetic effect after 24, 48 and, 72 hpi when analyzed with the Brain-Cousens model. The lack of fit test resulted in p-values greater than 0.05, representing a good fit of the data to the model. EC_{50} values were calculated to be 8.74 ppm at 24 hpi, 9.23 ppm after 48 hpi, and 7.85 ppm after 72 hpi (Table 13).

Table 13. Dose-response analysis using two hormetic models: Brain-Cousens model (BC.5) and Cedergreen-Ritz-Streibig model (CRS.5) using functions from the "drc" R package. Analysis performed with *F. oxysporum* and *F. proliferatum* td-Tom transformant isolates growing in vivo conditions after 24, 48, and 72 hours post-inoculation. EC_{50} values and the corresponding standard error were calculated only if the models proved a hormetic response. The fit of the dataset to the models was analyzed using the function modelFit, non-significant p-values (> 0.05) represent a good fit of the model.

Isolate	**HPI**	**Brain-Cousens model**		**Cedergreen-Ritz-Streibig model**		**Lack of fit test (p value)**	
		EC_{50}	**Standard error**	**EC_{50}**	**Standard error**	**BC.5**	**CRS.5**
FO-A1R1-4	24	13.84	3.53	NA	NA	0.21	NA
	48	16.96	3.37	10.71	6.67	0.00	0.03
	72	12.36	1.88	NA	NA	0.00	NA
FP-A7R8	24	8.74	1.72	NA	NA	0.15	NA
	48	9.23	1.50	NA	NA	0.11	NA
	72	7.85	1.12	NA	NA	0.09	NA

EC_{50}= effective concentration at which the growth is inhibited 50% compared to the control, NA= not applicable, the model analyzed did not found a hormetic effect.

DISCUSSION

Significant mycelial growth stimulation was observed at subinhibitory doses of iprodione in *Fusarium oxysporum* and *F. proliferatum* td-Tom transformant isolates growing on onion epidermis slides. Hormetic stimulatory responses of both pathogens on plant tissue were higher than the stimulation observed on amended media (Chapter III). These results are in concordance with previous studies that analyzed hormetic effects of fungicides on plant pathogens in vitro and/or in vivo (Cong et al. 2019b; Di et al. 2016a; Di et al. 2015; Garzón et al. 2011; Lu et al. 2018; Pradhan et al. 2017a; Zhang et al. 2019; Zhou et al. 2014).

In vivo, hormetic responses can result in an increase of mycotoxin production. Wheat plants inoculated with *Fusarium graminearum* macroconidia and sprayed with 1/100 dilution of prothioconazole + fluoxastrobin resulted in a significant increase of the mycotoxin DON (> 8 µg/kg) at 48 h after application compared to the control; nonetheless, the same results were observed in vitro. In addition, the study found an increase in hydrogen peroxide production after 4 hours of application of sublethal doses of the fungicides. These findings lead the author to conclude that the accumulation of hydrogen peroxide as a result of exposure to sublethal doses of prothioconazole + fluoxastrobin might be the starting point of a cascade of reactions resulting in DON biosynthesis (Audenaert et al. 2010). Interestingly, recent studies performed in plants have reported the production of reactive chemical species (e.g., ROS) as possible biological mechanisms of hormesis (Agathokleous et al. 2020). Another study reported the increase of fungal biomass and DON production of two chemotypes of *F.*

graminearum (3ADON and 15ADON) inoculated on wheat heads and treated with sublethal doses of propiconazole and tebuconazole in the field. Wheat treated with propiconazole (125 mg/L) showed a higher concentration of DON and fungal biomass (measured as DNA concentration with qPCR). However, this result was found in only one sample from ten analyzed. The author reported that the inconsistent results might have occurred because mycotoxin biosynthesis is affected by several factors in the field (Kulik et al. 2012).

Even though the present study did not analyze the production of mycotoxins on onion tissue, a preliminary experiment demonstrated that the *F. proliferatum* wild type isolate used in this study produced higher amounts of fumonisin B1 on corn treated with subinhibitory doses of iprodione. However, the results were not consistent between repetitions and replicates thus demonstrating they were not statistically significant (Anasi Castillo 2016).

Fungicide application is an important part of integrated pest management programs. Efficient use of pesticides, fertilizers and improved seeds have increased the quality and yield of agricultural crops (Fernandez-Cornejo et al. 2014). According to the USDA National Agricultural Statistics Service, more than $17,000 million were expended on chemicals purchases during 2017 in the USA alone (USDA-NASS 2019).

After application, fungicides can dilute in the environment due to the effect of biotic and abiotic factors (e.g., volatilization, drift, degradation by non-target microorganisms) (Derbalah et al. 2003; Duke 2017). For example, the environmental dissipation of iprodione is mainly controlled by bacteria that degrade the fungicide

initially into 3,5-dichlorophenyl-carboxamide, later on to 3,5-dichlorophenylurea-acetate, and finally into 3,5-dichloroaniline. The latter is one of the main soil and water agricultural contaminants (Campos et al. 2017; Campos et al. 2015; Yang et al. 2018). Additionally, improper application caused by miscalibrated equipment, incorrect timing or frequency of application, reduction of the treatment rate because of cost-saving practices, dilution of fungicides on recirculating systems, among others, represent scenarios where pathogens are at high risk to develop fungicide resistance and/or hormesis, thus becoming a serious problem in agriculture (Brent and Hollomon 2007; Halley et al. 2008; Hofman and Solseng 2004; Pradhan et al. 2017a). Furthermore, subinhibitory doses of fungicides could occur even if the recommended fungicide dosage was applied to the crop. For example, the concentration of azoles (propioconazole and tebuconazole) on wheat heads after 24 hours of spraying ranged from zero to 1.04 and 6.51 mg/kg causing an overproduction of DON by *F. graminearum* (Kulik et al. 2012).

Fusarium oxysporum and *F. proliferatum* are ubiquitous fungi that inhabit soils, host, and non-hots plants (Leslie and Summerell 2008). Because of their cosmopolitan habits, both pathogens are at risk of exposure to subinhibitory doses of fungicides that drift from agricultural fields. Onion production relies on fungicides to control pathogenic fungi in the field and dipping bulbs in fungicide solutions to prevent postharvest damage during storage (Behrani et al. 2015; Cramer 2000; Grinstein et al. 1992). *Fusarium* species have been found every year in onion production fields, with economic losses ranging from >20% to up 50% in highly infested fields (Gutierrez and Cramer 2005; Stivers 1999). Moreover, pathogen infecting bulbs can be unnoticeable until the infection worsens in storage, causing losses up to 30% (Haapalainen et al. 2016; Ko et al. 2002;

Rasiukevičiūtė et al. 2016). Hormetic responses to fungicides can exacerbate these detrimental effects. Our study demonstrated that *F. oxysporum* and *F. proliferatum* could grow over 20% larger than the control under the effect of subinhibitory doses of iprodione on onion tissue. However, it is recommended to perform additional studies of the infection process of *F. oxysporum* and *F. proliferatum* in onion bulbs treated with subinhibitory doses of fungicides compared to a fungicide-free control, under storage conditions to determine how our findings extend to postharvest conditions.

Mycotoxin contamination of onions is another important economic issue and public health risk. The two *Fusarium* species used in this study have been reported to produce different mycotoxins on infected plants (Dissanayake et al. 2009a; Stankovic et al. 2007; Zohri et al. 1992). Moreover, a probable link between subinhibitory doses of fungicides, environmental factors, and enhanced mycotoxin production have been reported in several *Fusarium* species (Audenaert et al. 2010; Cendoya et al. 2020; D'mello et al. 1998; Kulik et al. 2012; Magan et al. 2002; Marín et al. 2013; Matthies et al. 1999). Future studies could examine how growth stimulation of *Fusarium* correlates with mycotoxin production in onion during storage.

CHAPTER V

DIFFERENTIAL GENE EXPRESSION ANALYSIS OF CANDIDATE GENES OF *Fusarium proliferatum* GROWING UNDER SUPPRESSIVE AND SUBINHIBITORY DOSES OF IPRODIONE USING REVERSE TRANSCRIPTASE REAL-TIME PCR (RT-qPCR).

INTRODUCTION

There are two main hypotheses to explain hormetic mechanisms: an overcompensation response to the disruption of homeostasis of an organism (Calabrese 1999, 2001), or a direct stimulatory response that happens when the organism adapts to the stressor and the maximum stimulation is the limit of its biological plasticity (Calabrese and Baldwin 2001, 2002). Both responses seem to be related and regulated by similar molecular mechanisms because they result in the same quantitative hormetic features (Calabrese and Baldwin 2002; Calabrese and Mattson 2011).

Calabrese (2013) described hormetic mechanisms at the molecular level in response to different stressors. The author proposed that there were two main ways stressors could mediate the stimulatory/inhibitory responses characteristic of hormesis: either through receptor-mediated processes or through the interference of cell signaling pathways. The hormetic dose/concentration response could be characterized in three different ways: (1) when both the low dose stimulation and the high dose inhibition phase

are controlled by the same receptor/cell signaling pathway, (2) when the low dose stimulation and high dose inhibition are controlled by two separate mechanisms, and (3) when only the mechanism controlling the low dose stimulation phase is known but the mechanism mediating the high dose inhibition is not.

These mechanisms have been mostly studied in human or other animal cells. However, studies on plants have concluded that the molecular mechanisms behind hormetic responses are very complex and vary according to plant genotype, species, and stressors (Agathokleous et al. 2020). Plants under hormetic effects tend to display mild responses to stressors, which often involve producing reactive oxygen species, hormones, antioxidants, and proteins such as those in the heat shock family (Agathokleous et al. 2019, 2020).

There are few studies that have tried to understand the molecular mechanisms behind fungicide hormesis. Hu et al. (2019) demonstrated that low doses of boscalid increased the mycelial growth and virulence of *S. sclerotiorum* in vitro and in planta. However, no significant differences were found in the expression levels of three virulence-related genes: cutinase (*SsCut*), endopolygalacturonase (*SsPG1*), and acetylhydrolase (*SSOaH1*) (Hu et al. 2019). In another study, sublethal doses of carbendazim (0.02 µg/ml and 0.05 µg/ml) did not produce significant changes in the relative expression of five virulence-related genes in *Botrytis cinerea*: pectin methylesterase (*Bcpme1*), endopolygalactuonase (*Bcpg2*), cutinase (*CutA*), xylanase (*Xyn11A*) and NADPH oxidase gene (*BcnoxA*) (Cong et al. 2019).

The overexpression of genes related to the biosynthesis of mycotoxins has been linked with the presence of sublethal doses of different fungicides and other biotic and abiotic factors in *Fusarium* spp. Propiconazole and tebuconazole caused overexpression of *tri* genes, which are part of the trichothecenes biosynthesis pathways in *F. graminearum* (Kulik et al. 2012). The fumonisin related gene (*FUM1*) was significantly overexpressed in *F. proliferatum* and *F. verticilloides* under the effect of low doses of tebuconazole and water stress (Marín et al. 2013). Popiel et al. (2017) described a stimulation in the expression of trichothecene and zearalenone genes in *F. graminearum* and *F. culmorum* growing at sublethal doses of fungicides. However, the upregulation of mycotoxin biosynthetic genes was also observed at a suppressive dose of carbendazim when the fungicide was applied to mycelia during the stationary growth phase (Popiel et al. 2017).

Mitogen-activated protein kinase (MAPK) cascades contribute to the regulation of cellular responses to different stressors in eukaryotes, including fungi (Hayes et al. 2014). Three MAPKs that have been described in most ascomycetes, including *F. oxysporum* and *F. proliferatum,* are essential for development, stress response, and virulence (Segorbe et al. 2017). MAPK gene homologs to FUS3/KSS1 in yeast mediates hyphal growth, conidiation, spore germination, and virulence responses in *F. proliferatum* (*FPK1*) (Zhao et al. 2011) and in *F. oxysporum* (*FMK1*) (Di Pietro et al. 2001). MAP kinase-related (*MPK1)* genes mediate changes in the cell wall in response to stress (Segorbe et al. 2017). Also, the high osmolarity glycerol gene (*HOG1*) regulates responses to osmotic stress, sensitivity to fungicides (iprodione, fludioxonil), growth, and sporulation in *Fusarium* (Ádám et al. 2008; Nagygyörgy et al. 2011).

Iprodione is a dicarboxamide classified in the FRAC group 2, along with vinclozolin and procymidone. It is widely used in different vegetables, fruits, ornamentals, and turf (Stammler et al. 2019) to control plant pathogens such as *Botrytis* spp., *Monilia* spp., *Sclerotinia* spp., *Alternaria* spp., *Rhizoctonia solani*, among others. Dicarboxamides are considered chemicals with a high risk of developing fungicide resistance, especially in *Botrytis cinerea* (Brent and Hollomon 2007).

Dicarboxamides interfere with the osmotic regulation pathways of the histidine kinase and mitogen-activated cascades. The two-component histidine kinase (*Os1*) is believed to be the target molecule of this group of chemicals. This hypothesis was proposed after finding mutations of this gene in *Botrytis cinerea* isolates with resistance to dicarboxamides (Cui et al. 2002; Oshima et al. 2002).

The objective of this study was to investigate changes in the relative expression of 5 candidate genes related to growth, virulence, and stress responses in *Fusarium proliferatum* under the effect of suppressive and subinhibitory doses of iprodione using RT-qPCR.

MATERIAL AND METHODS

Fusarium proliferatum inoculum and experiment preparation

Fusarium proliferatum wild type isolate FP-A7WT was used in this experiment because it showed the higher mycelial growth stimulation (> 20% at the MSD) in the in vitro experiments with cellophane sheets. Iprodione treatments were prepared following the previously described protocol with cellophane sheets (Chapter III).

The treatments tested included a suppressive dose, the maximum stimulation dose (Chapter III), and a fungicide-free control. The experimental design consisted of three biological replicates per treatment, with 10 technical replicates each. Inoculated petri dishes were sealed with parafilm and incubated in a growth chamber (Percival Scientific, Perry, IA) at 22±2 ºC in the dark for 72 hours.

Petri dishes were scanned 72-hours post-inoculation (hpi) using a CanoScan 8400F (Canon, Melville, NY) and the mycelial growth area was measured using the software ImageJ 1.52a (Abràmoff et al. 2004).

RNA extraction and cDNA synthesis

Mycelium growing over cellophane sheets of the ten technical replicates per treatment per replicate were scrapped using spatulas and pooled together. Each harvested mycelium was placed in a screw-cap microcentrifuge tube containing RNAlater™-ICE (Thermo Fisher Scientific, Waltham, MA) and glass beads. To avoid degradation, mycelia were stored at -20 ºC until RNA extraction.

Before RNA extraction, RNAlater ™-ICE (Ambion, Inc., Austin, TX) was removed by pipetting from the tubes and mycelia were immediately flash-frozen in liquid nitrogen. Mycelia was lysed once using a bead beater (FastPrep®-24 Instrument, MP Biomedicals, Santa Ana, CA, USA) at 4 m/s for 20 seconds. RNA was extracted using a Monarch Total RNA Miniprep Kit (New England Biolabs, Ipswich, MA, USA) following the manufacturers' protocol, including the steps for DNA removal. RNA quantity was measured using Qubit™ RNA HS Assay Kit (Thermo Fisher Scientific, Waltham, MA, USA). RNA quality was measured using Nanodrop 1000 spectrophotometer (NanoDrop

Technologies, Wilmington, DE, USA) and RNA integrity was checked with an agarose gel electrophoresis.

Complementary DNA (cDNA) was synthetized from approx. 100ng of total RNA using the Verso cDNA synthesis kit (Thermo Fisher Scientific, Waltham, MA) with 500 ng/µl of anchored Oligo (dT) primer in a final volume of 20µl, according to the manufacturers' protocol. cDNA was kept at -20 ºC until use.

In order to check for DNA contamination and to verify the synthesis of the cDNA, an endpoint PCR was performed to amplify the Beta-actin gene (Table 14), using primers designed to flank an intron of the gene (Nunez-Rodriguez et al. 2020).

Analysis to find the best reference gene

To find the most suitable reference gene to be used in the differential gene expression (DGE) analysis, the stability of translation elongation factor (TEF), beta-actin, and β-tubulin (TUB2) was tested using the primers reported in **Table 15**.

The RT-qPCR assay was performed using 5 standards of known concentration (ranging from 1 ng/µl to 0.0001 ng/µl). Standards were prepared from PCR products of each gene that were purified using the QiAquick PCR purification kit (Qiagen, Inc., Valencia, CA) following the manufacturer's protocol. The concentration of the purified products was measured using Qubit™ dsDNA HS Assay Kit (Thermo Fisher Scientific, Waltham, MA, USA) and adjusted to 1 ng/µl, from which 10-fold dilutions were prepared.

The RT-qPCR for stability assay included three biological replicates of each treatment, a non-template control, and five standards of known concentration, with 3 technical replicates each. The reaction was performed in a final volume of 20 µl containing: 10 µl of PowerUP SYBR green master mix (Thermo Fisher Scientific, Waltham, MA), 1.5 µl of cDNA, 1.25 µl of each primer (5µM) for β tubulin and TEF genes, or 3.2 µl of each primer (5µM) in the case of beta-actin. The reaction volume was completed with nuclease-free water. Amplification reactions were carried out using a Rotor-Gene 6000 real-time PCR cycler (Qiagen, Inc., Valencia, CA).

Cycling parameters included an initial activation step of 2 min at 50 ºC and 5 min at 95 ºC followed by 40 cycles of 95 ºC for 60 seconds, 55 ºC for 30 seconds for beta-actin and β tubulin, and 53 ºC for TEF, followed by 72 ºC for 30 seconds, ending with a final extension of 5 min at 72 ºC. A high resolution melting analysis was included to identify dimers and non-specific amplification. Acquisition on the green channel was recorded at the end of each extension step. Temperature for the melting curve analysis ranged from 50 ºC to 99 ºC, increasing 0.25 ºC every 2 seconds.

Gene expression stability was analyzed using two software packages: geNorm (Vandesompele et al. 2002) and BestKeeper (Pfaffl et al. 2004). In addition, a web-based tool, RefFinder, that includes an analysis based on the comparative Delta-Ct method was used (Xie et al. 2012).

Table 15. Primers used to amplify reference genes

Primer name	Gene	Sequence 5'-3'	Product size (bp)	Primer efficiency	Literature
Proli 1F	TEF	GTCACGTGTCAAGCAGCGA	188	0.72	(Amatulli et al. 2012)
TEF 1R		GCGACAACATACCAATGACG			
Act-7q	Beta-actin	ATGTCACCACCTTCAACTCCA	150/200*	0.9	(Nunez-Rodriguez et al. 2020)
Act-9q		TGGAAGAAGGAGCAAGGGCA			
B-tubulin-F	β tubulin (TUB2)	GCGCATGAGTGTCTACTTCAAC	190/137*	0.9	This study
B-tubulin-R		AAGTTGTCGGGACGGAAGAG			

* These primers amplify larger products when DNA contamination is present.

Differential gene expression analysis

The differential gene expression of five genes (high-osmolarity glycerol (HOG1), fumonisin 1 (FUM1), heat shock protein 70 (HSP70), a histidine kinase homolog to Fus3 and Kss1 in *Saccharomyces cerevisiae* (FPK1), and β tubulin) was tested using primers listed in Table 16. Primer efficiencies were determined using four standards of known concentration, as described above.

The RT-qPCR for the DGE analysis was performed for the three biological replicates of each treatment with 3 technical replicates of each. The selected reference gene, beta-actin, was amplified alongside each of the target genes but in a separate tube. Two repetitions over time using the same parameters were performed.

The RT-qPCR reaction was performed in a final volume of 20 µl containing 10 µl of PowerUP SYBR green master mix (Thermo Fisher Scientific, Waltham, MA, USA), 3.2 µl of each primer (5 µM), 1.5 µl of cDNA, and 2.1 µl of nuclease-free water. The β tubulin reaction was prepared as described above. The amplification reaction was carried

out using a Rotor-Gene 6000 real-time PCR cycler (Qiagen, Inc., Valencia, CA). Cycling conditions were similar to those described before.

Relative expression of candidate genes was estimated using the delta Ct method (Livak and Schmittgen 2001) using the R package "pcr" (Ahmed and Kim 2018). The function "pcr_analyze" was used, Ct values of target genes were normalized with Ct values of the reference gene (beta-actin) in order to find the delta Ct. Then, the delta Ct value of the fungicide-free control group was used to calibrate the expression and to obtain the double delta Ct. This analysis was conducted using the average Ct value of the technical replicates of each biological replicate. Finally, a t-test was performed to analyze the statistical significance of the relative expression between treatments and the control group using the "pcr_test" function.

The R package Tidyverse was used to generate bar graphs and boxplots that represent the estimated relative expression of each candidate gene (Wickham et al. 2019).

Table 16. List of primers used in the differential gene expression analysis.

Primer name	Gene	Sequence 5'-3'	Product size	Primer efficiency	Literature
Hog1-1q	HOG1	AGGTTGATATTTGGAGTGCCG	245	0.92	(Lemos et al. 2018)
Hog1-1qt1		CAGATCAATAGCCGAATCGTC			
FUM1P2-F	FUM1	CCCCCATCATCCCGAGTAT	64	0.95	(Jurado et al. 2010)
FUM1P2-R		TGGGTCCGATAGTGATTTGTCA			
HSP70-F	Heat shock protein 70	GCCATTCCAGAAGACTTACCAA	140	0.94	(Jian et al. 2019)
HSP70-R		TGAGTTCCAACAGGGCAAAA			
FPK1-F	MAP kinase	GACACTCATTCTGGACGTGC	101	0.98	This study
FPK1-R		TCTTGAAGGGAAGCGATCGA			
B-tubulin-F	β tubulin protein (TUB2)	GCGCATGAGTGTCTACTTCAAC	190/137*	0.9	This study
B-tubulin-R		AAGTTGTCGGGACGGAAGAG			
Act-7q	Beta-actin	ATGTCACCACCTTCAACTCCA	150/200*	0.9	(Nunez-Rodriguez et al. 2020)
Act-9q		TGGAAGAAGGAGCAAGGGCA			

RESULTS

Analysis to find the best reference gene

Primers for TEF were excluded from the analysis because their efficiency was suboptimal (0.72). geNorm found that beta-actin and β tubulin genes were equally stable in all the treatments analyzed (Figure 33).

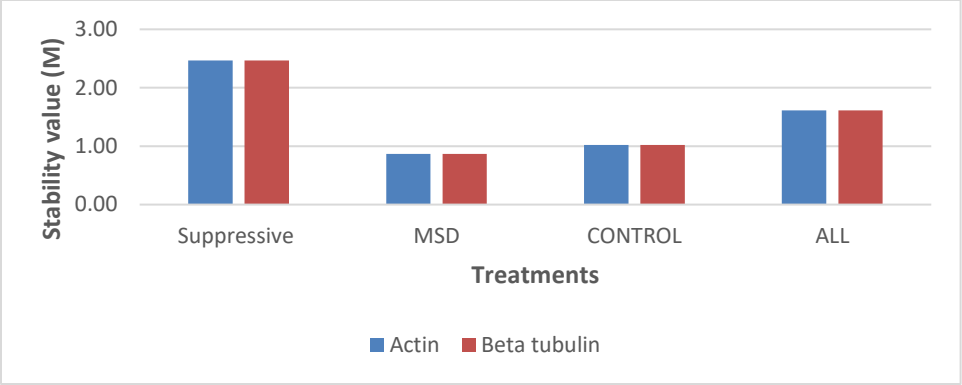

Figure 33. Gene stability analysis using geNorm. The stability value (M) was equal in all conditions analyzed. The stability value (M) for both genes was equal in the suppressive dose, maximum stimulation dose (MDS), non-amended control, and when samples from three conditions were together (All)

BestKeeper showed that β tubulin was the most stable gene. Ct standard deviation was larger on the beta-actin gene in all conditions, with the suppressive dose having the largest difference in standard deviation (Figure 34).

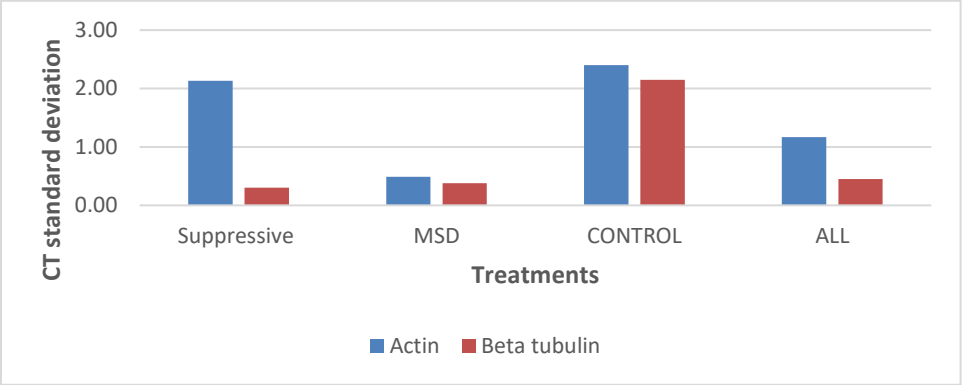

Figure 34. Gene stability analysis using BestKeeper. Bar represents the Ct standard deviation of each gene in the different treatments.

In the RefFinder analysis, beta-actin and β tubulin were equally stable in the 3 treatments (suppressive dose, MSD, and control).

Two software used for the analysis of the most stable gene, geNorm and RefFinder, agreed that both genes were equally stable in the conditions analyzed. On the other hand, BestKeeper found beta-tubulin to be the most stable.

Since both actin and β tubulin had the same stability, actin was selected as the reference for all further analysis based on the results of geNorm and RefFinder, since BestKeeper is often considered inferior to geNorm package (Maroufi et al. 2010).

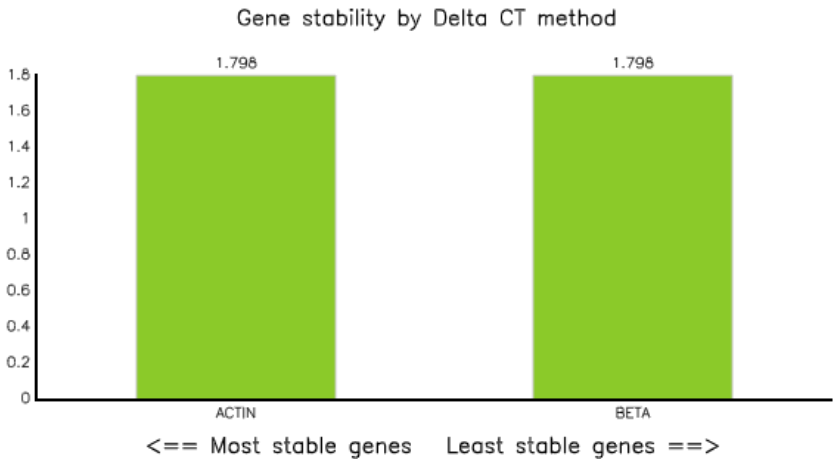

Figure 35. Gene stability analysis using the web tool RefFinder. Bars represent the average of the standard deviation of Ct in all treatments together.

Differential gene expression analysis

Fusarium proliferatum growing at the MSD of iprodione showed no significant changes in the relative expression of the analyzed five candidate genes compared to the fungicide-free control. This result was consistent after two repetitions of the experiment over time (Figure 36).

However, the suppressive dose of iprodione caused changes in the relative expression of FUM1, HOG1, and HSP70 genes compared with the fungicide-free control.

The expression levels of FUM1 gene were significantly lower than the control. Its expression was 0.1-fold lower than the control (p-value = 0). The HOG1 and the HSP70 genes showed increased expression levels compared to the control in the two repetitions analyzed. HOG1 was 1.52-fold greater with p-value = 0.01 and HSP70 was 2.51-fold greater with p-value = 0.01.

Additionally, the suppressive dose caused a significant increase in the expression of the mitogen-activated protein kinase (MAPK) FPK1, 1.86-fold larger than the control (p-value = 0.003) in the second repetition only.

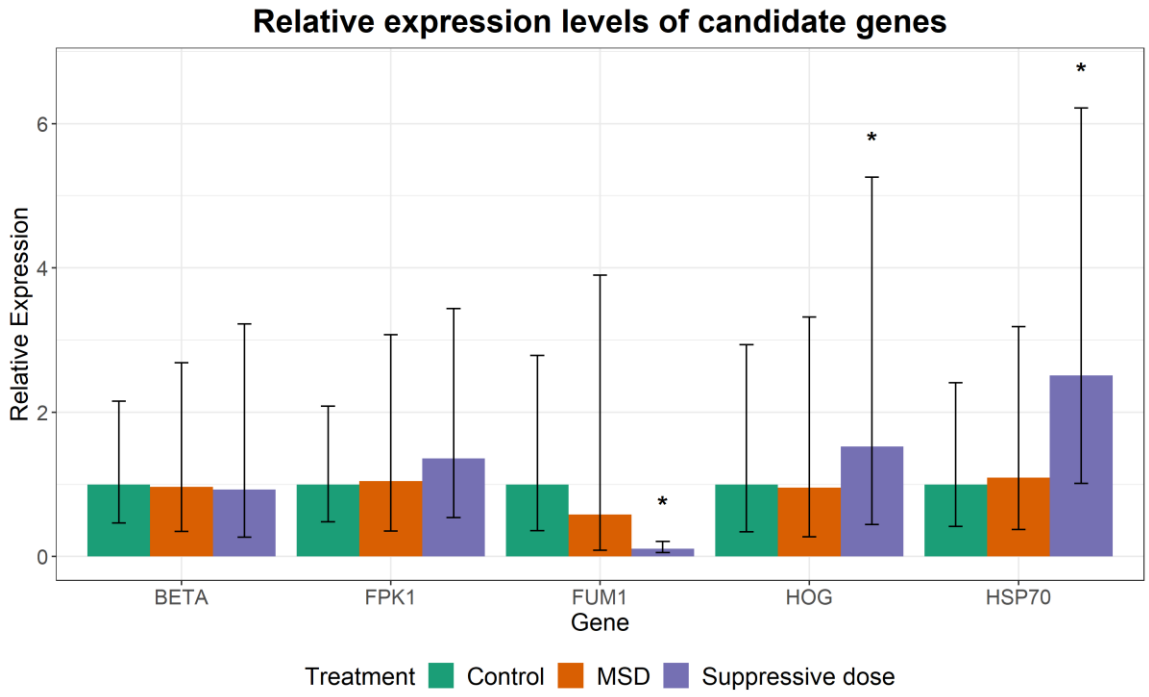

Figure 36. Relative expression levels of five candidate genes of *F. proliferatum* growing on the suppressive iprodione dose, hormetic maximum stimulation dose, and a fungicide-free control. Beta-actin was used as reference gene and the expression values were normalized to the fungicide-free control. Significant changes in the relative expression of the genes compared to the control dose are indicated with an asterisk (p-value < 0.05). Error bars represent the upper and lower limits of the relative expression. The graphic represents the results of the experiment repeated two times over time.

A large variation in the relative expression of FUM1 gene between biological replicates was found in the second repetition of the experiment. Nonetheless, biological variation was smaller for HOG1 and HSP70 genes during the same repetition (**Figure 37**).

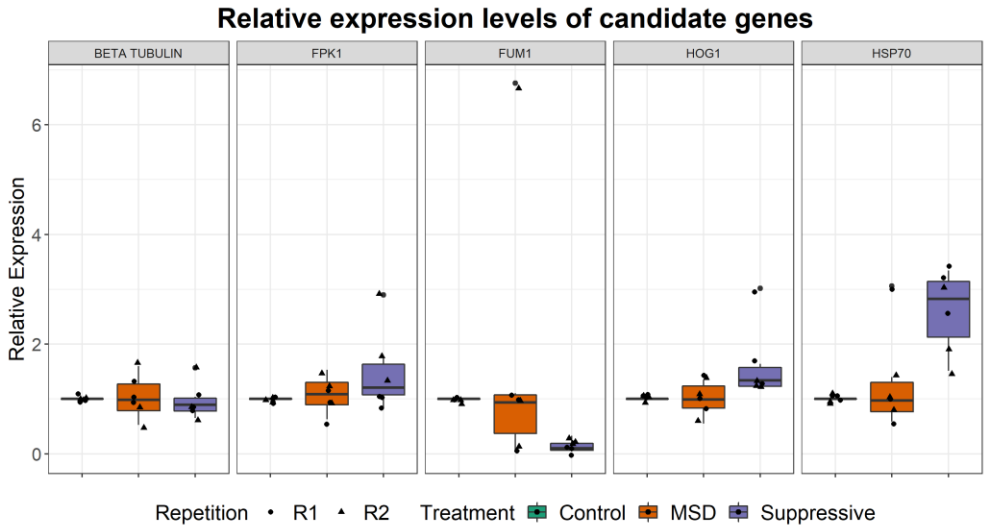

Figure 37. Box plot of the relative expression levels of five candidate genes of *F. proliferatum* growing on the suppressive iprodione dose (Suppressive), the maximum stimulation dose (MSD), and a fungicide-free control (Control). Experimental results of the first repetition and second repetition. Beta-actin was used as reference gene and the expression values were normalized to the fungicide-free control

DISCUSSION

At the maximum stimulation dose, iprodione did not affect the relative expression of 5 candidate genes associated with virulence, response to stress, and growth, compared to the fungicide-free control. This finding is similar to two previous studies that analyzed changes in the relative expression of virulence genes of *S. sclerotiorum* and *B. cinerea* during exposure to subinhibitory doses of fungicides (Cong et al. 2019; Hu et al. 2019).

Interestingly, the suppressive dose of iprodione affected the expression of FUM1, HOG1, HSP70; these changes were statistically significant (p-value < 0.05). High variability between replicates affected the ability of the statistical analyses to identify hormetic responses. In order to address this issue, increasing the number of biological replicates and repetitions is strongly recommended.

Marin et al. (2013) analyzed the effect of four temperatures (20, 25, 30, and 35 °C), three levels of water potential (-0.7, -2.8, and -7.0 MPa), and two tebuconazole concentrations (E_{50} and ED_{90}) on the relative expression of the FUM1 gene on *F. verticilliodes* and *F. proliferatum.* FUM1 overexpression was observed even at the higher fungicide concentration (ED_{90}), but sublethal doses of the fungicide (ED_{50}) were shown to cause more stimulation. Additionally, temperatures between 20°C to 30°C and mild water stress-induced FUM1 overexpression, suggesting that they were also important factors regulating the expression of this gene. However, our study did not find changes in the expression of FUM1 gene under subinhibitory doses of iprodione. Even though the experiment was carried out at low temperature (22±2°C), water stress was not a condition included in our analysis. The latter might have a key role in the fumonisin biosynthesis since increased water stress has been shown to result in a higher induction of FUM1 in both *F. verticilloides* and *F. proliferatum* (Jurado et al. 2008; Marín et al. 2010). Also, it is possible that FUM1 expression requires higher doses of iprodione to differentially express than the dose used in this assay since this dose was selected base on the growth stimulation, and it is not unusual for different endpoints to have different dose-responses to a stressor in the same biological system.

Although several studies have reported overproduction of mycotoxins under the effect of sublethal doses of fungicides (Audenaert et al. 2010; Cendoya et al. 2020; D'mello et al. 1998; Kulik et al. 2012; Magan et al. 2002; Marín et al. 2013; Matthies et al. 1999), the factors controlling mycotoxin biosynthesis are complex. Different stress conditions can cause enhanced production of mycotoxins. For example, *F. proliferatum* grown under nitrogen starvation showed enhanced expression levels of the FUM1 and FUM8 genes (Kohut et al. 2009) in one study, while another study in the same pathogen described the accumulation of fumonisins at pH 10 and pH 5 after 10 days, with the accumulation being greater at pH 10 (Li et al. 2017). Different sources of carbohydrates can also affect fumonisin production. In *F. proliferatum*, using sucrose as the only carbohydrate source increased fumonisin production while using fructose as the only source did not. Moreover, the genes FUM1, FUM8 and FUM15 were upregulated when the fungi grew on sucrose (Jian et al. 2019).

The overexpression of the HOG1 gene of *F. proliferatum* caused by the suppressive dose of iprodione was expected based on previous literature reports. Dicarboximides overactivate the HOG1 pathway causing fungi to become more sensitive against the fungicide and to accumulate glycerol (Hayes et al. 2014). A study showed that mutant *F. oxysporum* isolates lacking the HOG1 gene were more tolerant to iprodione and increased colony growth compared to the wild type (Segorbe et al. 2017), suggesting that HOG1 may be highly expressed in wild type isolates when exposed to iprodione. Studies of the metabolic pathways activated by phenylpyrroles, which are believed to have the same molecular target as the dicarboximides, have shown that the overexpression of the HOG1 gene can be detrimental to filamentous fungi (Kilani and

Fillinger 2016). This can be corroborated in the present study where *F. proliferatum* isolates growing at the suppressive dose of iprodione resulted in an increased expression of the HOG1 gene and a reduced mycelial growth area. On the other hand, at the hormetic dose (MSD) the relative expression of HOG1 was similar to that of the non-treated control suggesting that small concentrations of iprodione did not activate the HOG1 cascade and thus fungal growth was not affected.

Heat shock proteins (HSPs) in fungi play roles in response to different stressors such as oxidation, fungicides, pH, osmolarity, and temperature (Hagiwara et al. 2016). In *Saccharomyces cerevisiae*, the 70 kDa-heat shock proteins (HSP70s) are involved in the processes of protein biosynthesis and degradation (Craig et al. 1995). Even though heat shock proteins have been found to be upregulated during the hormetic responses in plants (Agathokleous et al. 2020), during this study the expression level of HSP70 did not change in *F. proliferatum* isolates growing at the MSD compared to the fungicide-free control. A study in *Neurospora crassa* reported that heat shock protein genes HSP30, HSP70, and HSP88 expression levels did not change in the presence of the fungicide fludioxinil, which simulates osmotic stress similar to iprodione (Noguchi et al. 2007). Furthermore, a study in *F. graminearum* found that two HSP70 proteins were involved in the sensitivity to the fungicide carbendazim but not to other fungicides, such as iprodione and fludioxonil (Liu et al. 2017b). In our study, overexpression of the HSP70 was found in *F. proliferatum* growing at the suppressive dose, in response to the stress caused by the high dose of iprodione (Hagiwara, 2016).

No significant changes in the expression of the MAPK gene FPK1 were observed at suppressive and hormetic doses of iprodione. Contrary to the HOG1 gene response to

iprodione and fludioxonil, *F. oxysporum* FPK1 mutants showed decreased resistance to the fungicides and higher resistance to osmotic stress. Thus, the authors suggested this gene might act antagonistically to the HOG1 pathway in stress responses (Segorbe et al. 2017). Similarly, mutants of the Fus3 gene of *Beauveria bassiana* were more sensitive to fludioxonil (Liu et al. 2017a). Furthermore, this gene has different functions in different infection processes, which vary among fungi (Jiang et al. 2018). For example, in *Alternaria alternata* this gene has been associated with resistance to copper fungicides (Lin et al. 2010); the FUS3 ortholog in *F. verticillioides* (MK1) has been reported to regulate secondary metabolite synthesis pathways (fumonisin biosynthesis) (Guo et al. 2016), while PMK1 gene controlled appressorium formation and invasive growth in *Magnaporthe oryzae* (Li et al. 2012). Further analysis will be necessary to better explain the role of FUS3 gene in *Fusarium proliferatum* (gene FPK1) at suppressive and subinhibitory doses of iprodione.

Also, no significant changes in the expression of β tubulin gene were observed neither at the hormetic dose nor at the suppressive dose of iprodione. Since β tubulin genes play roles in microtubule assembly and hyphal growth (Liu et al. 2013; Zhao et al. 2014), this study had the hypothesis that an increase in the relative gene expression of this gene might be associated with the increased hyphal growth observed at the MSD. However, the results of the present study do not support the role of β tubulin in growth stimulation due to exposure to iprodione. Thus, the molecular mechanisms responsible for growth stimulation remain unknown. The genes selected for this study were selected based on previous literature, but, given that this effort was unsuccessful, it was proposed

to change approaches and to conduct RNA-Seq analysis to identify differentially expressed genes during hormetic responses, which is the focus of chapter VI.

CHAPTER VI

IDENTIFICATION AND ANALYSIS OF DIFFERENTIALLY EXPRESSED GENES (DEG) OF *Fusarium proliferatum* GROWING AT THE SUBINHIBITORY DOSE OF IPRODIONE USING RNA-SEQ

INTRODUCTION

RNA sequencing (RNA-seq) has become the tool of choice for the analysis of gene expression levels between different conditions (Costa-Silva et al. 2017). The rapid expansion and acceptance of this technology rely on the advantages it has over previous technologies for transcriptome analysis based on hybridization (e.g., microarrays) (Wolf 2013). Some of the benefits of this technology over microarrays are that previous knowledge of the genomic sequences of interest is not required; it has higher sensitivity, which allows detecting a larger range of expression levels; also, RNA-seq allows detection of splicing events, has low background signal, and is highly reproducible (Wang et al. 2009; Wolf 2013). Furthermore, the widespread availability of analytical tools and the decrease of prices for next-generation sequencing assays are factors that contribute to the increased popularity of RNA-sequencing (Costa-Silva et al. 2017; González 2014).

RNA-seq analysis of fungicide hormesis has not been studied in detail. Although Somani, et al. (2019) reported a transcriptomic analysis in *Cochliobolus sativus* (S. Ito &

Kurib.) Drechsler ex Dastur comparing the gene expression levels at three different times post treatment (3h, 6h, and 12h) with sublethal doses of propiconazole. These treatments did not stimulate mycelial growth. Nonetheless, genes that belong to the steroid biosynthesis pathway and transferase enzymes, which are directly related to the mode of action of propiconazole, were upregulated. Other differentially expressed genes highlighted in the article were a cytochrome P450 family protein (ent-kaurene oxidase) that was found as the most upregulated enzyme, ABC transporters (41 genes up and downregulated), proteins related to oxidative stress, among others (Somani et al. 2019).

Another study used RNA-seq to study induced iprodione-resistant mutants of *Botrytis cinerea* compared to their wildtypes. Changes in gene expression were analyzed between mutants and wild type isolates, treated or non-treated with iprodione. Seven hundred twenty genes were differentially expressed in the mutant compared with the wildtype after iprodione treatment. ABC transporters were upregulated on iprodione treated isolates (mutant and wild type) and downregulated on non-treated isolates. Nine cytochrome P450 coding genes were upregulated on iprodione mutants treated or not. Genes with level of expression changes mostly belong to the following categories: zinc finger proteins, aspartic proteinases, amino acid metabolism, drug sensitivity related genes, glutathione-S transferases, zinc fingers proteins, and carbohydrate metabolism (Maqsood et al. 2020).

Samaras et al. (2020) performed a transcriptome analysis of *Penicillium expansum* multidrug resistant and sensitive isolates. Differentially expressed genes between these two phenotypes were analyzed before and after being treated with fludioxonil. The analysis was performed over time (0h, 1h, 2h, and 4h after treatment)

and it demonstrated that the most upregulated genes were found after 4 h of being in contact with the fungicide. A larger number of DE genes were found in resistant isolates. Functional analyzes showed that the most upregulated genes were: glutathione S-transferase, dihydrolipoamide succinyltranferase, Acetyl-CoA N-acyltransferase, CoA-tranferase family III, ABC, and Major Facilitator Superfamily (MFS) transporters (Samaras et al. 2020).

The objective of this project was to analyze the transcriptome of *Fusarium proliferatum* growing at subinhibitory doses of the fungicide iprodione in order to identify genes involved in the regulation of hormetic responses, as well as pathways and molecular mechanisms potentially responsible for hormetic stimulation. This work aims to provide a framework for future studies of fungicide hormesis.

MATERIAL AND METHODS

Fusarium proliferatum inoculum and experiment preparation

This experiment was performed using *Fusarium proliferatum* wild type isolate FP-A7WT. The isolate was inoculated on SNA media amended with iprodione and a fungicide-free control and covered with cellophane sheets treated with the same fungicide dose or water, in the case of the control. The two treatments compared were the maximum stimulation dose (MSD) of iprodione at 72 hpi (0.55 ppm, Chapter III) and a fungicide-free control; each with three biological replicates (named H1, H2 and H3, and C1, C2 and C3, respectively). Each biological replicate included 15 technical replicates each. Petri dishes were incubated in a Percival growth chamber (Percival Scientific, Perry, IA) at 22± 2ºC in the dark for 72 hours. The experiment was performed at this time

because preliminary assays showed that the largest amount of RNA, necessary to fulfill RNA-seq requirements, was obtained at 72hpi.

RNA extraction and sequencing

Total RNA of each treatment was extracted following the protocol described in Chapter V. The RNA obtained from the 15 technical replicates of each biological replicate was pooled to obtain enough RNA for the assays that followed.

RNA quantity was measured using Qubit™ RNA HS Assay Kit (Thermo Fisher Scientific, Waltham, MA, USA). RNA quality was measured using Nanodrop 1000 spectrophotometer (NanoDrop Technologies, Wilmington, DE, USA), OD260/230 ratios equal to or greater than 2 were selected as a reference of purity. RNA integrity was checked with an agarose gel electrophoresis and Agilent Bioanalyzer 2100 (Agilent Technologies Inc., Santa Clara, CA). Samples with RNA integrity number (RIN) greater than 8 were selected for sequencing.

Library preparation and RNA sequencing were done by Novogene Bioinformatics Technology Co., Ltd. Using the Illumina platform to obtain 150bp paired-end reads.

Differential gene expression analysis

Bioinformatics analysis of high-throughput data was performed using the resources of the High-Performance Computing Center at Oklahoma State University. The quality of the raw Illumina reads from the 6 samples sequenced were analyzed using FASTQC (Andrews 2010). Low quality reads and Illumina sequencing adapters were trimmed using Trimmomatic (Bolger et al. 2014).

Trimmed reads were mapped to the *Fusarium proliferatum* reference genome ET1 (Refseq accession: GCF_900067095.1) using HISAT2 (Kim et al. 2015). Reads that aligned to the reference genome where assembled using StringTie. Assembled transcripts were merged together with the reference annotation using "merge" mode of StringTie to generate a non-redundant set of transcripts. Finally, transcripts abundances were estimated using StringTie to generate a counts matrix for each sample (Pertea et al. 2016).

The R packages edgeR (Robinson et al. 2010), DESeq2 (Love et al. 2014), and NOISeq (Tarazona et al. 2015; Tarazona et al. 2011) were used to perform the differential gene expression analysis. DEGs were analyzed by a comparison between iprodione treated samples and the fungicide-free controls, using the latter as reference.

For edgeR and NOISeq, data was normalized using the trimmed mean of M values (TMM) method. For DESeq2, data was normalized using the software internal normalization algorithm (median of ratios). Furthermore, the R package 'fdrtool' was integrated into the DESeq2 analysis with the aim to normalize p-values distribution (Strimmer 2008).

Differentially expressed genes were selected based on a false discovery rate of 5% (FDR, p-value < 0.05) in edgeR and DESeq2 and based on the parameter q = 0.95 in NOISeq.

Functional annotation

Functional annotation was performed only for the DEGs that were found using DESeq2. Protein names and identity for most proteins were retrieved based on the

annotation of the reference genome. Differentially expressed, newly assembled transcripts were identified by homology against the Uniprot/Swissprot database. Carbohydrate-Active enzymes were predicted using the dbCAN2 meta server (Yin et al. 2012; Zhang et al. 2018). Secondary metabolites were predicted using antiSMASH fungal version (Medema et al. 2011), and the Secondary Metabolites tool of InterProScan (SMIPS) (Wolf et al. 2015). Additionally, protein sequences from the DEGs were blasted against the Pathogen Host Interactions (PHI) (Urban et al. 2019) database, using 50% of identity, 50% query coverage, and e-value of 1e-5 as thresholds. Secreted proteins were identified using SignalP v. 5.0 (Almagro Armenteros et al. 2019). Putative fungal effectors were identified with EffectorP (Sperschneider et al. 2016) and ApoplastP (Sperschneider et al. 2018). Gene Ontology (GO) terms were retrieved from Uniprot (Bairoch et al. 2005) based on the annotation of the reference gene (Refseq accession: GCF_900067095.1). An enrichment analysis of GO terms was performed using the R package topGO (Alexa and Rahnenfuhrer 2020). KEGG terms and pathways were annotated with KOBAS 3.0 webserver (Xie et al. 2011) using *F. verticilliodes* as reference. An overrepresentation analysis of the KEGG pathways was performed using the R package clusterProfiler (Yu et al. 2012).

Validation analysis of selected differentially expressed genes using RT-qPCR

Changes in the expression of 6 selected differentially expressed (DE) genes (Table 17), found to be upregulated in the previous analysis, were validated using RT-qPCR. Primers for all these genes were designed using Primer 3 (Untergasser et al. 2012) from transcript sequences (Table 18).

Assay preparation and RNA extraction were performed as previously described. cDNA synthesis was performed with the protocol described in Chapter V. Primer efficiencies were analyzed using five standards of known concentration (ranging from 1 ng/µl to 0.0001 ng/µl) prepared as described in Chapter V.

The experimental design consisted of two treatments, a hormetic dose (Dose H) and a fungicide-free control, with 4 biological replicates each. RT-qPCR was performed using 3 technical replicates per biological replicate of each treatment and of a non-template control. The experiment was repeated once. Beta-actin was used as reference gene (Nunez-Rodriguez et al. 2020). Target and reference genes were amplified simultaneously (separate tubes).

The RT-qPCR reaction for the target genes was performed in a final volume of 20 µl containing: 10 µl of PowerUP SYBR green master mix (Thermo Fisher Scientific, Waltham, MA, USA), 3 µl of each primer (5 µM), 2 µl of cDNA and 2 µl of nuclease-free water. The beta-actin reaction was prepared as described before (Chapter V). The amplification reaction was carried out using a Rotor-Gene 6000 real-time PCR cycler (Qiagen, Inc., Valencia, CA). Cycling conditions were similar to those described in Chapter V.

Analysis of the gene expression was performed using the R package “pcr” (Ahmed and Kim 2018) (Chapter V).

Table 17. Differentially expressed genes selected for validation using RT-qPCR.

Sequence ID	Putative function	Log2FC	padj
MSTRG.11506	Related to multidrug resistance-associated protein	7.00	0.007392
MSTRG.14423	Related to cytochrome P450 monooxygenase (LovA)	3.50	2.15E-05
MSTRG.3874	Related to N6-hydroxylysine acetyl transferase	2.55	4.79E-13
MSTRG.2194	Related to beta-mannanase	2.01	4.72E-08
MSTRG.11760	Related to cytochrome P450 monooxygenase (LovA)	1.46	3.24E-12
MSTRG.13401	Mannan endo-1,6-alpha-mannosidase	1.00	3.24E-12

Table 18. Primers designed with Primer3 for RT-qPCR validation

Sequence ID	Primers	Product size	Tm	GC%
MSTRG.11506	CAGCGACAGTGAAGTGGAA	195	58.49	52.63
	TGGCGAGAGCATTGAAGTAG		59.17	50
MSTRG.14423	TGGACGCCTGTTATTGCTC	243	59.81	52.63
	CGCCTCATTATTCTTCCTCTG		58.94	47.63
MSTRG.3874	GTCAACGGATGGTCGAGAAG	120	60.66	55
	GGAGAACGAGGATCAGCAAC		59.81	55
MSTRG.2194	GGCAACACCAACACAGGAA	216	60.56	52.63
	GCATCCAAAGTAGGCACAGTAAG		60.2	47.83
MSTRG.11760	GCGTCAAGCTACAGTTCATCC	140	59.9	52.38
	CATATCACGGAGTCGCTCTTC		59.85	52.38
MSTRG.13401	CGATGGCAGATTCCCTTTAC	169	59.53	50
	GGTCGATGTAGTTGACGTTCC		59.47	52.38

RESULTS

RNA sequencing and mapping

The sequenced libraries produced between 39 to 47 million reads for all of the samples. The quality index (Q30) was higher than 90% in all replicates and the GC content was between 52.33% and 52.89% (Table 19).

After quality checks and trimming of low-quality reads and adapters, more than 90% of the reads survived. The number of reads after trimming was between 36 to 44 million reads per sample. The percentage of the reads mapped to the *F. proliferatum* reference genome was between 82.08% and 89.16%. Mapped reads were used in the differential expression analysis.

Table 19. Statistics for the data quality of sequencing

Treatment	Sample	Raw reads	Effective (%)	Error (%)	Q30(%)	GC (%)
Fungicide-free control	C1	40,564,684	97.90	0.03	93.78	52.73
	C2	47,612,856	95.57	0.02	94.32	52.89
	C3	40,130,026	97.79	0.02	94.66	52.69
Hormetic fungicide dose (MSD)	H1	41,661,914	97.85	0.03	93.93	52.33
	H2	42,142,346	98.35	0.02	94.46	52.79
	H3	39,239,210	93.27	0.03	94.30	52.61

Differential gene expression analysis

During the data quality check of the mapped reads, one biological replicate of each condition (C2 and H1) did not cluster with the samples of their respective conditions: treated or untreated. This was observed during the hierarchical clustering analysis of sample-to-sample distances plotted using the DESeq2 package (Figure 38).

Treated refers to the samples of *F. proliferatum* grown under the fungicide subinhibitory dose while untreated were the fungicide-free control samples. Those outlier samples were eliminated from further analyses.

Analysis of the data from two biological repetitions using edgeR identified a total of 78 DE genes, 25 downregulated and 53 upregulated based on a false discovery rate of 5% (FDR, p-value < 0.05). Log2 fold change (Log2FC) of upregulated genes ranged from 0.94 to 11.79 and downregulated from -9.66 to -0.74.

NOISeq analysis, based on the parameter q = 0.95, identified 58 DE genes, 44 upregulated and 14 downregulated. Log2FC of upregulated genes ranged from 0.12 to 9.8 and downregulated from -7.63 to -0.28.

Finally, with the DESeq2 package, a total of 177 DE genes were identified, 117 upregulated and 60 downregulated with an adjusted p-value < 0.05. Log2FC values of upregulated genes ranged from 0.47 to 11.25 and downregulated from -9.08 to -0.46.

Twenty-three DE genes were found by the three software packages. Another 46 DE genes were found by DESeq2 and edgeR which are the packages that shared the higher number of similar genes. The NOIseq package shared a different set of 9 DE genes with DESeq2, and another set of 6 DE genes with edgeR (Figure 39). Since most of the differentially expressed genes were identified using DESeq2, the results obtained from this software were chosen to carry out further analyses.

Figure 3 shows a heatmap with the hierarchical cluster of the DEGs with the highest fold-changes (Log2FC >2). It is interesting to note that there were several uncharacterized proteins amongst the most differentially expressed genes as well as

several proteins that have not been fully characterized (those with names starting with "Related to"). Some of the newly assembled transcripts obtained with StringTie were also among the most differentially expressed proteins.

Of the 177 DEGs identified with DESeq2, 45 (25%) of them were annotated as uncharacterized proteins, 108 (61%) were not fully annotated ("probable" and "related to" proteins) and 18 (10%) are newly assembled transcripts, some of which fall under the two previous categories. This is an issue that arises from the reference annotation of *F. proliferatum*. Of the 16,136 genes in the reference annotation, 7,610 (47%) were uncharacterized proteins, 6,146 (38%) were "related to" known proteins, and 2,154 (13%) were "probable" proteins. These numbers showcase how the genome annotation of *Fusarium proliferatum* is still lacking and needs to be improved.

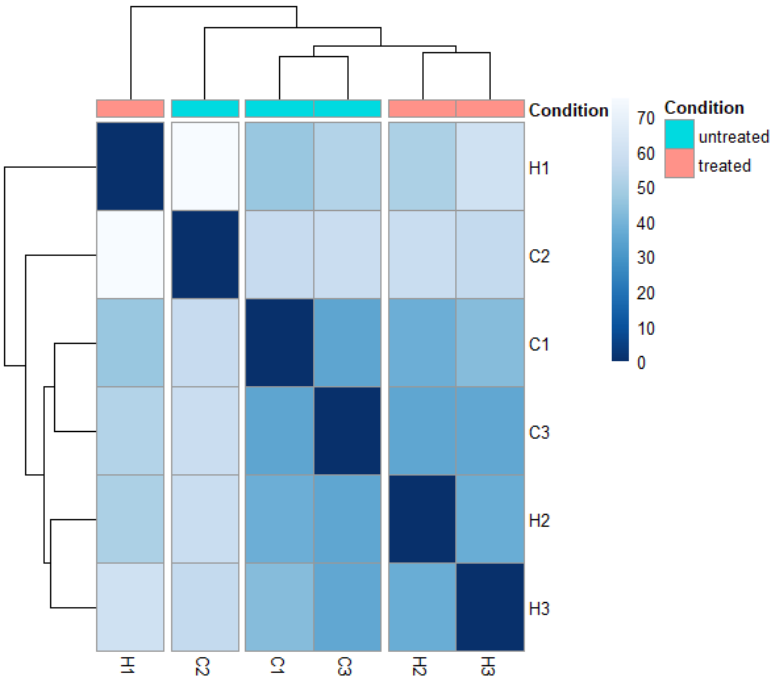

Figure 38. Hierarchical clustering heatmap analysis obtained using DESeq2 package representing sample to sample distances of two conditions: **untreated** that represents *F. proliferatum* growing on fungicide-free control (C1, C2, and C3) and **treated** represents the hormetic dose (H1, H2, and H3). Two outliers can be observed clustering outside each respective category (H1 and C2).

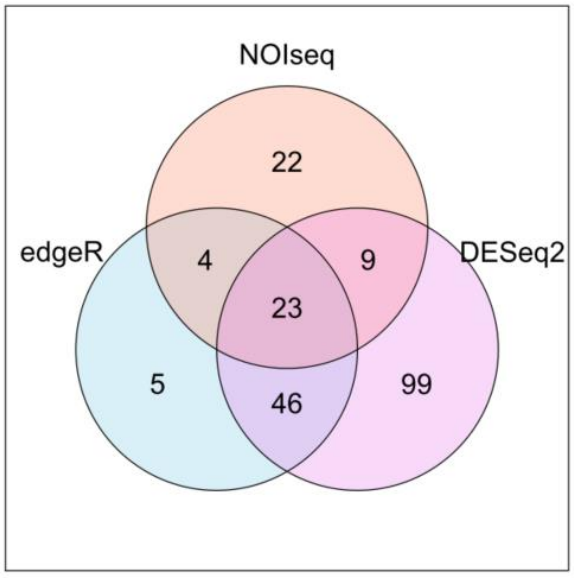

Figure 39. Venn diagram showing the number of differentially expressed genes found by three packages used: DESeq2, edgeR, and NOIseq. Analysis comparing the expression

levels of *F. proliferatum* growing under two conditions: treated (subinhibitory dose of iprodione) and untreated (fungicide-free control).

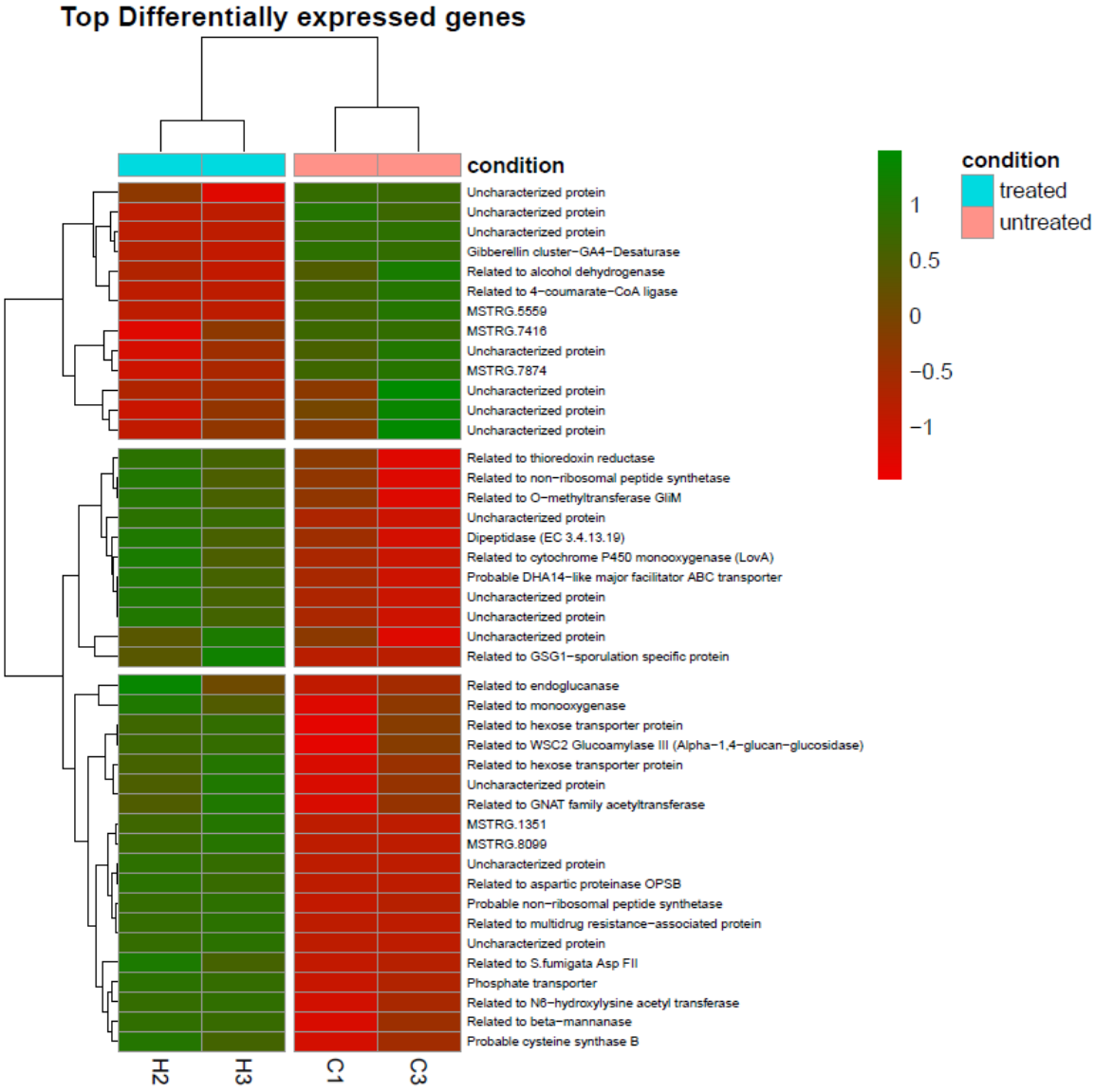

Figure 40. Hierarchical clustering heatmap analysis representing the most differentially expressed genes in *F. proliferatum* growing under two conditions: treated (subinhibitory dose of iprodione) and untreated (fungicide-free control). Gene expression fold changes are represented by colors, upregulated genes by green and downregulated by red. Genes with log2 fold-changes greater than 2 are represented.

Functional annotation

According to the dbCAN2 metaserver, 24 upregulated genes were identified as carbohydrate-active enzymes, 21 of whom had a signal peptide. Most of them (n=14) belonged to the glycoside hydrolase family (GH), three had auxiliary activities (AA), one belonged to the polysaccharide lyase family (PL), four belonged to the carbohydrate esterases class (CE), and two were identified as carbohydrate-binding modules (CBMs) (Supplementary Table 1). Moreover, seven of them were identified as putative fungal effectors with location on the apoplast: MSTRG.6762, MSTRG.7788, MSTRG.8765, MSTRG.10249, MSTRG.10924, MSTRG.10970, and MSTRG.12682.

Additionally, other 36 DE genes were predicted to have a signal peptide by SignalP-5.0 (total genes with signal peptide = 57). Of those genes, fifteen were putative fungal effectors, eleven were probably secreted into the apoplast (MSTRG.194, MSTRG.242, MSTRG.4543, MSTRG.5181, MSTRG.6762, MSTRG.7788, MSTRG.8765, MSTRG.10249, MSTRG.10924, MSTRG.10970 and MSTRG.12682) and the rest were non-apoplastic (MSTRG.212, MSTRG.4050, MSTRG.9957, and MSTRG.10230) (Supplementary Table 2).

According to antiSMASH fungal version (Medema et al. 2011) and the Secondary Metabolites tool from InterProScan (SMIPS) (Wolf et al. 2015), there were four upregulated genes that encoded for secondary metabolites. Three were defined as non-ribosomal peptide synthetases (MSTRG.6651, MSTRG.14424 and MSTRG.3875) and one was a polyketide synthase (MSTRG.2410).

A blastp search of the pathogen-host interaction (PHI) database found that 23 genes had putative pathogen-host interaction phenotypes, 15 were upregulated and 8 were downregulated (Supplementary Table 3). Even though a few of these phenotypes indicated that mutants for these genes might have reduced virulence, most of these genes (14 out of 23) were annotated to unaffected pathogenicity phenotypes.

A total of 117 out of the 177 DEGs had at least one associated GO term. Enrichment analysis of GO terms done with TopGO did not produce significant results because of the small number of genes, and because almost 40% of them did not have a GO annotation. Nonetheless, the most abundant GO terms were classified into three categories: biological processes (BP), cellular components (CC), and molecular functions (MF). In the first category, the most abundant GO terms (15 genes total) were related with carbohydrate metabolic processes (GO:0005975); in cellular component category, 46 genes were associated with membrane (GO:0016020), and in molecular function, 62 genes were associated with catalytic activity (GO:0003824) and 9 with nucleotide binding (GO:0000166). Other GO terms present in a lesser number of genes are summarized in Figure 41.

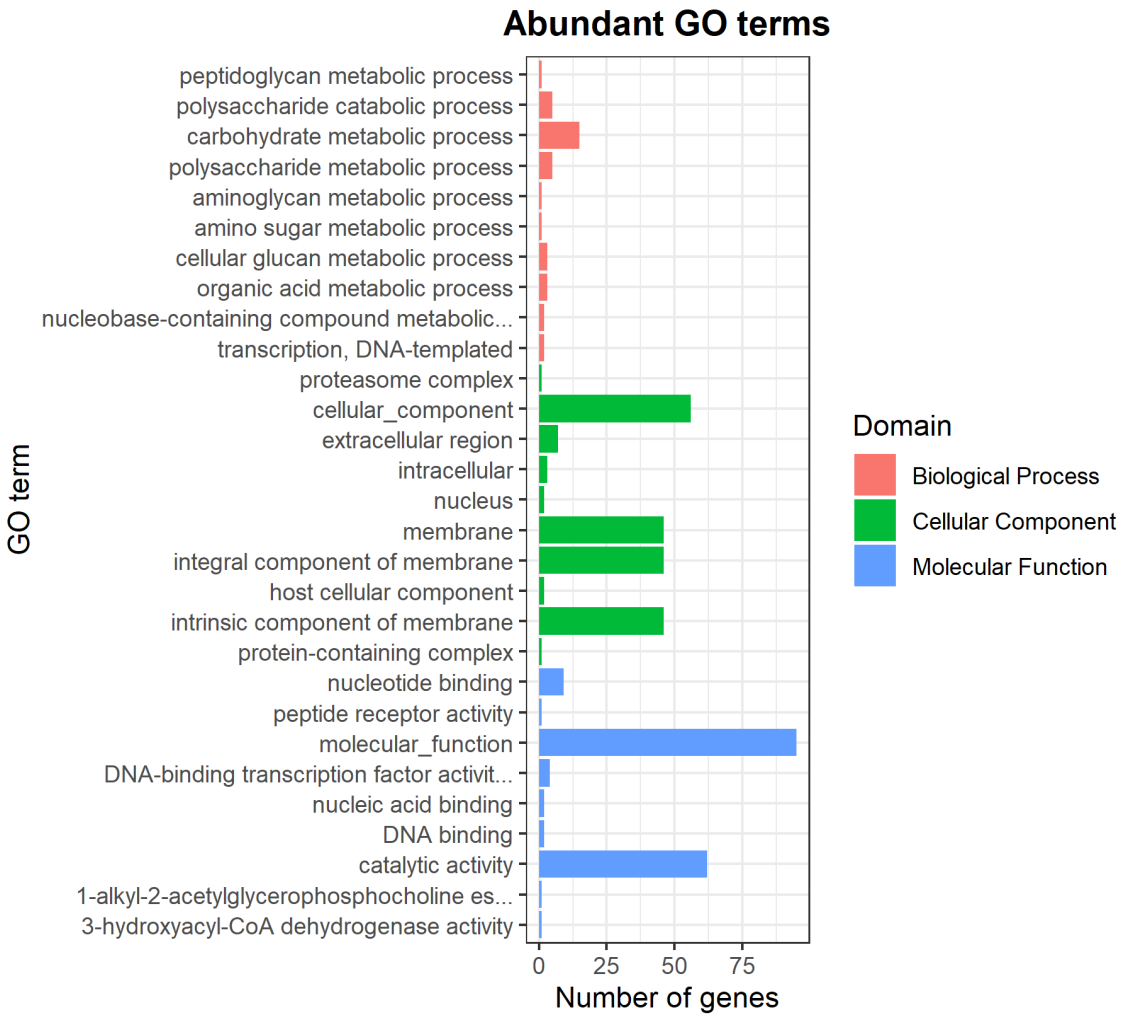

Figure 41. Gene Ontology (GO) classifications of differentially expressed genes of *F. proliferatum* growing under two conditions: treated (subinhibitory dose of iprodione) and untreated (fungicide-free control). GO terms are classified in three categories: Biological Process (pink), cellular component (green), and molecular function (blue).

The nucleotide sequences of the DEG were submitted to the KOBAS 3.0 webserver to be annotated using *F. verticilloides* as a reference. The overrepresentation analysis using clusterProfiler identified five overrepresented KEGG pathways among the DE genes, MAPK signaling (fvr04011), starch and sucrose metabolism (fvr00500), ABC transporters (fvr02010), fructose and sucrose metabolism (fvr00051), and linoleic acid

metabolism (fvr00591) (Figure 42). Genes associated with the MAPK pathway were downregulated (Supplementary Table 4).

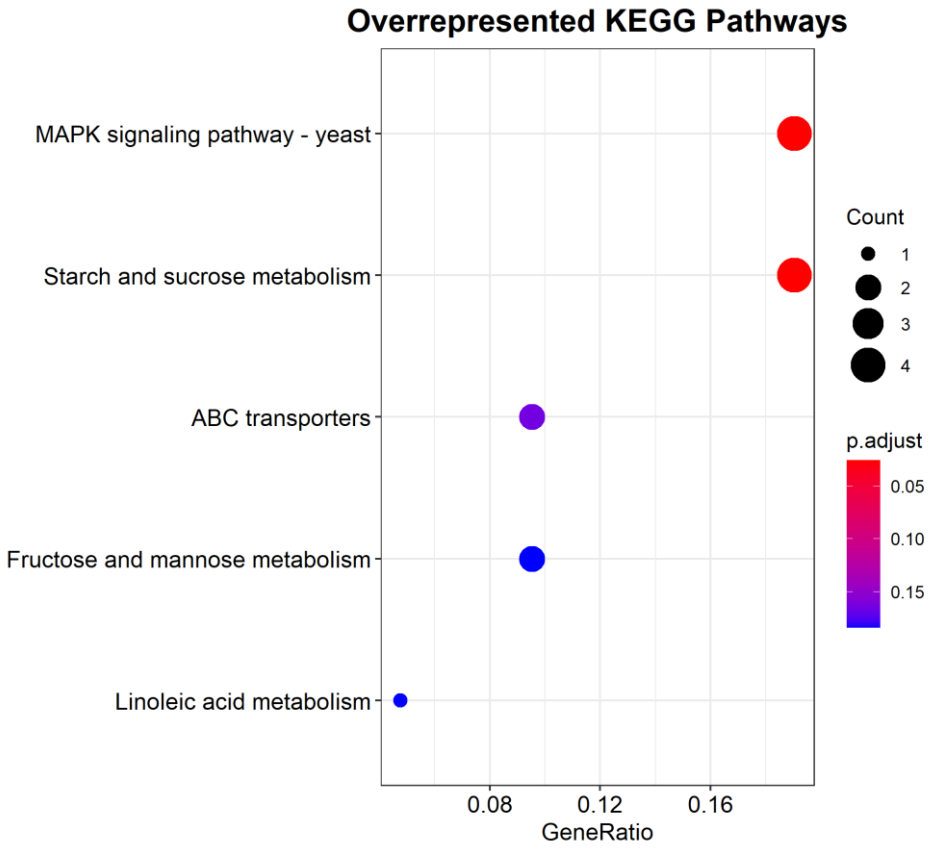

Figure 42. Most abundant KEGG pathways on differentially expressed genes of *F. proliferatum* growing under two conditions: treated (subinhibitory dose of iprodione) and untreated (fungicide-free control).

Real-time quantitative PCR (RT-qPCR) validation of differentially expressed genes

Six upregulated genes were selected based on their putative function and Log2FC to perform a RT-qPCR validation. Genes MSTRG.2194, MSTRG.11760, and MSTRG.13401, identified as related to beta-mannanase, cytochrome P450 monooxygenase (LovA), and mannan endo-1,6-alpha-mannosidase, respectively, were

significantly overexpressed compared to the fungicide-free control (p-value < 0,05); thus, changes in their expression levels were validated. Additionally, a cytochrome P450 monooxygenase (LovA) gene (MSTRG.14423) and a gene related to N6-hydroxylysine acetyl transferase (MSTRG.3874) were overexpressed according to RNA-Seq but the change in their relative expression was not significantly different (p-value >0.05) in the RT-qPCR analysis. Finally, the expression of the most upregulated gene according to the RNA-seq analysis, related to a multidrug resistance-associated protein (MSTRG.11506), was not confirmed with RT-qPCR (Figure 43).

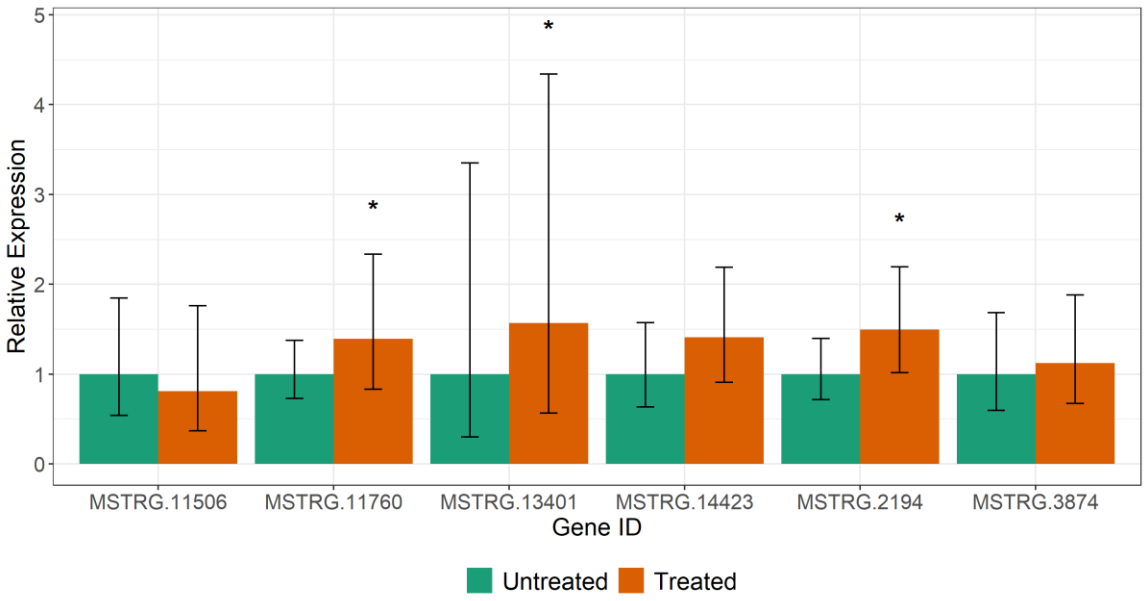

Figure 43. Validation of six differentially expressed of *F. proliferatum* growing on the hormetic maximum stimulation dose (treated) and a fungicide-free control (untreated). Beta-actin was used as reference gene and the expression values were normalized to the fungicide-free control. Significant changes in the relative expression of the genes compared to the control dose are indicated with an asterisk (p-value < 0.05). Error bars represent the upper and lower limits of the relative expression. The graphic represents the results of the experiment repeated two times over time.

DISCUSSION

This study found differences at the transcriptomic level of *Fusarium proliferatum* treated with a subinhibitory dose of iprodione compared with the untreated fungicide-free control. Changes in the expression of 177 genes were observed, 117 genes were upregulated and 60 were downregulated on the iprodione-treated isolates. According to the KEGG pathway analysis, one of the most represented pathways in the DEGs was the ABC transporters (ATP-binding cassette superfamily transporters). These are part of the two major efflux transporters mechanisms that fungi use to transport endogenous or exogenous toxicants (e.g., host and non-host toxins, mycotoxins, plant defense compounds, antibiotics, and fungicides) (Del Sorbo et al. 2000). The presence of fungicides resulted in overexpression of these transporters, which have also been identified as mechanisms of fungicide resistance in several plant pathogens (De Waard et al. 2006; Hulvey et al. 2012; Kretschmer et al. 2009).

Two upregulated genes (MSTRG.3873 and MSTRG.1047) belong to different subfamilies of transporters: subfamily C (ABCC1) that has multi-drug resistance-associated domains, and subfamily B (ABCB1) that has multi-drug resistance domains (Lee et al. 2011). Upregulation of an ABCC transporter (FgABCC9) was described in *F. graminearum* during plant infection as a response to salicylic acid and tebuconazole; subsequently, the authors suggested that FgABCC9 gene had a role in the mitigation of fungicide effects (Qi et al. 2018). Furthermore, RNA-seq analysis of *Sclerotinia homeocarpa* isolates with multidrug resistance to fungicides (propiconazole, iprodione, boscalid, and flurprimidol) displayed significant overexpression of ABC transporters and genes encoding for cytochrome P450 after propiconazole treatment. RT-qPCR confirmed

these same results when the fungus was in contact with the other fungicides, including iprodione (Sang et al. 2018). A different study demonstrated similar results when the dollar spot pathogen was treated with chlorothalonil (Green et al. 2018).

This study also found overexpression of two cytochrome P450 (CYP450) encoding genes. One of them (MSTRG.11760) had similarity to a cytochrome P450 monooxygenase and was upregulated in a *F. proliferatum* isolate treated with a subinhibitory dose of iprodione. This result was further validated with RT-qPCR. The expression of the second CYP450 gene (MSTRG.14423) was upregulated in the RNA-Seq assay, but the result was not validated with RT-qPCR (p-value = 0.056).

Cytochrome P450 enzymes have key functions in different cellular processes including detoxification of xenobiotic compounds, thus representing an important defense mechanism to environmental stressors (Črešnar and Petrič 2011). Shin et al. (2017) described the molecular functions of 119 putative P450 monooxygenases present in the *F. graminearum* genome by constructing a genome-wide deletion mutant library of those genes. The effects of the mutations were analyzed on vegetative growth, conidiogenesis, sexual development, virulence, mycotoxin production, and sensitive to fungicides: tebuconazole, difenoconazole, epoxiconazole, propiconazole, and prochloraz. Five P450 genes were demonstrated to have functions on virulence and plant infection and 17 P450 mutants were sensitivity to fungicides. Authors concluded that P450 genes had redundant functions on fungal development and detoxification (Shin et al. 2017).

The present work demonstrated that subinhibitory doses of iprodione resulted in the overexpression of both, ABC transporters and cytochrome P450 genes which is in

concordance with a study that analyzed the effects of sublethal doses of other fungicides (propiconazole) (Somani et al. 2019). Further analyses are required to functionally characterize the P450 gene found overregulated with the aim to find if it is involved in cellular processes other than detoxification.

The term “carbohydrate metabolic process” (GO:0005975) is one of the most abundant GO terms in the biological process category. Fifteen upregulated DEGs (MSTRG.8874, MSTRG.2194, MSTRG.10924, MSTRG.4177, MSTRG.8765, MSTRG.3917, MSTRG.3878, MSTRG.6690, MSTRG.11253, MSTRG.6762, MSTRG.13401, MSTRG.11261, MSTRG.10201, MSTRG.1095, and MSTRG.6798) were annotated with this term, all but one of them have been found to be carbohydrate-active enzymes (CAZymes) and four (MSTRG.4177, MSTRG.8765, MSTRG.10924 and MSTRG.6762) of them were also found to be putative effectors. CAZymes synthetized by plant pathogenic organisms can be involved in the degradation of the plant cell wall as well as in other plant-pathogen interactions (Zhao et al. 2013). Confirming this is the fact that fourteen of the previously mentioned DEG were identified to code for cell wall degrading enzymes (CWDEs) including cellulose-degrading enzymes such as glucanase, endoglucanase, and hemicellulose-degrading enzymes such as arabinofuranosidase, xylodase, xylanase, alpha-mannosidase and beta-mannanase.

Of the several kinds of CAZymes that fungi can produce, CWDEs are among the most important because fungi require them to get access to their host and to utilize carbohydrates released from host cells as nutrients (Zhao et al. 2013). Plant cell walls are complex structures that act as a barrier to limit pathogen attack (Hématy et al. 2009), thus

fungi have developed a wide arsenal of CWDE to overcome this barrier (King et al. 2011).

Studies on fungal transcriptome changes have found upregulation of CWDEs during the infection of lupin by *Pythopthora parasitica* (Blackman et al. 2015), as well as an increase of the CWDEs in *Magnaporte oryzae* when growing *in planta* when compared with in vitro (Mathioni et al. 2011). In the current study, the upregulation of the CWDEs was found in *F. proliferatum* isolates growing at subinhibitory doses of iprodione. Even though, previous studies using mutants for CWDEs were not able to expose any of these enzymes as key pathogenicity factors, the large number of CWDEs encoded by plant pathogens is a compelling argument in favor of considering them as virulence factors (Kubicek et al. 2014). These observations suggest that the overexpression of CWDEs in *F. proliferatum* at hormetic doses of the fungicide may produce an increase in virulence. Furthermore, in this study, the differential expression of two CWDE genes, MSTRG.13401, encoding for a mannan endo-1,6-alpha-mannosidase, and MSTRG.2194, with similarity to a beta-mannanase, was validated using RT-qPCR, since both were significantly overexpressed (p-value <0.05).

Another gene selected for validation with RT-qPCR was MSTRG.3874, that is related to N6-hydroxylysine acetyl transferase involved with siderophore biosynthetic processes. Results of RT-qPCR demonstrated a tendency towards overexpression however these changes were not statistically significant (p-value >0.05). Siderophores help with iron intake, however other functions have been described (e.g., virulence) (Khan et al. 2018). In *F. graminearum* a siderophore with a putative function of L -

Ornithine N 5 monooxygenase (SID1) is required for virulence in wheat (Greenshields et al. 2007).

The most up- and downregulated genes found during this analysis were annotated as uncharacterized proteins. About 25% of the DEGs were uncharacterized proteins, which makes analyzing the data and drawing conclusions more difficult. The success of the functional analysis of the RNA-seq data is based in the availability of functional data for the species being studied (Conesa et al. 2016). A good analysis requires having gene models of enough quality, which are not available for all organisms. Most non-model organism genomes have not received the extensive curation and experimental validation that model species have. Thus, resulting in poor genome annotations that were generated by automated pipelines that most of the time obtain information from distantly-related orthologs (Hosmani et al. 2019). Currently, genomes of the most important plant pathogens still have incomplete genomes and annotations (Pedro et al. 2019). For this reason, it is important to improve the annotation of the reference genomes that are publicly available for non-model organisms. This can be done, by re-annotating the reference genomes using new information that was perhaps not available the first time, by using community-driven annotation efforts (Hosmani et al. 2019; Pedro et al. 2019) or by validating uncharacterized genes experimentally to know their proper functions.

Data presented in this study showed that subinhibitory doses of iprodione on *F. proliferatum* caused the upregulation of different processes in the fungal cell that might be associated with the mechanisms of hormetic responses. Namely, detoxification processes mediated by ABC transporters and cytochrome P450 enzymes, production of secondary metabolites, a probable increase of virulence factors, and increased

carbohydrate metabolism. Further studies are necessary to better understand the mechanism of hormesis in plant pathogens. Furthermore, because hormesis is a time-specific response an RNA-seq study at different points in time will provide a broader perspective and will help to expand the catalog of pathways differentially regulated during hormetic responses.

REFERENCES

Abawi, G., and Lorbeer, J. 1971. Pathological histology of four onion cultivars infected by *Fusarium oxysporum* f. sp. *cepae*. Phytopathology 61:1164-1169.

Abd-Elrazik, A., Fahmy, F., Amein, A., and El-Amein, A. 1990. Role of onion seeds in transmission of damping-off causal fungi and chemical control of the disease. Assiut Journal of Agricultural Sciences 21:173-193.

Abràmoff, M. D., Magalhães, P. J., and Ram, S. J. 2004. Image processing with ImageJ. Biophotonics international 11:36-42.

Agathokleous, E., and Calabrese, E. J. 2019. Hormesis: The dose response for the 21st century: The future has arrived. Toxicology:152249.

Agathokleous, E., Kitao, M., and Calabrese, E. J. 2018. Environmental hormesis and its fundamental biological basis: rewriting the history of toxicology. Environmental research 165:274-278.

Agathokleous, E., Kitao, M., and Calabrese, E. J. 2020. Hormesis: highly generalizable and beyond laboratory. Trends in Plant Science 1076-1086.

Ahmed, M., and Kim, D. R. 2018. pcr: an R package for quality assessment, analysis and testing of qPCR data. PeerJ 6:e4473.

Alam, S., Joyce, D., and Wearing, A. 1996. Effects of equilibrium relative humidity on in vitro growth of *Botrytis cinerea* and *Alternaria alternata*. Australian Journal of Experimental Agriculture 36:383-388.

Alexa, A., and Rahnenfuhrer, J. 2020. topGO: Enrichment Analysis for Gene Ontology. in: R package version 2.42.0.

Alexander, N. J., Proctor, R. H., and McCormick, S. P. 2009. Genes, gene clusters, and biosynthesis of trichothecenes and fumonisins in *Fusarium*. Toxin reviews 28:198-215.

Almagro Armenteros, J. J., Tsirigos, K. D., Sønderby, C. K., Petersen, T. N., Winther, O., Brunak, S., von Heijne, G., and Nielsen, H. 2019. SignalP 5.0 improves signal peptide predictions using deep neural networks. Nature Biotechnology 37:420-423.

Amatulli, M. T., Spadaro, D., Gullino, M. L., and Garibaldi, A. 2012. Conventional and real-time PCR for the identification of *Fusarium fujikuroi* and *Fusarium proliferatum* from diseased rice tissues and seeds. European Journal of Plant Pathology 134:401-408.

Anasi Castillo, G. E. 2016. Evaluación de la producción de fumonisinas en *Fusarium proliferatum* en respuesta a dosis subinhibitorias de fungicida (Iprodiona). PUCE.

Andrews, S. 2010. FastQC: a quality control tool for high throughput sequence data. 2010.

Antoniou, C., Savvides, A., Christou, A., and Fotopoulos, V. 2016. Unravelling chemical priming machinery in plants: the role of reactive oxygen–nitrogen–sulfur species in abiotic stress tolerance enhancement. Current opinion in plant biology 33:101-107.

Anttila, A., Bhat, R. V., Bond, J. A., Borghoff, S. J., Bosch, F. X., Carlson, G. P., Castegnaro, M., Cruzan, G., Gelderblom, W. C., and Hass, U. 2002. IARC monographs on the evaluation of carcinogenic risks to humans: Some traditional herbal medicines, some mycotoxins, naphthalene and styrene. IARC monographs on the evaluation of carcinogenic risks to humans 82.

Armengol, J., Moretti, A., Perrone, G., Vicent, A., Bengoechea, J., and García-Jiménez, J. 2005. Identification, incidence and characterization of *Fusarium proliferatum* on ornamental palms in Spain. European Journal of Plant Pathology 112:123-131.

Armitage, A. D., Taylor, A., Hulin, M. T., Jackson, A. C., Harrison, R. J., and Clarkson, J. P. 2019. Draft genome sequence of an onion basal rot isolate of *Fusarium proliferatum*. Microbiology resource announcements 8.

Audenaert, K., Callewaert, E., Höfte, M., De Saeger, S., and Haesaert, G. 2010. Hydrogen peroxide induced by the fungicide prothioconazole triggers deoxynivalenol (DON) production by *Fusarium graminearum*. BMC Microbiology 10:112.

Bairoch, A., Apweiler, R., Wu, C. H., Barker, W. C., Boeckmann, B., Ferro, S., Gasteiger, E., Huang, H., Lopez, R., and Magrane, M. 2005. The universal protein resource (UniProt). Nucleic acids research 33:D154-D159.

Bakker, M. G., Brown, D. W., Kelly, A. C., Kim, H.-S., Kurtzman, C. P., Mccormick, S. P., O'Donnell, K. L., Proctor, R. H., Vaughan, M. M., and Ward, T. J. 2018. Fusarium mycotoxins: a trans-disciplinary overview. Canadian Journal of Plant Pathology 40:161-171.

Bargen, S. v., Martinez, O., Schadock, I., Eisold, A. M., Gossmann, M., and Büttner, C. 2009. Genetic variability of phytopathogenic *Fusarium proliferatum* associated with crown rot in *Asparagus officinalis*. Journal of phytopathology 157:446-456.

Baty, F., Ritz, C., Charles, S., Brutsche, M., Flandrois, J.-P., and Delignette-Muller, M.-L. 2015. A toolbox for nonlinear regression in R: the package nlstools. Journal of Statistical Software 66:1-21.

Bayraktar, H., and Dolar, F. S. 2011. Molecular identification and genetic diversity of *Fusarium* species associated with onion fields in Turkey. Journal of Phytopathology 159:28-34.

Behrani, G., Syed, R., Abro, M., Jiskani, M., and Khanzada, M. 2015. Pathogenicity and chemical control of basal rot of onion caused by *Fusarium oxysporum* f. sp. *cepae*. Pakistan Journal of Agriculture, Agricultural Engineering and Veterinary Sciences 31:60-70.

Belz, R. G., and Piepho, H.-P. 2012. Modeling effective dosages in hormetic dose-response studies. PLOS ONE 7:e33432.

Blackman, L. M., Cullerne, D. P., Torrena, P., Taylor, J., and Hardham, A. R. 2015. RNA-Seq analysis of the expression of genes encoding cell wall degrading enzymes during infection of lupin (*Lupinus angustifolius*) by *Phytophthora parasitica*. PLOS ONE 10:e0136899.

Bolger, A. M., Lohse, M., and Usadel, B. 2014. Trimmomatic: a flexible trimmer for Illumina sequence data. Bioinformatics 30:2114-2120.

Brain, P., and Cousens, R. 1989. An equation to describe dose responses where there is stimulation of growth at low doses. Weed Research 29:93-96.

Brayford, D. 1996. *Fusarium oxysporum* f sp *cepae*. Mycopathologia 133:39-40.

Brent, K., and Hollomon, D. 2007. Fungicide resistance in crop pathogens: How can it be managed? 2nd Rev. Edn. Online. Fungicide Resistance Action Committee (FRAC). CropLife International, Brussels, Belgium.

Calabrese, E. J. 2004. Hormesis: from marginalization to mainstream: a case for hormesis as the default dose-response model in risk assessment. Toxicology and applied pharmacology 197:125-136.

Calabrese, E. J. 2005. Toxicological awakenings: the rebirth of hormesis as a central pillar of toxicology. Toxicology and applied pharmacology 204:1-8.

Calabrese, E. J. 2008. Hormesis: why it is important to toxicology and toxicologists. Environmental Toxicology and Chemistry: An International Journal 27:1451-1474.

Calabrese, E. J. 2013. Hormetic mechanisms. Critical reviews in toxicology 43:580-606.

Calabrese, E. J. 2017. Perspectives on Hormesis and Implications for Pesticides. Pages 83-100 in: Pesticide Dose: Effects on the Environment and Target and Non-Target Organisms. ACS Publications.

Calabrese, E. J., and Baldwin, L. A. 1997a. A quantitatively-based methodology for the evaluation of chemical hormesis. Human and Ecological Risk Assessment: An International Journal 3:545-554.

Calabrese, E. J., and Baldwin, L. A. 1997b. The dose determines the stimulation (and poison): development of a chemical hormesis database. International Journal of Toxicology 16:545-559.

Calabrese, E. J., and Baldwin, L. A. 1998. Hormesis as a biological hypothesis. Environmental Health Perspectives 106:357-362.

Calabrese, E. J., and Baldwin, L. A. 1999. Chemical hormesis: its historical foundations as a biological hypothesis. Toxicologic pathology 27:195-216.

Calabrese, E. J., and Baldwin, L. A. 2000. The marginalization of hormesis. Human & experimental toxicology 19:32-40.

Calabrese, E. J., and Baldwin, L. A. 2002. Defining hormesis. Human & experimental toxicology 21:91-97.

Calabrese, E. J., and Blain, R. 2005. The occurrence of hormetic dose responses in the toxicological literature, the hormesis database: an overview. Toxicology and applied pharmacology 202:289-301.

Calabrese, E. J., and Blain, R. B. 2011. The hormesis database: the occurrence of hormetic dose responses in the toxicological literature. Regulatory Toxicology and Pharmacology 61:73-81.

Calabrese, E. J., and Mattson, M. P. 2011. Hormesis provides a generalized quantitative estimate of biological plasticity. Journal of cell communication and signaling 5:25-38.

Calabrese, E. J., and Mattson, M. P. 2017. How does hormesis impact biology, toxicology, and medicine? NPJ aging and mechanisms of disease 3:1-8.

Calabrese, E. J., Baldwin, L. A., and Holland, C. D. 1999. Hormesis: a highly generalizable and reproducible phenomenon with important implications for risk assessment. Risk Analysis 19:261-281.

Calabrese, E. J., Agathokleous, E., Kozumbo, W. J., Stanek III, E. J., and Leonard, D. 2019. Estimating the range of the maximum hormetic stimulatory response. Environmental research 170:337-343.

Campos, M., Perruchon, C., Vasilieiadis, S., Menkissoglu-Spiroudi, U., Karpouzas, D., and Diez, M. 2015. Isolation and characterization of bacteria from acidic pristine soil environment able to transform iprodione and 3, 5-dichloraniline. International Biodeterioration & Biodegradation 104:201-211.

Campos, M., Karas, P. S., Perruchon, C., Papadopoulou, E. S., Christou, V., Menkissoglou-Spiroudi, U., Diez, M. C., and Karpouzas, D. G. 2017. Novel insights into the metabolic pathway of iprodione by soil bacteria. Environmental Science and Pollution Research 24:152-163.

Cedergreen, N., Ritz, C., and Streibig, J. C. 2005. Improved empirical models describing hormesis. Environmental Toxicology and Chemistry: An International Journal 24:3166-3172.

Cendoya, E., Nichea, M. J., del Pilar Monge, M., Zachetti, V. G., Chiacchiera, S. M., and Ramirez, M. L. 2020. Effect of fungicides commonly used for Fusarium head blight management on growth and fumonisin production by *Fusarium proliferatum*. Revista Argentina de Microbiología https://doi.org/10.1016/j.ram.2019.12.005 .

Chang, K., Hwang, S., Conner, R., Ahmed, H., Zhou, Q., Turnbull, G., Strelkov, S., McLaren, D., and Gossen, B. 2015. First report of *Fusarium proliferatum* causing root rot in soybean (*Glycine max* L.) in Canada. Crop Protection 67:52-58.

Conesa, A., Madrigal, P., Tarazona, S., Gomez-Cabrero, D., Cervera, A., McPherson, A., Szcześniak, M. W., Gaffney, D. J., Elo, L. L., and Zhang, X. 2016. A survey of best practices for RNA-seq data analysis. Genome biology 17:13.

Cong, M.-L., Zhang, B., Zhang, K., Li, G., and Zhu, F. 2019a. Stimulatory effects of sublethal doses of carbendazim on the virulence and sclerotial production of *Botrytis cinerea*. Plant Disease 103:2385-2391.

Cong, M., He, S., Zhang, J., Luo, C., and Zhu, F. 2019b. Hormetic Effects of Mixtures of Carbendazim and Iprodione on the Virulence of *Botrytis cinerea*. Plant disease 103:95-101.

Conn, K., Lutton, J., and Rosenberger, S. 2012. Onion disease guide: a practical guide for seedsmen, growers and agricultural advisors. Senminis Vegetable Seeds. Woodland.

Conner, R., Hwang, S., and Stevens, R. 1996. *Fusarium proliferatum*: A new causal agent of black point in wheat. Canadian Journal of Plant Pathology 18:419-423.

Costa-Silva, J., Domingues, D., and Lopes, F. M. 2017. RNA-Seq differential expression analysis: An extended review and a software tool. PLOS ONE 12:e0190152.

Cramer, C. S. 2000. Breeding and genetics of Fusarium basal rot resistance in onion. Euphytica 115:159-166.

Črešnar, B., and Petrič, Š. 2011. Cytochrome P450 enzymes in the fungal kingdom. Biochimica et Biophysica Acta (BBA)-Proteins and Proteomics 1814:29-35.

Cui, W., Beever, R. E., Parkes, S. L., Weeds, P. L., and Templeton, M. D. 2002. An osmosensing histidine kinase mediates dicarboximide fungicide resistance in *Botryotinia fuckeliana* (*Botrytis cinerea*). Fungal Genetics and Biology 36:187-198.

D'mello, J. F., Macdonald, A. M., Postel, D., Dijksma, W. T., Dujardin, A., and Placinta, C. M. 1998. Pesticide use and mycotoxin production in *Fusarium* and *Aspergillus* phytopathogens. European Journal of Plant Pathology 104:741-751.

De Waard, M. A., Andrade, A. C., Hayashi, K., Schoonbeek, H. j., Stergiopoulos, I., and Zwiers, L. H. 2006. Impact of fungal drug transporters on fungicide sensitivity, multidrug resistance and virulence. Pest Management Science: formerly Pesticide Science 62:195-207.

Dean, R., Van Kan, J. A. L., Pretorius, Z. A., Hammond-Kosack, K. E., Di Pietro, A., Spanu, P. D., Rudd, J. J., Dickman, M., Kahmann, R., Ellis, J., and Foster, G. D. 2012. The Top 10 fungal pathogens in molecular plant pathology. Molecular Plant Pathology 13:414-430.

Del Sorbo, G., Schoonbeek, H.-j., and De Waard, M. A. 2000. Fungal transporters involved in efflux of natural toxic compounds and fungicides. Fungal genetics and biology 30:1-15.

Deng, C., Zhao, Q., and Shukla, R. 2000. Detecting hormesis using a non-parametric rank test. Human & Experimental Toxicology 19:703-708.

Deng, C., Graham, R., and Shukla, R. 2001. Detecting and estimating hormesis using a model-based approach. Human and Ecological Risk Assessment 7:849-866.

Derbalah, A. S. H., Nakatani, N., and Sakugawa, H. 2003. Distribution, seasonal pattern, flux and contamination source of pesticides and nonylphenol residues in Kurose River water, Higashi-Hiroshima, Japan. Geochemical Journal 37:217-232.

Devreese, M., De Backer, P., and Croubels, S. 2013. Overview of the most important mycotoxins for the pig and poultry husbandry. Vlaams Diergeneeskundig Tijdschrift 82:171-180.

Di, Y.-L., Zhu, Z.-Q., Lu, X.-M., and Zhu, F.-X. 2015. Pathogenicity stimulation of *Sclerotinia sclerotiorum* by subtoxic doses of carbendazim. Plant Disease 99:1342-1346.

Di, Y.-L., Cong, M.-L., Zhang, R., and Zhu, F.-X. 2016a. Hormetic effects of trifloxystrobin on aggressiveness of *Sclerotinia sclerotiorum*. Plant Disease 100:2113-2118.

Di, Y.-L., Lu, X.-M., Zhu, Z.-Q., and Zhu, F.-X. 2016b. Time course of carbendazim stimulation on pathogenicity of *Sclerotinia sclerotiorum* indicates a direct stimulation mechanism. Plant Disease 100:1454-1459.

Dissanayake, M., Tanaka, S., and Ito, S. 2009a. Fumonisin B1 production by *Fusarium proliferatum* strains isolated from *Allium fistulosum* plants and seeds in Japan. Letters in Applied Microbiology 48:598-604.

Dissanayake, M. L. M. C., Kashima, R., Tanaka, S., and Ito, S.-i. 2009b. Pathogenic variation and molecular characterization of Fusarium species isolated from wilted Welsh onion in Japan. Journal of General Plant Pathology 75:37-45.

Duke, S. O. 2017. Pesticide dose–A parameter with many implications. Pages 1-13 in: Pesticide Dose: Effects on the Environment and Target and Non-Target Organisms. ACS Publications.

Edel-Hermann, V., and Lecomte, C. 2019. Current Status of *Fusarium oxysporum* Formae Speciales and Races. Phytopathology 109:512-530.

Elmer, W. H. 2015. Management of Fusarium crown and root rot of asparagus. Crop Protection 73:2-6.

Elzhov, T. V., Mullen, K. M., Spiess, A.-N., and Bolker, B. 2016. minpack.lm: R Interface to the Levenberg-Marquardt Nonlinear Least-Squares Algorithm Found in MINPACK, Plus Support for Bounds. R Package Version 1.2-1.

FAOSTAT. 2018. Top 10 Country production of Onions, dry. in: Country by commodity Food and Agriculture Organization of the United Nations.

Fernandez-Cornejo, J., Nehring, R. F., Osteen, C., Wechsler, S., Martin, A., and Vialou, A. 2014. Pesticide use in US agriculture: 21 selected crops, 1960-2008. USDA-ERS Economic Information Bulletin.

Flores, F. 2010. Effect of low doses of pesticides on soilborne pathogens: An approach to the hormetic response. Oklahoma State University.

Flores, F. J., and Garzón, C. D. 2013. Detection and assessment of chemical hormesis on the radial growth in vitro of oomycetes and fungal plant pathogens. Dose-Response 11:dose-response. 12-026.

FRAC. 2020. Fungicide Resistance Action Committee - FRAC Code List 2020: Fungal control agents sorted by cross resistance pattern and mode of action (including FRAC Code numbering).

Futane, A., Dandnaik, B., Salunkhe, S., Jadhav, P., and Magar, S. 2018. Management of storage diseases of onion by using different fungicides and antibiotics. International Journal of Current Microbiology and Applied Sciences 7:1149-1158.

Galván, G. A., Koning-Boucoiran, C. F., Koopman, W. J., Burger-Meijer, K., González, P. H., Waalwijk, C., Kik, C., and Scholten, O. E. 2008. Genetic variation among *Fusarium* isolates from onion, and resistance to Fusarium basal rot in related Allium species. European Journal of Plant Pathology 121:499-512.

Gálvez, L., Urbaniak, M., Waśkiewicz, A., Stępień, Ł., and Palmero, D. 2017. *Fusarium proliferatum*–Causal agent of garlic bulb rot in Spain: Genetic variability and mycotoxin production. Food Microbiology 67:41-48.

Gao, M.-L., Luan, Y.-S., Yu, H.-N., and Bao, Y.-M. 2016. First report of tomato leaf spot caused by *Fusarium proliferatum* in China. Canadian Journal of Plant Pathology 38:400-404.

Garzón, C. D., and Flores, F. J. 2013. Hormesis: Biphasic dose-responses to fungicides in plant pathogens and their potential threat to agriculture. Agricultural and Biological Sciences. Fungicides–Showcases of Integrated Plant Disease Management from Around the World 12:311-328.

Garzón, C. D., Molineros, J. E., Yánez, J. M., Flores, F. J., del Mar Jiménez-Gasco, M., and Moorman, G. W. 2011. Sublethal doses of mefenoxam enhance Pythium damping-off of geranium. Plant Disease 95:1233-1238.

Gawehns, F., Ma, L., Bruning, O., Houterman, P. M., Boeren, S., Cornelissen, B. J., Rep, M., and Takken, F. L. 2015. The effector repertoire of *Fusarium oxysporum* determines the tomato xylem proteome composition following infection. Frontiers in Plant Science 6:967.

González, I. 2014. Statistical analysis of RNA-Seq data. Universidad de Toulouse.

Gordon, T. R. 2017. *Fusarium oxysporum* and the Fusarium wilt syndrome. Annual Review of Phytopathology 55:23-39.

Gordon, T. R., Swett, C. L., and Wingfield, M. J. 2015. Management of Fusarium diseases affecting conifers. Crop Protection 73:28-39.

Green, R., Sang, H., Im, J., and Jung, G. 2018. Chlorothalonil biotransformation by cytochrome P450 monooxygenases in *Sclerotinia homoeocarpa*. FEMS Microbiology Letters 365:fny214.

Greenshields, D. L., Liu, G., Feng, J., Selvaraj, G., and Wei, Y. 2007. The siderophore biosynthetic gene SID1, but not the ferroxidase gene FET3, is required for full *Fusarium graminearum* virulence. Molecular Plant Pathology 8:411-421.

Grinstein, A., Elad, Y., Temkin-Gorodeiski, N., Rivan, Y., and Frankel, H. 1992. Reduced volume application of fungicides for the control of onion rots. Phytoparasitica 20:293.

Grothendieck, G. 2013. nls2: Non-linear regression with brute force. R Package Version 0.2.

Gutierrez, J. A., and Cramer, C. S. 2005. Screening short-day onion cultivars for resistance to fusarium basal rot. HortScience 40:157-160.

Gutleb, A. C., Morrison, E., and Murk, A. J. 2002. Cytotoxicity assays for mycotoxins produced by Fusarium strains: a review. Environmental Toxicology and Pharmacology 11:309-320.

Haapalainen, M., Latvala, S., Kuivainen, E., Qiu, Y., Segerstedt, M., and Hannukkala, A. 2016. *Fusarium oxysporum*, *F. proliferatum* and *F. redolens* associated with basal rot of onion in Finland. Plant Pathology 65:1310-1320.

Hagiwara, D., Matsubayashi, Y., Marui, J., Furukawa, K., Yamashino, T., Kanamaru, K., Kato, M., Abe, K., Kobayashi, T., and Mizuno, T. 2007. Characterization of the NikA histidine kinase implicated in the phosphorelay signal transduction of *Aspergillus nidulans,* with special reference to fungicide responses. Bioscience, Biotechnology, and Biochemistry 71:844-847.

Halley, S., Van Ee, G., Hofman, V., Panigrahi, S., and Gu, H. 2008. Fungicide deposition measurement by spray volume, drop size, and sprayer system in cereal grains. Applied Engineering in Agriculture 24:15-21.

Hayes, B. M., Anderson, M. A., Traven, A., van der Weerden, N. L., and Bleackley, M. R. 2014. Activation of stress signalling pathways enhances tolerance of fungi to chemical fungicides and antifungal proteins. Cellular and Molecular Life Sciences 71:2651-2666.

Hématy, K., Cherk, C., and Somerville, S. 2009. Host–pathogen warfare at the plant cell wall. Current Opinion in Plant Biology 12:406-413.

Hofman, V., and Solseng, E. 2004. Spray equipment and calibration. North Dakota State University Extension Service.

Hosmani, P. S., Shippy, T., Miller, S., Benoit, J. B., Munoz-Torres, M., Flores-Gonzalez, M., Mueller, L. A., Wiersma-Koch, H., D'Elia, T., and Brown, S. J. 2019. A quick guide for student-driven community genome annotation. PLOS Computational Biology 15:e1006682.

Houterman, P. M., Speijer, D., Dekker, H. L., de Koster, C. G., Cornelissen, B. J., and Rep, M. 2007. The mixed xylem sap proteome of *Fusarium oxysporum*-infected tomato plants. Molecular Plant Pathology 8:215-221.

Hu, S., Xu, Q., Zhang, Y., and Zhu, F. 2019. Stimulatory effects of boscalid on virulence of *Sclerotinia sclerotiorum* indicate hormesis may be masked by inhibitions. Plant Disease https://doi.org/10.1094/PDIS-07-19-1421-RE.

Hulvey, J., Popko, J. T., Sang, H., Berg, A., and Jung, G. 2012. Overexpression of ShCYP51B and ShatrD in *Sclerotinia homoeocarpa* isolates exhibiting practical field resistance to a demethylation inhibitor fungicide. Applied and Environmental Microbiology 78:6674-6682.

Hunt, D. L., and Bowman, D. 2004. A parametric model for detecting hormetic effects in developmental toxicity studies. Risk Analysis: An International Journal 24:65-72.

Isack, Y., Benichis, M., Gillet, D., and Gamliel, A. 2014. A selective agar medium for isolation, enumeration and morphological identification of *Fusarium proliferatum*. Phytoparasitica 42:541-547.

Jakše, M., and Bohanec, B. 2003. Haploid induction in onion via gynogenesis. Pages 281-285 in: Doubled Haploid Production in Crop Plants. Springer.

Jimenez, M., Logrieco, A., and Bottalico, A. 1993. Occurrence and pathogenicity of *Fusarium* species in banana fruits. Journal of Phytopathology 137:214-220.

Jurado, M., Marín, P., Callejas, C., Moretti, A., Vázquez, C., and González-Jaén, M. T. 2010. Genetic variability and fumonisin production by *Fusarium proliferatum*. Food Microbiology 27:50-57.

Kalman, B., Abraham, D., Graph, S., Perl-Treves, R., Meller Harel, Y., and Degani, O. 2020. Isolation and Identification of *Fusarium* spp., the Causal Agents of Onion (Allium cepa) Basal Rot in Northeastern Israel. Biology 9:69.

Khan, A., Singh, P., and Srivastava, A. 2018. Synthesis, nature and utility of universal iron chelator–Siderophore: A review. Microbiological research 212:103-111.

Kim, D., Langmead, B., and Salzberg, S. L. 2015. HISAT: a fast spliced aligner with low memory requirements. Nature Methods 12:357-360.

King, B. C., Waxman, K. D., Nenni, N. V., Walker, L. P., Bergstrom, G. C., and Gibson, D. M. 2011. Arsenal of plant cell wall degrading enzymes reflects host preference among plant pathogenic fungi. Biotechnology for Biofuels 4:4.

Ko, S.-S., Chang, W.-N., Wang, J.-F., Cherng, S.-J., and Shanmugasundaram, S. 2002. Storage variability among short-day onion cultivars under high temperature and high relative humidity, and its relationship with disease incidence and bulb characteristics. Journal of the American Society for Horticultural Science 127:848-854.

Kretschmer, M., Leroch, M., Mosbach, A., Walker, A.-S., Fillinger, S., Mernke, D., Schoonbeek, H.-J., Pradier, J.-M., Leroux, P., and De Waard, M. A. 2009. Fungicide-driven evolution and molecular basis of multidrug resistance in field populations of the grey mould fungus *Botrytis cinerea*. PLOS Pathogens 5:e1000696.

Kubicek, C. P., Starr, T. L., and Glass, N. L. 2014. Plant cell wall–degrading enzymes and their secretion in plant-pathogenic fungi. Annual review of phytopathology 52:427-451.

Kulik, T., Łojko, M., Jestoi, M., and Perkowski, J. 2012. Sublethal concentrations of azoles induce tri transcript levels and trichothecene production in *Fusarium graminearum*. FEMS Microbiology Letters 335:58-67.

Kumar, V., Neeraj, S. S., and Sagar, N. A. 2015. Post harvest management of fungal diseases in onion—a review. International Journal of Current Microbiology and Applied Sciences 4:737-752.

Lacy, M., and Roberts, D. 1982. Yields of onion cultivars in Midwestern organic soils infested with *Fusarium oxysporum* f. sp. *cepae* and Pyrenochaeta terrestris. Plant Disease V66:1003-1006.

Lee, S., Son, H., Lee, J., Lee, Y.-R., and Lee, Y.-W. 2011. A putative ABC transporter gene, ZRA1, is required for zearalenone production in *Gibberella zeae*. Current Genetics 57:343.

Leoni, C., de Vries, M., ter Braak, C. J., van Bruggen, A. H., and Rossing, W. A. 2013. *Fusarium oxysporum* f. sp. *cepae* dynamics: in-plant multiplication and crop sequence simulations. European Journal of Plant Pathology 137:545-561.

Leslie, J. F., and Summerell, B. A. 2008. The Fusarium laboratory manual. John Wiley & Sons.

Lombard, L., Sandoval-Denis, M., Lamprecht, S. C., and Crous, P. 2019. Epitypification of *Fusarium oxysporum*–clearing the taxonomic chaos. Persoonia: Molecular Phylogeny and Evolution of Fungi 43:1.

Love, M. I., Huber, W., and Anders, S. 2014. Moderated estimation of fold change and dispersion for RNA-seq data with DESeq2. Genome Biology 15:550.

Lu, X., Zhang, R., Cong, M., Li, J., and Zhu, F. 2018. Stimulatory effects of flusilazole on virulence of *Sclerotinia sclerotiorum*. Plant Disease 102:197-201.

Ma, L.-J., Van Der Does, H. C., Borkovich, K. A., Coleman, J. J., Daboussi, M.-J., Di Pietro, A., Dufresne, M., Freitag, M., Grabherr, M., and Henrissat, B. 2010. Comparative genomics reveals mobile pathogenicity chromosomes in *Fusarium.* Nature 464:367-373.

Ma, Z., Yan, L., Luo, Y., and Michailides, T. J. 2007. Sequence variation in the two-component histidine kinase gene of *Botrytis cinerea* associated with resistance to dicarboximide fungicides. Pesticide Biochemistry and Physiology 88:300-306.

Magan, N., Hope, R., Colleate, A., and Baxter, E. 2002. Relationship between growth and mycotoxin production by *Fusarium* species, biocides and environment. Pages 685-690 in: Mycotoxins in Plant Disease. Springer.

Maqsood, A., Wu, C., Ahmar, S., and Wu, H. 2020. Cytological and Gene Profile Expression Analysis Reveals Modification in Metabolic Pathways and Catalytic Activities Induce Resistance in *Botrytis cinerea* Against Iprodione Isolated From Tomato. International Journal of Molecular Sciences 21:4865.

Marín, P., de Ory, A., Cruz, A., Magan, N., and González-Jaén, M. T. 2013. Potential effects of environmental conditions on the efficiency of the antifungal tebuconazole controlling *Fusarium verticillioides* and *Fusarium proliferatum* growth rate and fumonisin biosynthesis. International Journal of Food Microbiology 165:251-258.

Mathioni, S. M., Beló, A., Rizzo, C. J., Dean, R. A., and Donofrio, N. M. 2011. Transcriptome profiling of the rice blast fungus during invasive plant infection and in vitro stresses. BMC Genomics 12:49.

Matthies, A., Walker, F., and Buchenauer, H. 1999. Interference of selected fungicides, plant growth retardants as well as piperonyl butoxide and 1-aminobenzotriazole in trichothecene production of *Fusarium graminearum* (strain 4528) in vitro/Eingriff ausgewählter Fungizide, Pflanzenwachstumshemmer sowie Piperonylbutoxid und 1-Aminobenzotriazol in die Trichothecen-Produktion von *Fusarium graminearum* (Stamm 4528) in vitro. Zeitschrift für Pflanzenkrankheiten und Pflanzenschutz/Journal of Plant Diseases and Protection:198-212.

McGovern, R. 2015. Management of tomato diseases caused by *Fusarium oxysporum*. Crop Protection 73:78-92.

Medema, M. H., Blin, K., Cimermancic, P., de Jager, V., Zakrzewski, P., Fischbach, M. A., Weber, T., Takano, E., and Breitling, R. 2011. antiSMASH: rapid identification, annotation and analysis of secondary metabolite biosynthesis gene clusters in bacterial and fungal genome sequences. Nucleic Acids Research 39:W339-W346.

Michielse, C. B., and Rep, M. 2009. Pathogen profile update: *Fusarium oxysporum*. Molecular Plant Pathology 10:311-324.

Mohan, S., Bijman, V., and Knott, E. 1997. Bulb rot of onions caused by *Fusarium proliferatum*. Phytopathology 87:S67.

Munkvold, G. P. 2017. *Fusarium* species and their associated mycotoxins. Pages 51-106 in: Mycotoxigenic Fungi. Springer.

Musser, S. M., and Plattner, R. D. 1997. Fumonisin composition in cultures of *Fusarium moniliforme, Fusarium proliferatum*, and *Fusarium nygami*. Journal of Agricultural and Food Chemistry 45:1169-1173.

NCBI. 1988. Taxonomy [*Fusarium oxysporum*]. Bethesda (MD): National Library of Medicine (US).

Nguyen, T. T. X., Dehne, H.-W., and Steiner, U. 2016. Histopathological assessment of the infection of maize leaves by *Fusarium graminearum*, *F. proliferatum*, and *F. verticillioides*. Fungal Biology 120:1094-1104.

Nunez-Rodriguez, J. C., Ruiz-Roldán, C., Lemos, P., Membrives, S., and Hera, C. 2020. The phosphatase Ptc6 is involved in virulence and MAPK signalling in *Fusarium oxysporum*. Molecular Plant Pathology 21:206-217.

O'Donnell, K., Sutton, D. A., Rinaldi, M. G., Magnon, K. C., Cox, P. A., Revankar, S. G., Sanche, S., Geiser, D. M., Juba, J. H., and Van Burik, J.-A. H. 2004. Genetic diversity of human pathogenic members of the *Fusarium oxysporum* complex inferred from multilocus DNA sequence data and amplified fragment length polymorphism analyses: evidence for the recent dispersion of a geographically widespread clonal lineage and nosocomial origin. Journal of Clinical Microbiology 42:5109-5120.

O'Donnell, K., Sutton, D. A., Rinaldi, M. G., Sarver, B. A., Balajee, S. A., Schroers, H.-J., Summerbell, R. C., Robert, V. A., Crous, P. W., and Zhang, N. 2010. Internet-accessible DNA sequence database for identifying fusaria from human and animal infections. Journal of Clinical Microbiology 48:3708-3718.

O'Donnell, K., Kistler, H. C., Cigelnik, E., and Ploetz, R. C. 1998. Multiple evolutionary origins of the fungus causing Panama disease of banana: concordant evidence from nuclear and mitochondrial gene genealogies. Proceedings of the National Academy of Sciences 95:2044-2049.

O'Donnell, K., Gueidan, C., Sink, S., Johnston, P. R., Crous, P. W., Glenn, A., Riley, R., Zitomer, N. C., Colyer, P., and Waalwijk, C. 2009. A two-locus DNA sequence database for typing plant and human pathogens within the *Fusarium oxysporum* species complex. Fungal Genetics and Biology 46:936-948.

Ochiai, N., Fujimura, M., Motoyama, T., Ichiishi, A., Usami, R., Horikoshi, K., and Yamaguchi, I. 2001. Characterization of mutations in the two-component histidine kinase gene that confer fludioxonil resistance and osmotic sensitivity in the os-1 mutants of *Neurospora crassa*. Pest Management Science: formerly Pesticide Science 57:437-442.

Oshima, M., Fujimura, M., Banno, S., Hashimoto, C., Motoyama, T., Ichiishi, A., and Yamaguchi, I. 2002. A point mutation in the two-component histidine kinase BcOS-1 gene confers dicarboximide resistance in field isolates of *Botrytis cinerea*. Phytopathology 92:75-80.

Özer, N., and Köycü, N. 1998. Evaluation of seed treatments for controlling *Aspergillus niger* and *Fusarium oxysporum* on onion seed. Phytopathologia Mediterranea:33-40.

Palacios, S. A., Susca, A., Haidukowski, M., Stea, G., Cendoya, E., Ramirez, M. L., Chulze, S. N., Farnochi, M. C., Moretti, A., and Torres, A. M. 2015. Genetic variability and fumonisin production by *Fusarium proliferatum* isolated from durum wheat grains in Argentina. International Journal of Food Microbiology 201:35-41.

Parthasarathy, S., Rajamanickam, S., and Muthamilan, M. 2016. Allium diseases: A global perpective. Innovative Farming 1:171-178.

Pasanen, A.-L., Kalliokoski, P., Pasanen, P., Jantunen, M., and Nevalainen, A. 1991. Laboratory studies on the relationship between fungal growth and atmospheric temperature and humidity. Environment International 17:225-228.

Pedro, H., Yates, A. D., Kersey, P. J., and De Silva, N. H. 2019. Collaborative annotation redefines gene sets for crucial phytopathogens. Frontiers in Microbiology 10:2477.

Pertea, M., Kim, D., Pertea, G. M., Leek, J. T., and Salzberg, S. L. 2016. Transcript-level expression analysis of RNA-seq experiments with HISAT, StringTie and Ballgown. Nature Protocols 11:1650.

Poschenrieder, C., Cabot, C., Martos, S., Gallego, B., and Barceló, J. 2013. Do toxic ions induce hormesis in plants? Plant Science 212:15-25.

Pradhan, S., Flores, F. J., Melouk, H., Walker, N. R., Molineros, J. E., and Garzón, C. D. 2017a. Chemical hormesis on plant pathogenic fungi and oomycetes. Pages 121-133 in: Pesticide Dose: Effects on the Environment and Target and Non-Target Organisms. ACS Publications.

Pradhan, S., Flores, F. J., Molineros, J. E., Walker, N. R., Melouk, H., and Garzón, C. D. 2017b. Improved assessment of mycelial growth stimulation by low doses of mefenoxam in plant pathogenic *Globisporangium* species. European Journal of Plant Pathology 147:477-487.

Pradhan, S., Miller, L., Marcillo, V., Koch, A. R., Graf Grachet, N., Molineros, J. E., Walker, N. R., Melouk, H., and Garzon, C. D. 2019. Hormetic Effects of Thiophanate-Methyl in Multiple Isolates of *Sclerotinia homoeocarpa*. Plant Disease 103:89-94.

Proctor, R. H., Desjardins, A. E., and Moretti, A. 2009. Biological and chemical complexity of *Fusarium proliferatum*. Pages 97-111 in: The role of plant pathology in food safety and food security. Springer.

Proctor, R. H., Brown, D. W., Plattner, R. D., and Desjardins, A. E. 2003. Co-expression of 15 contiguous genes delineates a fumonisin biosynthetic gene cluster in *Gibberella moniliformis*. Fungal Genetics and Biology 38:237-249.

Proctor, R. H., Plattner, R. D., Brown, D. W., Seo, J.-A., and Lee, Y.-W. 2004. Discontinuous distribution of fumonisin biosynthetic genes in the *Gibberella fujikuroi* species complex. Mycological Research 108:815-822.

Qi, P.-F., Zhang, Y.-Z., Liu, C.-H., Zhu, J., Chen, Q., Guo, Z.-R., Wang, Y., Xu, B.-J., Zheng, T., and Jiang, Y.-F. 2018. *Fusarium graminearum* ATP-binding cassette transporter gene FgABCC9 is required for its transportation of salicylic acid, fungicide resistance, mycelial growth and pathogenicity towards wheat. International Journal of Molecular Sciences 19:2351.

R Core Team. 2019. R: A language and environment for statistical computing. R Foundation for Statistical Computing. Vienna, Austria.

Rasiukevičiūtė, N., Supronienė, S., and Valiuškaitė, A. 2016. Effective onion leaf fleck management and variability of storage pathogens. Open Life Sciences 11:259-269.

Ritieni, A., Fogliano, V., Randazzo, G., Scarallo, A., Logrieco, A., Moretti, A., Manndina, L., and Bottalico, A. 1995. Isolation and characterization of fusaproliferin, a new toxic metabolite from *Fusarium proliferatum*. Natural Toxins 3:17-20.

Ritz, C., Strebig, J. C., and Ritz, M. C. 2016. Package 'drc'. Creative Commons: Mountain View, CA, USA.

Ritz, C., Baty, F., Streibig, J. C., and Gerhard, D. 2015. Dose-response analysis using R. PlOS ONE 10:e0146021.

Robinson, M. D., McCarthy, D. J., and Smyth, G. K. 2010. edgeR: a Bioconductor package for differential expression analysis of digital gene expression data. Bioinformatics 26:139-140.

Samaras, A., Ntasiou, P., Myresiotis, C., and Karaoglanidis, G. 2020. Multidrug resistance of *Penicillium expansum* to fungicides: whole transcriptome analysis of MDR strains reveals overexpression of efflux transporter genes. International Journal of Food Microbiology 335:108896.

Sang, H., Hulvey, J. P., Green, R., Xu, H., Im, J., Chang, T., and Jung, G. 2018. A xenobiotic detoxification pathway through transcriptional regulation in filamentous fungi. Mbio 9:e00457-18. https://doi.org/10 .1128/mBio.00457-18.

Santos Pereira, C., C Cunha, S., and Fernandes, J. O. 2019. Prevalent mycotoxins in animal feed: Occurrence and analytical methods. Toxins 11:290.

Saravanakumari, K., Thiruvudainambi, S., Ebenezar, E., and Senthil, N. 2019. Efficacy of some fungicides and oil cake extracts against basal rot of onion caused by *Fusarium oxysporum*. International Journal of Farm Sciences 9:93-96.

Sasaki, K., Nakahara, K., Tanaka, S., Shigyo, M., and Ito, S.-i. 2015. Genetic and pathogenic variability of *Fusarium oxysporum* f. sp. *cepae* isolated from onion and Welsh onion in Japan. Phytopathology 105:525-532.

Schabenberger, O., Tharp, B. E., Kells, J. J., and Penner, D. 1999. Statistical tests for hormesis and effective dosages in herbicide dose response. Agronomy Journal 91:713-721.

Schulz, H. 1887. Zur lehre von der arzneiwirkung. Archiv für pathologische Anatomie und Physiologie und für klinische Medicin 108:423-445.

Schulz, H. 1888. Ueber hefegifte. Archiv für die gesamte Physiologie des Menschen und der Tiere 42:517-541.

Schwartz, H. F., and Mohan, S. K. 2008. Compendium of onion and garlic diseases and pests, Second Edition. American Phytopathological Society.

Segmüller, N., Ellendorf, U., Tudzynski, B., and Tudzynski, P. 2007. BcSAK1, a stress-activated mitogen-activated protein kinase, is involved in vegetative differentiation and pathogenicity in *Botrytis cinerea*. Eukaryotic Cell 6:211-221.

Shin, J. Y., Bui, D. C., Lee, Y., Nam, H., Jung, S., Fang, M., Kim, J. C., Lee, T., Kim, H., and Choi, G. J. 2017. Functional characterization of cytochrome P450 monooxygenases in the cereal head blight fungus *Fusarium graminearum*. Environmental Microbiology 19:2053-2067.

Sintayehu, A., Sakhuja, P., Fininsa, C., and Ahmed, S. 2011. Management of fusarium basal rot (*Fusarium oxysporum* f. sp. *cepae*) on shallot through fungicidal bulb treatment. Crop Protection 30:560-565.

Smith, G. W. 2018. Fumonisins. Pages 1003-1018 in: Veterinary toxicology. Elsevier.

Smith, R., Biscaro, A., Cahn, M., Daugovish, O., Natwick, E., Nunez, J., Takele, E., and Turini, T. 2011. Fresh-market bulb onion production in California. University of California Agriculture and Natural Services.

Somani, D., Adhav, R., Prashant, R., and Kadoo, N. Y. 2019. Transcriptomics analysis of propiconazole-treated *Cochliobolus sativus* reveals new putative azole targets in the plant pathogen. Functional & Integrative Genomics 19:453-465.

Southam, C. M. 1943. Effects of extract of western red-cedar heartwood on certain wood-decaying fungi in culture. Phytopathology 33:517-524.

Sperschneider, J., Dodds, P. N., Singh, K. B., and Taylor, J. M. 2018. ApoplastP: prediction of effectors and plant proteins in the apoplast using machine learning. New Phytologist 217:1764-1778.

Sperschneider, J., Gardiner, D. M., Dodds, P. N., Tini, F., Covarelli, L., Singh, K. B., Manners, J. M., and Taylor, J. M. 2016. EffectorP: predicting fungal effector proteins from secretomes using machine learning. New Phytologist 210:743-761.

Srivastava, S., Kadooka, C., and Uchida, J. Y. 2018. *Fusarium* species as pathogen on orchids. Microbiological Research 207:188-195.

Stankovic, S., Levic, J., Petrovic, T., Logrieco, A., and Moretti, A. 2007. Pathogenicity and mycotoxin production by *Fusarium proliferatum* isolated from onion and garlic in Serbia. European Journal of Plant Pathology 118:165-172.

Stebbing, A. 1997. A theory for growth hormesis. Belle Newsletter 6.

Steinkellner, S., Mammerler, R., and Vierheilig, H. 2005. Microconidia germination of the tomato pathogen *Fusarium oxysporum* in the presence of root exudates. Journal of plant interactions 1:23-30.

Stępień, Ł., Koczyk, G., and Waśkiewicz, A. 2011. Genetic and phenotypic variation of *Fusarium proliferatum* isolates from different host species. Journal of Applied Genetics 52:487.

Stewart, J., Otto, K., Cline, G., Dumroese, K., Klopfenstein, N., and Kim, M.-S. 2016. First report of *Fusarium proliferatum* causing Fusarium root disease on sugar pine (*Pinus lambertiana*) in a forest container nursery in California. Plant Disease. 100 (12): 2534. 100:2534.

Stivers, L. 1999. Crop profile: onions in New York. Cornell Cooperative Extension, Rochester, NY.

Stockmann-Juvala, H., and Savolainen, K. 2008. A review of the toxic effects and mechanisms of action of fumonisin B1. Human & Experimental Toxicology 27:799-809.

Strimmer, K. 2008. fdrtool: a versatile R package for estimating local and tail area-based false discovery rates. Bioinformatics 24:1461-1462.

Sullivan, D. M., Brown, B., Shock, C. C., Horneck, D. A., Stevens, R., Pelter, G., and Feibert, E. B. G. 2001. Nutrient management for onions in the Pacific Northwest. Pacific Northwest Extension.

Summerell, B. A., Salleh, B., and Leslie, J. F. 2003. A utilitarian approach to Fusarium identification. Plant Disease 87:117-128.

Szabadi, E. 1977. A model of two functionally antagonistic receptor populations activated by the same agonist. Journal of Theoretical Biology 69:101-112.

Tanaka, C., and Izumitsu, K. 2010. Two-component signaling system in filamentous fungi and the mode of action of dicarboximide and phenylpyrrole fungicides, fungicides, Odile Carisse, IntechOpen, DOI: 10.5772/13774, https://www.intechopen.com/books/fungicides/two-component-signaling-system-in-filamentous-fungi-and-the-mode-of-action-of-dicarboximide-and-phen

Tarazona, S., García-Alcalde, F., Dopazo, J., Ferrer, A., and Conesa, A. 2011. Differential expression in RNA-seq: a matter of depth. Genome research 21:2213-2223.

Tarazona, S., Furió-Tarí, P., Turrà, D., Pietro, A. D., Nueda, M. J., Ferrer, A., and Conesa, A. 2015. Data quality aware analysis of differential expression in RNA-seq with NOISeq R/Bioc package. Nucleic Acids Research 43:e140-e140.

Taylor, A., Vágány, V., Jackson, A. C., Harrison, R. J., Rainoni, A., and Clarkson, J. P. 2016. Identification of pathogenicity-related genes in *Fusarium oxysporum* f. sp. *cepae*. Molecular Plant Pathology 17:1032-1047.

Taylor, A., Vagany, V., Barbara, D., Thomas, B., Pink, D., Jones, J., and Clarkson, J. 2013. Identification of differential resistance to six *Fusarium oxysporum* f. sp. *cepae* isolates in commercial onion cultivars through the development of a rapid seedling assay. Plant Pathology 62:103-111.

Tini, F., Beccari, G., Onofri, A., Ciavatta, E., Gardiner, D. M., and Covarelli, L. 2020. Fungicides May Have Differential efficacies towards the main causal agents of Fusarium head blight of wheat. Pest Management Science.

Toit, L. d., Inglis, D., and Pelter, G. 2003. *Fusarium proliferatum* pathogenic on onion bulbs in Washington. Plant Disease 87:750-750.

Turrà, D., Segorbe, D., and Di Pietro, A. 2014. Protein kinases in plant-pathogenic fungi: conserved regulators of infection. Annual Review of Phytopathology 52:267-288.

Untergasser, A., Cutcutache, I., Koressaar, T., Ye, J., Faircloth, B. C., Remm, M., and Rozen, S. G. 2012. Primer3—new capabilities and interfaces. Nucleic Acids Research 40:e115-e115.

Urban, M., Cuzick, A., Seager, J., Wood, V., Rutherford, K., Venkatesh, S. Y., De Silva, N., Martinez, M. C., Pedro, H., Yates, A. D., Hassani-Pak, K., and Hammond-Kosack, K. E. 2019. PHI-base: the pathogen–host interactions database. Nucleic Acids Research 48:D613-D620.

USDA-NASS. 2019. 2017 Census of Agriculture. United States Summary and State Data. Volume 1. Geographic Area Series. Part 51.

USDA. 2020a. Vegetables 2019 Summary. in: Vegetables Annual Summary United States Department of Agriculture (USDA) Economis, Statistics and Market Information System.

USDA. 2020b. The PLANTS Database. National Plant Data Team, Greensboro, NC 27401-4901 USA. https://plants.sc.egov.usda.gov/java/ .

Viaud, M., Fillinger, S., Liu, W., Polepalli, J. S., Le Pêcheur, P., Kunduru, A. R., Leroux, P., and Legendre, L. 2006. A class III histidine kinase acts as a novel virulence factor in *Botrytis cinerea*. Molecular Plant-Microbe Interactions 19:1042-1050.

Wang, J., Bradley, C. A., Stenzel, O., Pedersen, D. K., Reuter-Carlson, U., and Chilvers, M. I. 2017. Baseline sensitivity of *Fusarium virguliforme* to fluopyram fungicide. Plant Disease 101:576-582.

Wang, Z., Gerstein, M., and Snyder, M. 2009. RNA-Seq: a revolutionary tool for transcriptomics. Nature reviews genetics 10:57-63.

Waśkiewicz, A., Stępień, Ł., Wilman, K., and Kachlicki, P. 2013. Diversity of pea-associated *F. proliferatum* and *F. verticillioides* populations revealed by FUM1 sequence analysis and fumonisin biosynthesis. Toxins 5:488-503.

Wickham, H., Averick, M., Bryan, J., Chang, W., McGowan, L. D. A., François, R., Grolemund, G., Hayes, A., Henry, L., and Hester, J. 2019. Welcome to the Tidyverse. Journal of Open Source Software 4:1686.

Wolf, J. B. 2013. Principles of transcriptome analysis and gene expression quantification: an RNA-seq tutorial. Molecular Ecology Resources 13:559-572.

Wolf, T., Shelest, V., Nath, N., and Shelest, E. 2015. CASSIS and SMIPS: promoter-based prediction of secondary metabolite gene clusters in eukaryotic genomes. Bioinformatics 32:1138-1143.

Wu, L., Conner, R., Wang, X., Xu, R., and Li, H. 2016. Variation in growth, colonization of maize, and metabolic parameters of GFP-and DsRed-labeled *Fusarium verticillioides* strains. Phytopathology 106:890-899.

Xie, C., Mao, X., Huang, J., Ding, Y., Wu, J., Dong, S., Kong, L., Gao, G., Li, C. Y., and Wei, L. 2011. KOBAS 2.0: a web server for annotation and identification of enriched pathways and diseases. Nucleic Acids Research 39:W316-322.

Xu, X., Bailey, J. A., and Cooke, B. 2003. Epidemiology of Mycotoxin Producing Fungi. Springer.

Yang, Z., Jiang, W., Wang, X., Cheng, T., Zhang, D., Wang, H., Qiu, J., Cao, L., Wang, X., and Hong, Q. 2018. An amidase gene ipaH is responsible for the initial degradation step of iprodione in strain *Paenarthrobacter* sp. YJN-5. Applied and Environmental Microbiology 84:e01150-18. https:// doi.org/10.1128/AEM.01150-18.

Yin, Y., Mao, X., Yang, J., Chen, X., Mao, F., and Xu, Y. 2012. dbCAN: a web resource for automated carbohydrate-active enzyme annotation. Nucleic Acids Research 40:W445-W451.

Yu, G., Wang, L.-G., Han, Y., and He, Q.-Y. 2012. clusterProfiler: an R package for comparing biological themes among gene clusters. Omics: a journal of integrative biology 16:284-287.

Yurchenko, E. G., Savchuk, N., Porotikova, E., and Vinogradova, S. 2019. First report of grapevine (*Vitis sp*.) cluster blight caused by *Fusarium proliferatum* in Russia. Plant Disease https://doi.org/10.1094/PDIS-05-19-0938-PDN

Zainudin, N. A. I. M., Hamzah, F. A., Kusai, N. A., Zambri, N. S., and Salleh, S. 2017. Characterization and pathogenicity of *Fusarium proliferatum* and *Fusarium verticillioides*, causal agents of Fusarium ear rot of corn. Turkish Journal of Biology 41:220-230.

Zhang, H., Yohe, T., Huang, L., Entwistle, S., Wu, P., Yang, Z., Busk, P. K., Xu, Y., and Yin, Y. 2018. dbCAN2: a meta server for automated carbohydrate-active enzyme annotation. Nucleic Acids Research 46:W95-W101.

Zhang, R., Zhang, Y., Xu, Q., Li, J., and Zhu, F. 2019. Hormetic Effects of Mixtures of Dimethachlone and Prochloraz on *Sclerotinia sclerotiorum*. Plant Disease 103:546-554.

Zhang, X., Ding, L., Kang, L., and Wang, Z.-Y. 2012. Estrogen receptor-alpha 36 mediates mitogenic antiestrogen signaling in ER-negative breast cancer cells. PLOS ONE 7:e30174.

Zhao, Z., Liu, H., Wang, C., and Xu, J.-R. 2013. Comparative analysis of fungal genomes reveals different plant cell wall degrading capacity in fungi. BMC Genomics 14:1-15.

Zhou, F., Liang, H.-J., Di, Y.-L., You, H., and Zhu, F.-X. 2014. Stimulatory effects of sublethal doses of dimethachlon on *Sclerotinia sclerotiorum*. Plant Disease 98:1364-1370.

Zhu, Y., Abdelraheem, A., Sanogo, S., Wedegaertner, T., Nichols, R. L., and Zhang, J. 2019. First report of cotton (Gossypium L.) wilt caused by *Fusarium proliferatum* in New Mexico, USA. Plant Disease.

Zohri, A., Sabah, A. M., and Abdel-Gawad, K. 1992. Fungal flora and mycotoxins associated with onion (*Allium cepa* L.) in Egypt. The Korean Journal of Mycology 20:302-308.

APPENDICES

SUPPLEMENTARY TABLES

Supplementary Table 1. Differentially expressed genes identified as carbohydrate-active enzymes using dbCAN2 metaserver.

GENE_ID	Log2FC	padj	Protein name	CAZyme assignment	SignalP
MSTRG.11261	0.975254	0.012057	Probable cellulase	CBM1+GH5_5	Yes
MSTRG.6798	0.865833	0.000193	Related to beta-mannosidase	GH2	Yes
MSTRG.1095	0.887965	0.019535	Glucanase (EC 3.2.1.-)	GH7+CBM1	Yes
MSTRG.10202	1.39967	8.05E-05		GH67	No
MSTRG.11334	1.246926	0.006416	GH115_C domain-containing protein	GH115	Yes
MSTRG.3888	1.494179	5.07E-05	Related to L-sorbosone dehydrogenase	AA12	Yes
MSTRG.13401	0.998963	3.24E-12	Mannan endo-1,6-alpha-mannosidase (EC 3.2.1.101)	GH76	No
MSTRG.13155	1.261478	9.27E-08	Related to putative arabinase	GH43	Yes
MSTRG.11253	1.124242	0.010367	Related to cellulose binding protein CEL1	AA9+CBM1	Yes
MSTRG.2194	2.014575	4.72E-08	Related to beta-mannanase	GH5_7	Yes
MSTRG.3917	1.259252	5.10E-05	Related to beta-mannanase	GH5+CBM1	Yes
MSTRG.6762	1.001506	0.006304	Related to deacetylase	CE4	No
MSTRG.7788	1.017913	0.041227	Probable acetylxylan esterase	CE1	Yes
MSTRG.10201	0.903171	0.043224	Glucanase (EC 3.2.1.-)	CBM1+GH6	Yes
MSTRG.3878	1.207099	0.000309	Beta-xylanase (EC 3.2.1.8)	GH10	Yes
MSTRG.12670	0.989153	0.03687	Related to cellulose-binding GDSL lipase/acylhydrolase	CE16	Yes
MSTRG.8765	1.581664	3.12E-08	Glucanase (EC 3.2.1.-)	GH7	Yes
MSTRG.6690	1.142131	0.016811	Related to xylosidase/arabinosidase	GH43_14	No
MSTRG.10249	1.514096	5.60E-08	Related to endoglucanase IV	AA9	No
MSTRG.10924	1.857588	0.012057	Related to alpha-L-arabinofuranosidase II	GH43_26	No
MSTRG.8874	6.172824	0.037668	Related to endoglucanase	GH5_22	No
MSTRG.11995	1.058251	0.024378	Related to lipase/acylhydrolase	CE2	Yes
MSTRG.10970	1.754173	0.000669	Pectate lyase (EC 4.2.2.2)	PL3_2	Yes
MSTRG.12682	1.3864	6.12E-05	Uncharacterized protein	GH134	Yes

Supplementary Table 2. Differentially expressed genes predicted as fungal effectors by SignalP-5.0 and Effector P

GENE_ID	Log2FC	padj	Protein name	SignalP-5.0	EffectorP
MSTRG.194	-1.07059	2.12E-06	EF-hand domain-containing protein	SP(Sec/SPI)	Effector
MSTRG.11261	0.975254	0.012057	Probable cellulase	SP(Sec/SPI)	Non-effector
MSTRG.1095	0.887965	0.019535	Glucanase (EC 3.2.1.-)	SP(Sec/SPI)	Non-effector
MSTRG.10972	0.982412	3.16E-08	Uncharacterized protein	SP(Sec/SPI)	Non-effector
MSTRG.212	-1.14224	2.01E-06	Uncharacterized protein	SP(Sec/SPI)	Effector
MSTRG.10202	1.39967	8.05E-05	Probable alpha-glucuronidase precursor	SP(Sec/SPI)	Non-effector
MSTRG.13959	1.152227	1.40E-06	Probable lipase	SP(Sec/SPI)	Non-effector
MSTRG.12705	1.421499	0.009729	Related to extracellular GDSL-like lipase/acylhydrolase	SP(Sec/SPI)	Non-effector
MSTRG.11223	-1.0483	0.007272	Related to tripeptidyl-peptidase I	SP(Sec/SPI)	Non-effector
MSTRG.5292	-0.66407	0.00163	Carboxypeptidase (EC 3.4.16.-)	SP(Sec/SPI)	Non-effector
MSTRG.10166	1.267826	0.001218	DM13 domain-containing protein	SP(Sec/SPI)	Non-effector
MSTRG.8339	-1.36405	0.004705	Related to alkaline protease (Oryzin)	SP(Sec/SPI)	Non-effector
MSTRG.2116	3.143294	2.55E-06	Uncharacterized protein	SP(Sec/SPI)	Non-effector
MSTRG.13124	2.30796	4.79E-13	Related to S.fumigata Asp FII	SP(Sec/SPI)	Non-effector
MSTRG.11334	1.246926	0.006416	GH115_C domain-containing protein	SP(Sec/SPI)	Non-effector
MSTRG.1876	1.873476	3.04E-07	Calpain-9	SP(Sec/SPI)	Non-effector
MSTRG.3888	1.494179	5.07E-05	Related to L-sorbosone dehydrogenase	SP(Sec/SPI)	Non-effector
MSTRG.2124	-0.58978	0.003972	Uncharacterized protein	SP(Sec/SPI)	Non-effector
MSTRG.242	-1.58197	0.048207	Uncharacterized protein	SP(Sec/SPI)	Effector
MSTRG.1917	0.64014	0.000578	Carboxylic ester hydrolase (EC 3.1.1.-)	SP(Sec/SPI)	Non-effector
MSTRG.2406	1.488803	0.004684	Probable fusarubin cluster-oxidoreductase	SP(Sec/SPI)	Non-effector
MSTRG.13401	0.998963	3.24E-12	Mannan endo-1,6-alpha-mannosidase (EC 3.2.1.101)	SP(Sec/SPI)	Non-effector
MSTRG.13155	1.261478	9.27E-08	Related to putative arabinase	SP(Sec/SPI)	Non-effector
MSTRG.2389	0.73955	0.000578	Uncharacterized protein	SP(Sec/SPI)	Non-effector
MSTRG.11159	0.586528	0.040047	Amine oxidase (EC 1.4.3.-)	SP(Sec/SPI)	Non-effector
MSTRG.10798	-2.24063	0.005177	Uncharacterized protein	SP(Sec/SPI)	Non-effector
MSTRG.11406	0.887244	0.026653	Uncharacterized protein	SP(Sec/SPI)	Non-effector
MSTRG.3958	6.584182	0.033529	Uncharacterized protein	SP(Sec/SPI)	Non-effector
MSTRG.4390	1.606719	1.13E-10	Related to zinc transporter	SP(Sec/SPI)	Non-effector
MSTRG.11253	1.124242	0.010367	Related to cellulose binding protein CEL1	SP(Sec/SPI)	Non-effector
MSTRG.4050	-2.13629	0.04652	Uncharacterized protein	SP(Sec/SPI)	Effector

MSTRG.2194	2.014575	4.72E-08	Related to beta-mannanase	SP(Sec/SPI)	Non-effector
MSTRG.10552	1.083737	0.018319	Related to ferric reductase Fre2p	SP(Sec/SPI)	Non-effector
MSTRG.3917	1.259252	5.10E-05	Related to beta-mannanase	SP(Sec/SPI)	Non-effector
MSTRG.4249	0.858509	0.014557	Probable isoamyl alcohol oxidase	SP(Sec/SPI)	Non-effector
MSTRG.4543	1.51234	0.019535	CHRD domain-containing protein	SP(Sec/SPI)	Effector
MSTRG.5181	0.937071	4.13E-05	Probable triacylglycerol lipase	SP(Sec/SPI)	Effector
MSTRG.6762	1.001506	0.006304	Related to deacetylase	SP(Sec/SPI)	Effector
MSTRG.7788	1.017913	0.041227	Probable acetylxylan esterase	SP(Sec/SPI)	Effector
MSTRG.10201	0.903171	0.043224	Glucanase (EC 3.2.1.-)	SP(Sec/SPI)	Non-effector
MSTRG.3878	1.207099	0.000309	Beta-xylanase (EC 3.2.1.8)	SP(Sec/SPI)	Unlikely effector
MSTRG.12670	0.989153	0.03687	Related to cellulose-binding GDSL lipase/acylhydrolase	SP(Sec/SPI)	Unlikely effector
MSTRG.6994	0.861382	0.043539	Uncharacterized protein	SP(Sec/SPI)	Non-effector
MSTRG.8765	1.581664	3.12E-08	Glucanase (EC 3.2.1.-)	SP(Sec/SPI)	Effector
MSTRG.4352	1.072319	0.006839	Probable fusarubin cluster-esterase	SP(Sec/SPI)	Non-effector
MSTRG.9957	-1.0018	0.018081	Uncharacterized protein	SP(Sec/SPI)	Effector
FPRO_14590	9.132446	5.22E-08	Related to aspartic proteinase OPSB	SP(Sec/SPI)	Non-effector
MSTRG.10230	-1.05227	0.044101	Uncharacterized protein	SP(Sec/SPI)	Effector
MSTRG.10249	1.514096	5.60E-08	Related to endoglucanase IV	SP(Sec/SPI)	Effector
MSTRG.10924	1.857588	0.012057	Related to alpha-L-arabinofuranosidase II	SP(Sec/SPI)	Effector
MSTRG.10352	0.883534	0.033496	Related to endopeptidase K	SP(Sec/SPI)	Non-effector
MSTRG.11436	-0.76698	0.002611	Carboxypeptidase (EC 3.4.16.-)	SP(Sec/SPI)	Non-effector
MSTRG.4393	1.422807	1.06E-11	Uncharacterized protein	SP(Sec/SPI)	Non-effector
MSTRG.11995	1.058251	0.024378	Related to lipase/acylhydrolase	SP(Sec/SPI)	Non-effector
MSTRG.2117	2.329262	0.000181	Related to WSC2 Glucoamylase III (Alpha-1,4-glucan-glucosidase)	SP(Sec/SPI)	Non-effector
MSTRG.10970	1.754173	0.000669	Pectate lyase (EC 4.2.2.2)	SP(Sec/SPI)	Effector
MSTRG.12682	1.3864	6.12E-05	Uncharacterized protein	SP(Sec/SPI)	Effector

Supplementary Table 3. Differentially expressed genes with Pathogen-host interaction annotations.

GENE_ID	Log2FC	padj	Protein name	PHI (Pathogen-Host Interaction database)
MSTRG.11261	0.975254	0.012057	Probable cellulase	unaffected pathogenicity
MSTRG.10899	-1.12944	0.033496	Related to HSP30 heat shock protein Yro1p	unaffected pathogenicity
MSTRG.6898	0.75645	0.001174	Probable ENA5-Plasma membrane P-type ATPase involved in Na+ and Li+ efflux	reduced virulence, loss of pathogenicity
MSTRG.8413	0.952551	0.03999	Related to integral membrane protein	unaffected pathogenicity
MSTRG.10366	-1.03827	0.016811	Probable PTR2-Di-and tripeptide permease	unaffected pathogenicity
MSTRG.3715	-1.2712	0.02004	Catalase (EC 1.11.1.6)	reduced virulence, unaffected pathogenicity
MSTRG.6318	-1.09574	0.007392	Related to pheromone receptor PRE-1	unaffected pathogenicity
MSTRG.1917	0.64014	0.000578	Carboxylic ester hydrolase (EC 3.1.1.-)	unaffected pathogenicity
MSTRG.6819	-0.83275	0.037668	Related to STB5-SIN3 binding protein	unaffected pathogenicity
MSTRG.11684	2.054285	4.79E-13	Probable cysteine synthase B	reduced virulence, unaffected pathogenicity
MSTRG.7760	0.617596	0.006165	Related to linoleate diol synthase	reduced virulence
MSTRG.8532	0.574606	0.016469	Probable Pls1 tetraspanin	unaffected pathogenicity
MSTRG.4249	0.858509	0.014557	Probable isoamyl alcohol oxidase	unaffected pathogenicity
MSTRG.5181	0.937071	4.13E-05	Probable triacylglycerol lipase	reduced virulence
MSTRG.14421	3.920494	5.30E-07	Probable DHA14-like major facilitator ABC transporter	chemistry target: sensitivity to chemical, unaffected pathogenicity, reduced virulence, unaffected pathogenicity, increased virulence (hypervirulence)
MSTRG.2410	0.69143	0.039969	Fusarubin cluster-polyketide synthase	unaffected pathogenicity
MSTRG.10177	-0.55415	0.018615	Probable developmental regulator flbA	unaffected pathogenicity
MSTRG.13740	-1.2414	4.63E-05	Related to 26S proteasome subunit RPN4	unaffected pathogenicity
MSTRG.13161	-0.46767	0.043698	Related to myo-inositol transport protein ITR1	unaffected pathogenicity
MSTRG.10249	1.514096	5.60E-08	Related to endoglucanase IV	unaffected pathogenicity
MSTRG.3875	2.175148	4.79E-13	Probable non-ribosomal peptide synthetase	reduced virulence, unaffected pathogenicity
MSTRG.8923	0.546425	0.018983	Related to myo-inositol transport protein ITR1	reduced virulence
MSTRG.10970	1.754173	0.000669	Pectate lyase (EC 4.2.2.2)	reduced virulence

Supplementary Table 4. Most overrepresented KEGG pathways in the DEGs

GENE_ID	Log2FC	padj	KEGG ID	KEGG description	padj
MSTRG.6601	-0.913276	0.001899	fvr04011	MAPK signaling pathway - yeast	0.002003
MSTRG.3715	-1.271198	0.001012			
MSTRG.6318	-1.095743	0.000347			
MSTRG.10177	-0.554145	0.000907			
MSTRG.11261	0.975253	0.000543	fvr00500	Starch and sucrose metabolism	0.020574
MSTRG.1095	0.887964	0.000986			
MSTRG.10201	0.903170	0.002254			
MSTRG.8765	1.581663	4.413E-09			
MSTRG.1047	0.915162	0.000261	fvr02010	ABC transporters	0.129983
MSTRG.3873	1.599655	1.337E-06			
MSTRG.7760	0.617596	0.000275	fvr00591	Linoleic acid metabolism	0.145464
MSTRG.2194	2.014575	7.185E-09	fvr00051	Fructose and mannose metabolism	0.145464
MSTRG.3917	1.259251	3.669E-06			

VITA

Viviana Estefania Freire Zapata

Candidate for the Degree of

Master of Science

Thesis: EFFECTS OF SUBINHIBITORY DOSES OF THE FUNGICIDE IPRODIONE ON THE PLANT PATHOGENS *Fusarium oxysporum* AND *F. proliferatum*

Major Field: Entomology and Plant Pathology

Biographical:

Education:

Completed the requirements for the Master of Science in Entomology and Plant Pathology at Oklahoma State University, Stillwater, Oklahoma in December, 2020.

Completed the requirements for the Bachelor of Science in Biotechnology Engineering at University of the Armed Forces – ESPE, Sangolquí, Ecuador in 2016.

Experience:

Graduate Research Assistant at Oklahoma State University, Stillwater, Oklahoma from January, 2019 to December, 2020.

Research Assistant, Institute of Biosecurity and Microbial Forensics, Stillwater, Oklahoma from June 2018 to November 2018.

Research Assistant, Oklahoma State University, Stillwater, Oklahoma from September 2017 to June 2018

Professional Memberships:

American Phytopathological Society (APS)